NOTICE

The quality of this microform is heavily dependent upon the quality of the original thesis submitted for microfilming. Every effort has been made to ensure the highest quality of reproduction possible.

If pages are missing, contact the university which granted the degree.

Some pages may have indistinct print especially if the original pages were typed with a poor typewriter ribbon or if the university sent us an inferior photocopy.

Previously copyrighted materials (journal articles, published tests, etc.) are not filmed.

Reproduction in full or in part of this microform is governed by the Canadian Copyright Act, R.S.C. 1970, c. C-30

AVIS

La qualité de cette microforme dépend grandement de la qualité de la thèse soumise au microfilmage. Nous avons tout fait pour assurer une qualité supérieure de reproduction.

S'il manque des pages, veuillez communiquer avec l'université qui a conféré le grade.

La qualité d'impression de certaines pages peut laisser à désirer, surtout si les pages originales ont été dactylographiées à l'aide d'un ruban usé ou si l'université nous a fait parvenir une photocopie de qualité inférieure.

Les documents qui font déjà l'objet d'un droit d'auteur (articles de revue, tests publiés, etc.) ne sont pas microfilmés.

La reproduction, même partielle, de cette microforme est soumise à la Loi canadienne sur le droit d'auteur, SRC 1970, c. C-30

Canada

Performance of a Frequency Hopped MFSK Multi-Access Mobile Cellular Radio Network Using Error Correcting Techniques

Clifford Ellement

~~A Thesis~~

In

The department

of

Electrical Engineering

Presented in Partial Fulfillment of the Requirements
for the Degree of Master of Engineering at
Concordia University
Montreal, Quebec, Canada

June 1987

ISBN 0-315-41616-5

Acknowledgements

The author wishes to express his gratitude to Dr. A.K. ElHakeem for his guidance, support, and patience during the entire delevopment and preparation of the thesis.

Also, a thanks to Dr. Le-Ngoc is required for sharing some of his insight on topics related to this work.

Thanks to Dr. J. Hayes for the opportunity to work on the research project which provided much support for the completion of the Master program.

ABSTRACT

Performance of a Frequency Hopped MFSK Multi-Access Mobile Cellular Radio Network Using Error Correcting Techniques

Clifford Ellement

The performance characteristics of a Spread-Spectrum Mobile Cellular Network with both data and voice users is investigated. Error correction schemes such as Automatic Repeat-Request (ARQ) and Forward-Error-Control (FEC) are employed to provide for a high-capacity network. A comparison of several FEC codes is performed under various load conditions to determine the best system performance in terms of the throughput, packet blocking, and packet delay.

An exact analysis is employed to determine the probability of bit error for a soft-limited Frequency-Hopped Multi-Access system and inturn is used for the averaging analysis of the uplink channel of the mobile cellular system.

Table of Contents

List of Figures

List of Tables

List of Symbols

A_{jI}	Inphase Random Variable for Interfering Users
A_{jq}	Quadrature Random Variable for Interfering Users
ARQ	Automatic-Repeat Request
B_d	Hamming Distance of a Code
B_l	Probability of Packet Blocking
C	Number of Cells in a Basic Cell Pattern
CDMA	Code Division Multiple Access
CS	Central Switch
$C(t)_j$	PN Code Sequence
DS	Direct Sequence
FEC	Forward Error Control
FH	Frequency Hopping
LPI	Low Probability of Intercept
L_s	Implementation Loss
MFSK	M-ary Frequency Shift Keying
MLS	Maximum length Sequence
M_d	Number of Data Users
M_v	Number of Voice Users
P(t)	Distribution of Silent Period
PG	Processing Gain
P_c	Probability of Correct Symbol
P_{dp}	Probability of Transmitting a Packet
P_{ds}	Average Probability of Transmitting a Packet
P_m	Probability of Incorrect Symbol Detection
PN	Pseudo-Random Code

P(n)	Average Probability of Transmitting a Packet
$P_{r_{ij}}$	Output PDF of Energy Detector
P_{vd}	Probability Silent Period
P_{vf}	Probability of Unsuccessful Transmission
$P_v(t)$	Distribution of Inter-Time Arrival
Q	Total Number of Frequency Tones
Q(t)	Distribution of Talking Period
Q_r	Co-Channel Interference Reduction Factor
R_c	Code Rate
R_d	Data Rate
R_{ij}	i th Energy Detector Output During j th Hop
R^{-n}	Received Power at Distance R
S_l	State In Markovian Diagram
SS	Spread-Spectrum
T_h	Hopping Period
T_l	Total Traffic in Uplink Channel
THRO	System Throughput Performance
UAN	User-Access Node
U_s	Total Number of Strong Users
U_t	Total Number of Weak Users
W_d	BaseBand signal Bandwidth
W_{ss}	Spread-Spectrum Bandwidth
Z_l	Random Variable of Receiver Combiner
$d_{\min}$	Minimum Distance of a Code
i_{jk}	Number of Weak Users in Hop j and Bank k
k_{jk}	Number of Strong Users in Hop j and Bank k

n	Propagation Constant
q	Average Retransmission Rate
t	Maximum Number of Correctable Bits
t_p	Duration of Packet Transmission
u	Probability of Voice Transmission
Θ_l	Data Phase Modulation
$\chi_{jl}(r)$	Output of The Soft-Limiter
$\psi_{\chi_{jl}}(\omega)$	Characteristic Function of the $\chi_{jl}(r)$ Distribution
$\psi_{Z_l}(\omega)$	Product of the L-Fold $\chi_{jl}(r)$ Convolution
λ_d	Probability of Data Transmission
λ_v	Probability of Voice Transmission
σ^2	Signal Variance
θ_{jj}	Phase Shift of Spread-Spectrum Signal
ω^{h_l}	Hopping Frequency

CHAPTER ONE

INTRODUCTION

Much concern is developing over the state of the existing mobile radio services. The need for better spectral efficient mobile communication systems are becoming more apparent as the demands for such services increase. With todays requirements for integrated voice and data services, demands are created for for new and diverse forms of data transmission requirements. The new generation mobile networks must have the capability of being spectrally efficient and have the ability to handle diverse forms of traffic.

The current mobile cellular radio systems are plagued with a host of problems, such as, boundary crossing, channel assignment, blocking, and co-channel interference. In this study, we investigate the performance of a Spread-Spectrum mobile radio network which has many advantages over the conventional mobile systems. Spread-Spectrum networks alleviate some of the spectral demands by increasing the user density in a small-cell system as well as significantly reducing the degradation in performance that normally arises from rapid fading conditions. There is no hard limit on the number of users that can access a Spread-Spectrum network. However, when the number of active users exceeds a designed value, the network performance degrades but gradually. Thus, mobile users can initiate a call at any time without being blocked due to a limited number of free channels in the network. Spread-Spectrum networks are also capable of handling various forms of traffic, such as required for integrated services.

Over the past few years, analysis in this area has been attempted and shown to be a viable form of communications. However, many considerations important to the compete network and transmission picture have not been included. We

propose an analysis which uncovers some of the concerns and trade-offs present when designing a integrated service mobile spread-spectrum network.

In Chapter Two, we introduce some of the relevant basic techniques used in Spread-Spectrum communications and develop certain criteria required for a SS multiple-access design. A Spread-Spectrum system proposed by [10] is examined as a brief introduction into the calculation of bit error probability for a SSMA system.

The development of an exact analysis for the probability of error of a multiple-access SS network is described in Chapter Three for various receiver and system designs. The investigation of the best system performance is performed for 2,4 and 8-FSK receivers with 2 and 4 hops/symbol system parameters. The results of which are used in Chapter Five where we analyze the throughput performance, blocking, and packet delay for a CDMA cellular mobile network employing error correction measures. Also in Chapter Five, we propose several network control signalling techniques and inter-station network design features.

Chapter Four introduces some of the basic mobile system designs in handling multi-user traffic requests and information routing schemes. Newly proposed mobile network architectures such as channel borrowing and Microcell designs are also investigated.

The study presented here is an overview of the choice of Spread-Spectrum system design for use in a multiple-access environment using exact analysis computation which has not been attempted in the available literature to the extent that we attempt. Our proposed mobile cellular radio network illustrates how a Spread-Spectrum system can be employed for the next generation mobile systems and gives some foresight of possible error coding and network topology techniques.

CHAPTER TWO

SPREAD-SPECTRUM DESIGN

2.1 Introduction

Code Division Multiple-Access (CDMA) networks use spread-spectrum techniques as the basis of transmission. Spread-spectrum signals have the characteristic that their bandwidth W_{ss} is much greater than the minimum bandwidth required to transmit the information being sent at rate R_d. The introduction of frequency redundancy to the baseband signal provides for many advantages over other signalling schemes and is known as the bandwidth expansion factor ($B_e = W_{ss}/R_d$). Some of the advantages with this bandwidth redundancy are immunity to interference in the radio channels, low probability of intercept, and anti-jamming capabilities.

Interference in radio channels are caused by a variety of sources. As in all digital radio links, there exists self-interference due to multi-path propagation of frequency selective fading, which can be reduced with the by employing spread-spectrum communications. Another form of unintentional interference, which will be discussed later in full, is the interference from other users in multiple-access communications systems. However, the latter type is not fatal to the network operation or to a specific channel as in other multi-access schemes.

Intentional interference also known as jamming arises when a hostile transmitter tries its best to confuse the intended receiver. This can be done by optimizing the time-frequency power of the jammer into certain portions of the spread-spectrum bandwidth (W_{ss}) at an optimum duty cycle. Again spread-spectrum systems have an inherent immunity to such forms of interference.

The factor which determines the ability of the spread-spectrum system to perform all of the above requirements is called the Processing Gain (PG) which is basically the bandwidth expansion or the time and frequency redundancy introduced into the system, denoted as $PG = W_{ss}/R_d$.

When confronted with a jamming signal either intentional or unintentional, the spread-spectrum receiver with its processing gain PG cannot always perform correctly. The capability of a receiver to operate in such hostile environments is called the jamming margin and is the measure of the required SNR at the receiver input. The jamming margin takes into consideration the implementation loss (L_s) and the SNR at the information output. We can then write

$$JammingMargin = PG - [L_s - (SNR)_{out}] \qquad (2.1)$$

An other important factor which makes spread-spectrum communications attactive is that the spreading is perform in a pseudo-random fashion. Thus the signal appears to be noise-like when transmitted at low power levels. This creates what is known as a Low-Probability of Intercept (LPI) signal and of coarse is required for security communications.

2.2 Generation of SS signals

There are a few methods of obtaining a spread-spectrum signal from a baseband signal. Two of the most common techniques are Direct Sequence (DS) and Frequency Hopping (FH). Bandwidth spreading is performed in a direct sequence system by combining a pseudorandom (PN) sequence C(t) (modulating at a rate of (R_c).) with the information sequence where the chip rate R_c is much greater than the information rate R_d. The resulting signal is a binary sequence having a PN binary rate (R_c) which is then modulated upto the radio frequency. Compared to the usual modulated signal spectrum, the spectrum of

the DS signal is spread by a factor of N which is the ratio of the PN sequence bit rate to the data bit rate.

For example, a simple form of spreading by direct sequence techniques is done so by employing Binary Phase-Shift Keying (BPSK) as shown if Figure (2.1). The binary information sequence D(t) is first combined with the pseudo-random sequence C(t) (Mod 2 addition) before it is sent to the BPSK transmitter. The output of the BPSK transmitter, now a Direct Sequence signal X(t), is shown in Figure (2.1)

$$X(t) = \sqrt{2P}\, C(t) \cos(\omega_0 t + \Theta_d(t)) \qquad (2.2)$$

where P is the transmitted power, ω_0 is the center SS frequency, and $\Theta_d(t)$ is the data phase modulation.

At the receiver, the received signal is first despread by binary addition with the same pseudo-random code as the transmitter assuming the two codes are synchronized. Then the signal is demodulated by the PSK receiver to obtain the original information sequence.

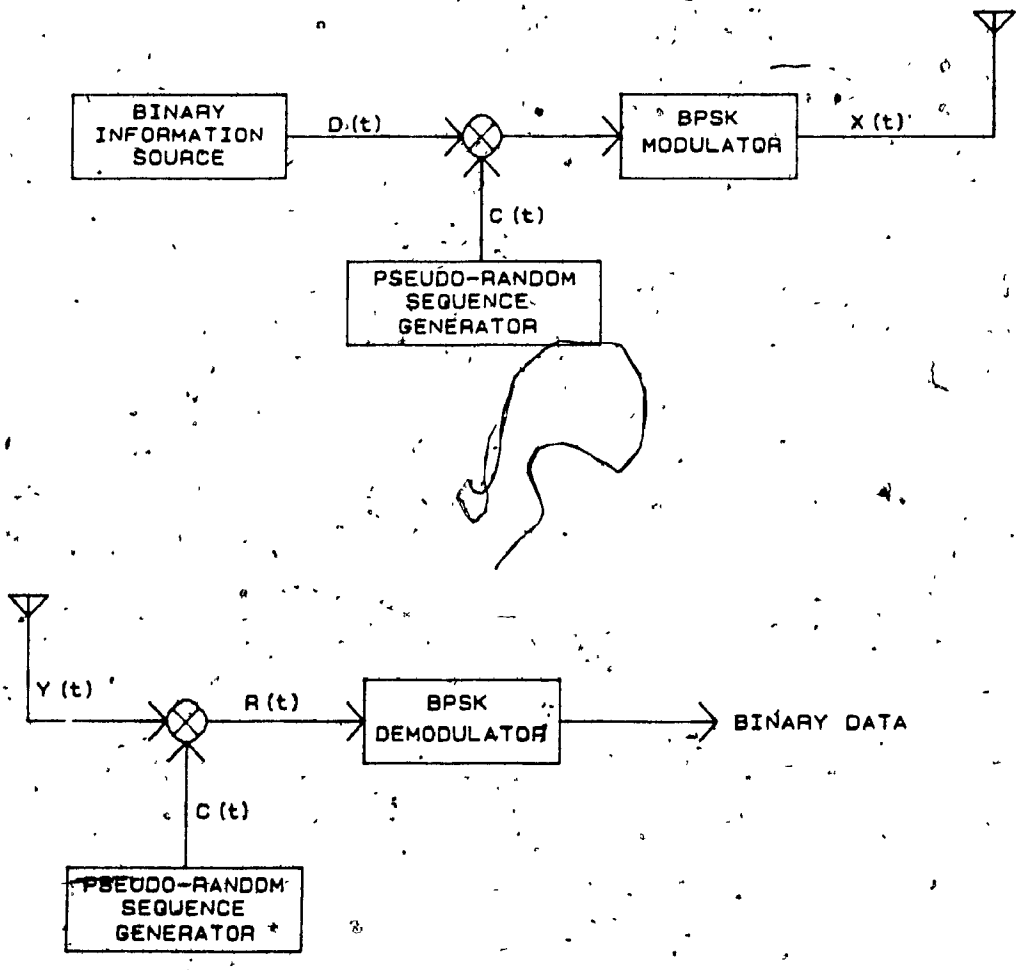

Figure (2.1) Direct Sequence Spread-Spectrum System.

The second method of spreading the spectrum is to change the frequency of the carrier frequency periodically. The carrier frequency is chosen from a set of frequencies which are spaced approximately the width of the data modulation spectrum apart. In this case the spreading code does not directly modulate the data-modulated carrier but is instead used to control the sequence of carrier frequencies. Because the transmitted signal appears as a data modulated carrier which is hopping from one frequency to the next, this type of spread-spectrum is called frequency hopping.

The modulation employed is usually either binary or M-ary Frequency Shift Keying (MFSK) and usually demodulated noncoherently. Consider a FH spread-spectrum system in which a BFSK scheme is employed as shown in Figure (2.2). The modulator selects one of two possible frequencies corresponding to the transmission of either a 1 or 0 for duration T_b. The ordinary BFSK signal can be written as

$$S(t) = \sqrt{2P}\ \sin[\omega_0 t + d_n\, \Delta\omega t_b] \tag{2.3}$$

where d_n are independent data bits

$$d_n = \begin{cases} 1 & with\ \ probability\ 1/2 \\ -1 & with\ \ probability\ 1/2 \end{cases} \tag{2.4}$$

The value of $\Delta\omega t_b$ is chosen such that any two possible data tones are orthogonal.

The output of the FSK modulator is then translated in frequency by the amount determined from the pseudo-random generator which selects a frequency from the frequency synthesizer. If the pseudo-random generator has m stages, then there are $2^m - 1$ possible frequency translations. The frequency hopping tone

of the BFSK signal becomes

$$X(t) = \sqrt{2P}\,\sin[\omega_0 t + \omega_n t + d_n \Delta\omega t] \qquad (2.5)$$

where ω_n is the particular hop frequency chosen for the n-th transmission interval.

Again at the receiver we have an identical PN code generator synchronized with the received signal to select the proper frequency from the frequency synthesizer. This is achieved by running an identical code sequence generator in time synchronism with the code sequence producing a hopping pattern of the receiver carrier. The local carrier hops in frequency synchronism with the received carrier so that only the BFSK signal appears as a difference frequency. After which a bank of filters tuned to each possible FSK frequency non-coherently decodes the symbol modulation in each time slot.

The constraining limitation on FH systems is the speed of the frequency synthesizers which must have the capability of changing frequencies very fast and with good accuracy. If the frequency accuracy is offset, the FSK demodulation will receive a tone which is misaligned with the tuned filters and cause decoding errors. The settling time of the frequency synthesizers is a major concern, since the decoding time lost in each transition adds to the energy lost in the filter output.

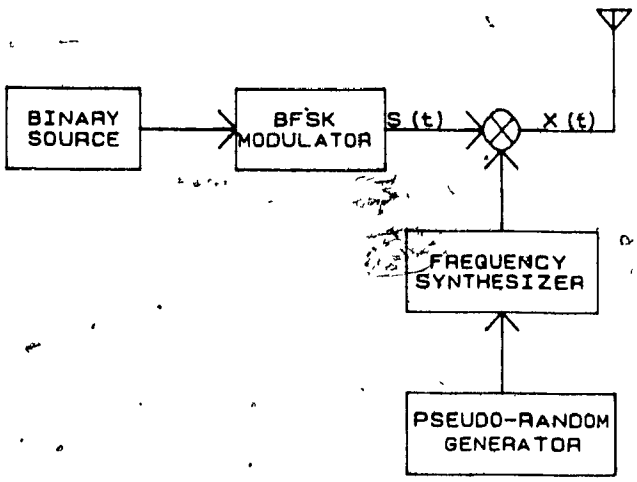

FH TRANSMITTER

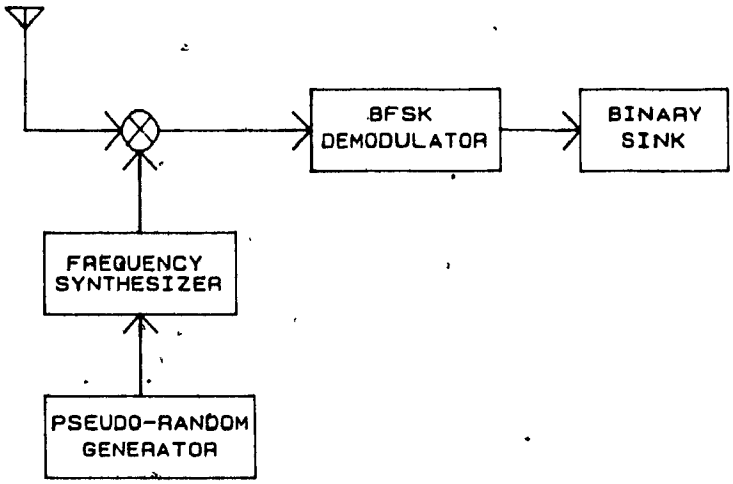

FH RECEIVER

Figure (2.2) Frequency Hopping Spread-Spectrum System.

When the hopping rate is faster than the the symbol rate producing a multiple- hop per symbol signal, it is considered as fast-hopping spread-spectrum. Slow-hopping on the other hand is so termed when the hopping rate equals or is less than the symbol rate.

There are two points of view one can take for a non-coherent FH/SS system. One is that the entire SS bandwidth W_{ss} is composed of one MFSK baseband signal where the redundancy is introduced in the M-ary component of the modulation scheme. The other view point is essentially a conventional BFSK or MFSK signal that has a shifting carrier frequency as shown in Figure (2.3). The FH system we consider in our analysis (in later chapters) consists of many MFSK non-overlapping baseband signals within the SS bandwidth W_{ss} and a fast frequency hopping scheme.

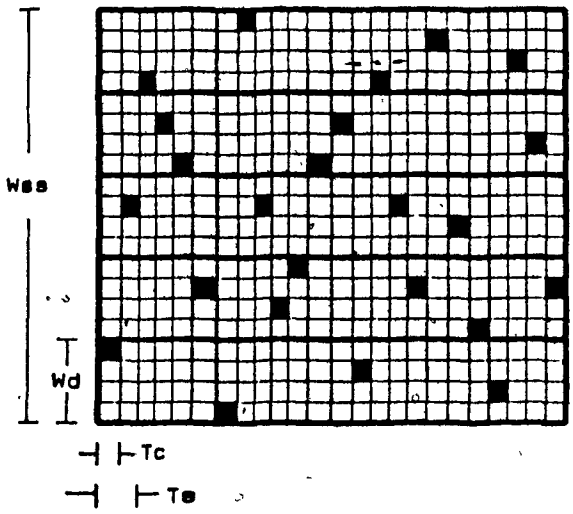

Figure (2.3) MFSK Signalling Strategy for FH systems.

2.3 Hybrid Spread-Spectrum Generation

By combining both DS and FH spreading techniques a third form of spreading technique is created which is called Hybrid SS system. The advantages of both systems are now combined into one system and providing a practical method of obtaining large spreading bandwidths. Figure (2.4) shows a FH/DS Hybrid transmitter. The output spectrum is composed of many DS spectra hopping over the entire SS bandwidth as dictated by a frequency hopping pattern.

The Hybrid transmitter in our example, employs both BPSK modulation and non-coherent frequency hopping schemes. The PN sequence in a Hybrid transmitter performs the selection of the hopping frequency as well as the binary addition with the information sequence. The binary information sequence is first modulated with the PN code sequence then it is frequency translated by the frequency synthesizer. Therefore, we can write the signal from the Hybrid transmitter as

$$S(t) = \sqrt{2P}\, C(t) \cos[\omega_h t + \omega_n t + d_n \Delta\omega t] \qquad (2.6)$$

The DS and FH pseudo-random sequences are synchronized with each other since both are sourced from the same clock. The DS code or chip rate is normally much faster than the rate of frequency hopping thus, the frequency from the synthesizer will remain the same over many C(t) bits. same.

The Hybrid receiver first dehops the incoming signal with the same requirements as the FH scheme. After which a baseband BPSK waveform is produced and decoded at the PSK demodulator.

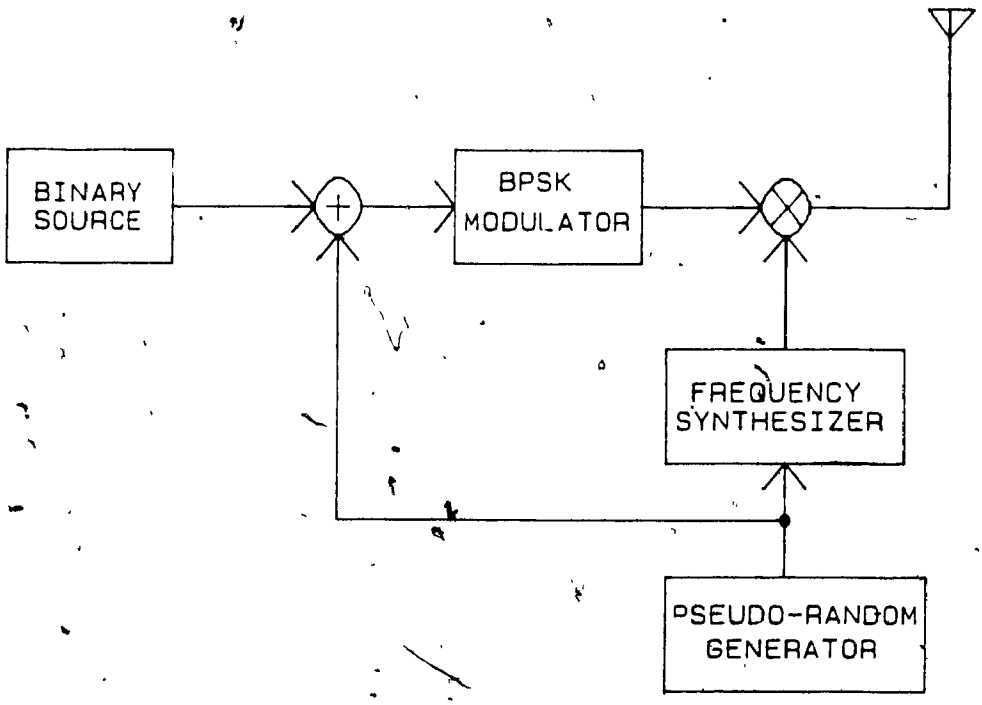

Figure (2.4) Hybrid Spread-Spectrum Transmitter

2.4 Pseudo-Random Sequences -

The binary sequence C(t), used for spreading and despreading the baseband signal is most commonly generated using shift registers. When a large array of shift registers are used, the sequence C(t) acts as a noise-like signal but is still deterministic. For practical SS systems C(t) is made to have a very wide bandwidth and for efficient despreading performance the sequence must be easy to track (regain synchronization), therefore a C(t) with a two-valued autocorrelation function is desirable.

The type of pseudo-random sequence we consider in this study are linear code sequences which are useful for interference rejection but fall short in performance for security measures. Non-linear codes, not treated here, also can be used for interference rejection and are better suited for security tactics.

In choosing a pseudo-random sequence, one wants a nonrepeating sequence to provide the most randomness possible to the DS or FH systems. Since all practical sequences must be finite (even though some are long enough to be almost considered infinite) the best sequence generators will give the longest sequence for the least amount of hardware. Thus we examine a class of code sequences that, by definition, are the largest codes that can be generated by a given shift-register of a given length. This class of sequences are known as Maximal Length Sequences (MLS). The maximum length of the MLS is $2^n - 1$ chips, where n is the number of stages in the shift-register. Thus, after $2^n - 1$ chips the sequence repeats itself again.

An important characteristic of MLS code sequences is that the number of ones in a sequence is always one less than the number of zeros. That is there are $2^n/2$ ones and $2^n/2 - 1$ zeros generated within a cycle of the MLS code. This characteristic is quite important in communication systems, since it provides a

very low DC component.

Another important property of MLS is the autocorrelation characteristics which can be stated as

$$\Theta = \begin{cases} 1.1 & k = ln \\ -1/n & k = 1/\ln \end{cases} \tag{2.7}$$

where l is any integer and N is the frequency period $(2^n - 1)$. For tracking purposes, a two-valued autocorrelation function such as the one described above is very important. For example, if we consider a 10 stage MLS sequence generator, there are $2^n - 1$ or 1023 chips per cycle and giving a peak to minimal autocorrelation value of 1024, a range of 30.1 dB. A high dB value for a given autocorrelation function will increase the receiver's ability to track the pseudo-random code and therefore remain synchronized when confronted with interfering signals as would be expected in CDMA networks.

The choice of a PN sequence when designing a FH/CDMA network, must also contain other important factors above the requirement listed above. The sequence size must be relatively large in order to randomize the frequency hopping as much as possible. Since there are many simultaneous users communicating in a CDMA network, each users PN sequence must differ from any other users PN sequence. To avoid two distinct transmitters interfering with each other, the Hamming distance between the two sequences must be s large as possible. Thus the cross-correlation of the two codes will be as small as possible.

2.5 Spread-Spectrum Multiple Access Networks

From the point of view of capacity, Spread-Spectrum Multiple Access (SSMA), also called Code-Division Multiple Access (CDMA), networks do not seem to be the most attractive, but when a network is required to provide a multiple-access scheme in a jamming or a mutual interference environment, CDMA networks are not only more attractive but also the only choice. The employment of CDMA in cellular mobile communications and packet switched radio becomes increasingly popular.

In CDMA systems, each user has access to the entire system bandwidth. One way of distinguishing the signals from one another is to give each user an address or unique code consisting of a fixed pattern in time and frequency, so the information to be transmitted is modulated onto the address. In a multipoint-to-point system, the base station receiver simultaneously detects and decodes several SS signal transmitted from spatially separated radios. Since all other users have a different code sequence, the receiver will detect the wanted signal even though all signal use the entire SS bandwidth. However, when the number of users become relatively large compared to the bandwidth, the probability that another user will effect the correct decision of the receiver will increase. The interference between users is a major limiting factor in the SSMA network capacity. The use of large processing gains results in a form of frequency diversity that significantly reduces the degradation in performance that normally arise from mutual interference.

The mobile station's code sequence, as stated before, cycles through its address sequences which is superimposed on the carrier with the data. A CDMA system can be designed in two basic formats. If the PN sequence is modulated directly on the carrier is it referred to as a direct-sequence CDMA (DS-CDMA). The second format uses the PN sequence to change the frequency of the carrier,

this is referred to as frequency hopped CDMA (FH-CDMA). We shall limit our following discussion and study to only frequency hopped multiple-access schemes (FH-CDMA).

As an example, we examine a CDMA network proposed by Goodman [11] for mobile-base communications. The network uses FH-MFSK modulation, in doing so, confines all M users to the same 20 MHz bandwidth. The SSMA system is analyzed with a simplified transmission model of white Gaussian noise and Rayleigh-distributed fading. The effect of mutual interference from the M-1 users on a specific intended signal is determined. Additional effects such as synchronization problems are not considered here.

By referring to Figure (2.5), the operation of the system is defined by the use of a time-frequency matrix. Every T seconds, k message bits are loaded into a shift-register and transferred as a k-bit word. During the basic signalling interval, for one symbol of $T = L\tau$ seconds, the code generator in the transmitter generates a sequence of L codes, each k-bits long. The address generator and the k-bit message word is added modulo-2^k producing a signal 2^k-FSK frequency hopped signal. The transmission rate per user is k-bits every $L\tau$ seconds, so that $R = k/L\tau$ bits/second.

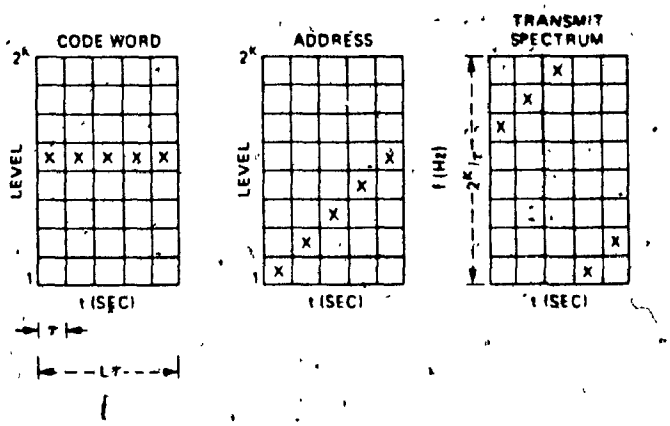

Figure (2.5) Time-Frequency Matrix

At the front-end of the receiver, the signal is first despread with the PN sequence and then decoded by the MFSK receiver. Interference by other users can be minimized by taking advantage of the time-diversity of the system. For an example of the receiver operation, a time-frequency matrix exhibits the intended signal as 'x' and the interfering signal as 'o'. In Figure (2.6), the first matrix on the left shows the input waveforms entering the despreader. The despreader frequencies are controlled by the code generator to produce the frequency hopping pattern illustrated in the middle matrix. After the despreading or mixing operation, the detection matrix includes the intended signal and the interfering signals as shown in the right most matrix. The MFSK receiver determines the correct symbol by choosing the matrix row with the largest number of entries by employing majority logic circuits. Errors can be caused by the insertion of tones due to other users which form a row with more or equal the number entries than the row with the transmitted signal.

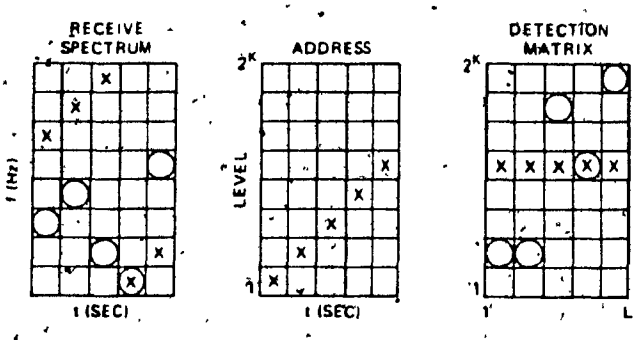

Figure (2.6) Time-Frequency Matrix of FH-MFSK Receiver.

To derive the probability of error, we consider first the probability that an interfering user is not sending a tone to the J,I position in the detection matrix, where J and I denote the row and column of the matrix respectively. The resulting probability is $1-2^{-k}$. Thus the probability that none of the $M-1$ interfering signals will send a tone to the J,I position is

$$P_d = \left[1-2^{-k}\right]^{M-1} \tag{2.8}$$

Given that the probability of detecting no tone in some matrix position is $1-P_d$ then the probability that a tone is transmitted to the J,I position is

$$P = \left\{1 - \left[1-2^{-k}\right]^{M-1}\right\} \tag{2.9}$$

The miss probability denoted as P_d, is defined as the probability of no tone detected in a matrix position conditional to a tone transmitted to that position and is written as

$$P_m = \left[1-\left(1-2^{-k}\right)^{M-1}\right](1-P_d) \tag{2.10}$$

The probability for overall insertion is the probability of false alarms (P_f) and the probability of error due to other users, thus we have $P_i = P + P_f - P_{pf}$. Where P_{pf} is the overlap of the two distributions. Now we can write the probability of m entries in row j as

$$P_s(m) = \binom{l}{m} P^m \ (1-P_i)^{l-M} \tag{2.11}$$

The upper bound on the bit error rate becomes

$$P_b = \left(\frac{2^{k-1}}{2^k-1}\right)\left[1-\sum_{i=1}^{L} P_c(i)[P(i,0)+1/2P(i,1)]\right] \tag{2.12}$$

where

$$P_c(i) = \binom{L}{i}(1-P_d)^i P_d^{L-i} \tag{2.13}$$

and

$$P(n,0) = \left[\sum_{M=0}^{n-1} P_s(M)\right]^{2^k-1} \tag{2.14}$$

The performance results of the system operating at a bit rate of 32 Kb/sec. in a Rayleigh fading environment and with parameters of k=8 and l=19 are

displayed below in Figure (2.9). It can be seen that the performance degrades gradually as the number of users increase. For example, with an average SNR of 25 dB, the system can accommodate up to 170 users before $P_b > 0.001$.

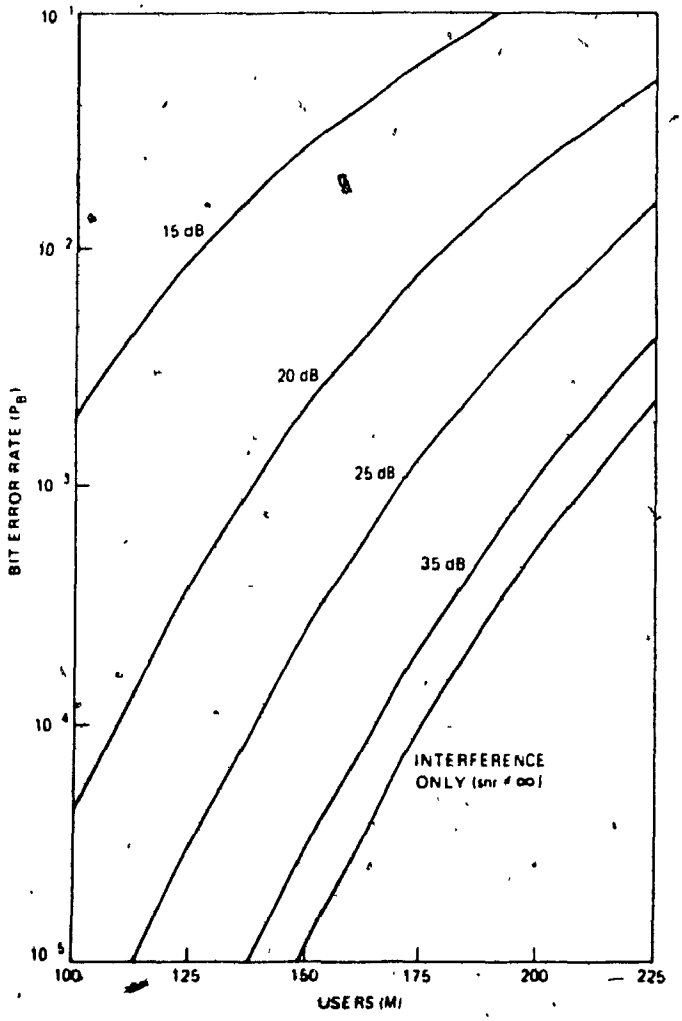

Figure (2.9) Performance Curves For FH-MFSK System.

CHAPTER THREE

EXACT ANALYSIS PERFORMANCE OF A SOFT-LIMITED FH/MFSK MULTIPLE-ACCESS SYSTEM IN NEAR-FAR SITUATIONS

3.1 Introduction

Multiple-access networks are increasingly being employed to satisfy the mobile communication needs of both metropolitan and rural areas. Recently, frequency-hopped spread-spectrum signaling has been used to alleviate some of the problems that plague multiple-access networks. In the past, SS systems were usually employed for military applications, but it is now becoming economically feasible and throughput cost effective to design packet switched cellular radio networks using spread-spectrum techniques.

In a mobile multiple-access environment, spread-spectrum multiple access offers many advantages over conventional multiple-access techniques. In metropolitan settings, the effect of multi-path fading is detrimental to a communication system; however, this can be overcome by the frequency diversity inherent in FH signals. Also, since there is no hard limit on the number of active users simultaneously on the network, any additional users over the permitted number will not be denied entry into the system. The additional users introduced into a spread-spectrum network will cause a "gentle degradation" throughout the entire network for all users.

In this chapter, we analyze the effect of strong (near) and weak (far) users for many different types of network designs. We consider systems using MFSK where $M = 2,4,6$ number of receiver banks, and systems with multiple hops per symbol, namely $L = 2$ and 4 hops/symbol. The average probability of error is determined by employing an exact analysis which includes summing

over all mutual interference conditions for various load situations (1 to 100 active users). The study includes a non-linear combining receiver which soft-limits the incoming signals at the end of each hop duration thus offsetting possible large power differential caused by a strong interference source. Non-coherent MFSK detection followed by summing over L hops and maximum likelihood decision constitutes the basic receiver structure following dehopping.

Other FHMA systems have been proposed in the past employing MFSK modulation methods. The work in [6] derives the performance of a FHMA multilevel FSK system with linear combining and hard-limiting. A Rayleigh fading channel is assumed and with interfering signals (other users) also experiencing Rayleigh fading with random phase shifts. Results were obtained for the probability of error (P_e) in terms of the number of active system users using probability bounds on the bit error rate. However, the results in [6] do not lead the true shape of the P_e curves. Theoretical developments by [10] addressed the same issue but considers no noise component nor random phase shifts of the interfering signals. The probability of error results were determined only on a majority logic decision rule and not true linear combining techniques for intended and interfering signals. The result obtained in [10] serves as a worst case analysis providing an approximation to the general shape of the P_e curves.

3.2 System Design

In frequency-hopped multiple-access (FHMA) spread-spectrum systems, each user's signal is hopped in a pseudorandom fashion in accordance with its own unique code which is also known as CDMA. The possibility of one or more users using the frequency hop at the same time exists, however, by pseudo-random hopping, the probability of these users overlapping over and

over again in other hop times will diminish as the processing gain increases. This allows many users to occupy the same spread-spectrum bandwidth W_{ss} without a dramatic number of bits in error within a packet.

The FH/FMSK transmitter employed in this study is depicted in Figure (3.1). The binary information is sent into the serial to parallel converter at rate R_b. The symbol rate out of the converter then will be $R_s = R_b/k = 1/T_s$, where $k = \log m$ is the symbol size. The baseband signal which consists of M frequency tones in the MFSK bandwidth is then mixed with the frequency-hopping tone f_h at the hopping rate $R_h = 1/T_h$. Therefore, the MFSK data bandwidth is $W_d = 2^k/T_h = M(L/k)/T_b$. The outcome of mixing the baseband MFSK signal and the frequency hop signal generates the spread-spectrum waveform with bandwidth W_{ss} as shown in Figure (3.2). To achieve frequency diversity each symbol encompasses L hops. Thus to have an orthogonal tone set, the tone spacing must be at least $1/T_h = k/(LT_b)$.

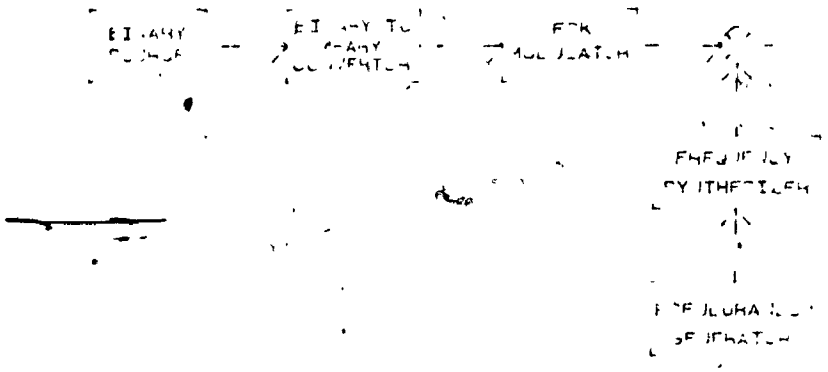

Figure (3.1). FH/MFSK transmitter.

bits in error within a packet.

The FH/FMSK transmitter is depicted in Figure (3.1), the binary information is sent into the serial to parallel converter at rate R_b. The symbol rate out of the converter then will be $R_s = R_b/k = 1/T_s$, where $k = \log m$ is the symbol size. The baseband signal which consistes of M frequency tones in the MFSK bandwidth is then mixed with the frequency-hopping tone f_h at the hopping rate $R_b = 1/T_h$. Therefore, the MFSK data bandwidth is $W_d = 2^k/T_h = M(L/k)/T_b$. The outcome of mixing the baseband MFSK signal and the frequency hop signal constitute the spread-spectrum bandwidth W_{ss} as shown in Figure (3.2). To achelve frequency diversity each symbol encompasses L hops. Thus to have an orthogonal tone set, the tone spacing must be at least $1/T_h = k/(LT_b)$.

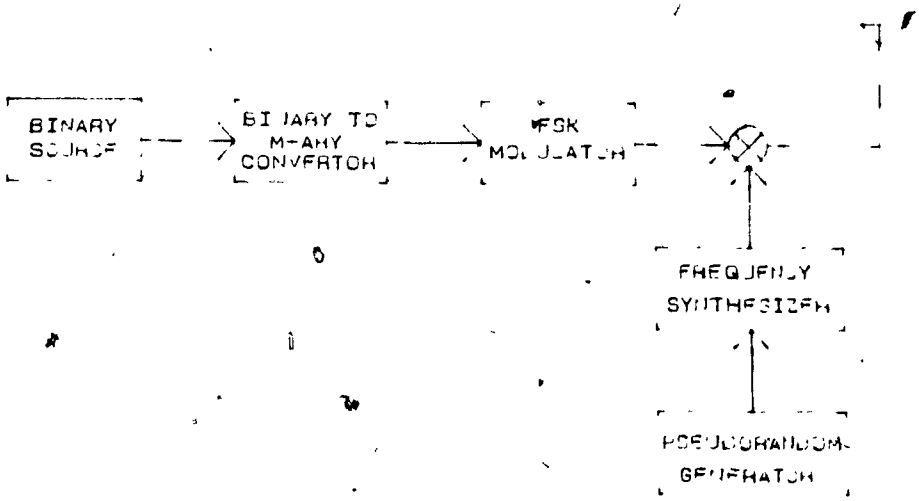

Figure (3.1). FH/MFSK transmitter.

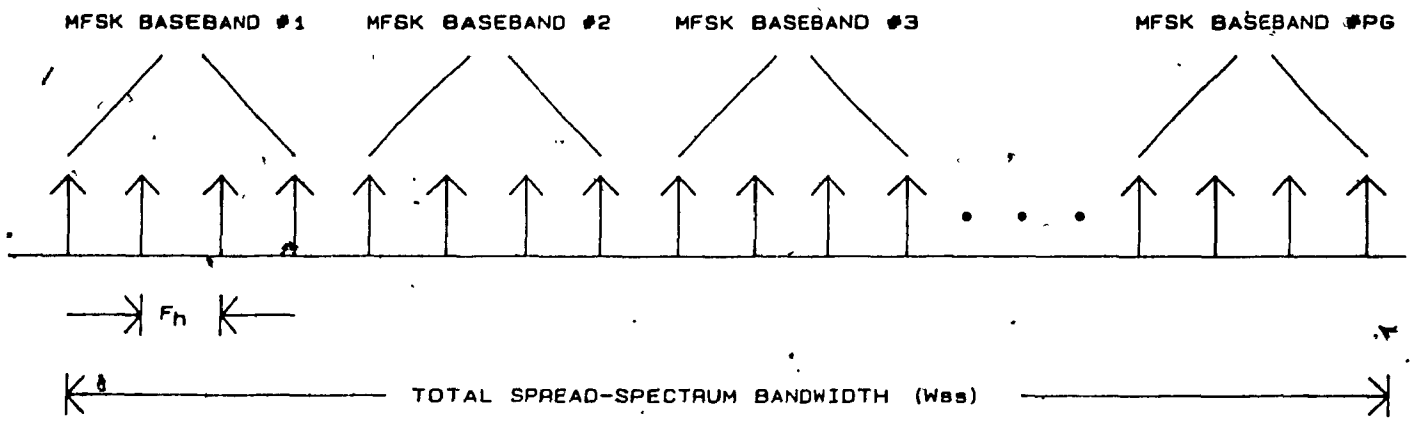

Figure (3.2). MFSK Baseband Allocations in The Spread-Spectrum Bandwidth.

The number of possible frequency tones generated by the FH transmitter (denoted as Q) is determined by the frequency synthesizer and the word size of the random sequence generator. For a word size of n bits, there are 2^n hopping frequencies to be mixed with the MFSK tone giving a total system bandwidth of $W_{ss} = 2^n W_d$ and 2^n non-overlapping MFSK bands. The amount of performance improvement that is achieved through the use of spread-spectrum is defined as the processing gain of the spread-spectrum system, ie. $PG = 2^n / M$.

The received FH/MFSK signal at rate R_h is dehopped at the front end of the receiver, Figure (3.3). We assume the receiver and the transmitted signals from the frequency hopping synthesizer are synchronized. Following dehopping the baseband waveform W_1 is fed into all of the M envelope detectors of the nonlinear combining receiver. The output of the envelope detectors are sampled every hop period T_h and fed through a soft-limiter prior to being accumulated in

the combiner circuit. At the end of L hops, the output of all receiver banks are compared and a choice is made at the decision circuit. The bank containing the largest value at the end of L hops is determined to be the bank containing the intended signal. Naturally, a symbol error is made if after L hops a different bank not containing the intended signal has a value larger than that of the intended receiver bank.

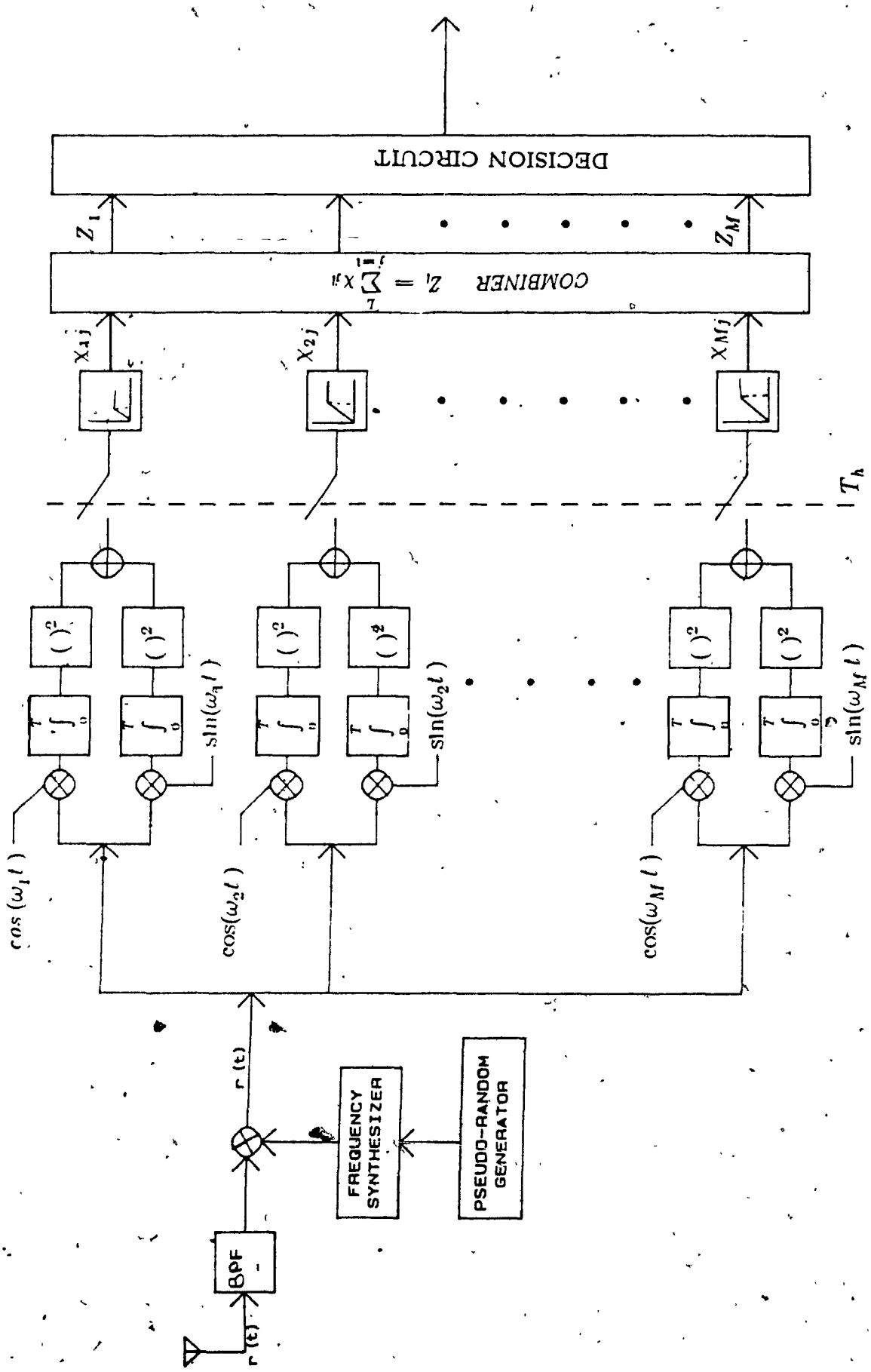

Figure (3.3). FH/MFSK receiver.

3.3 Analysis

Consider a FHMA system with a total of U_t low power users, each having its own independent pseudorandom code. There is, unfortunately, unintentional interference due to other users hopping into the same receiver bank as the intended signal during the same hop time. Two aspects of this scenario emerge, first; the interfering users may hop onto the same tone of the intended signal, but depending on the phase relation of the two or more tones the the signals may add or cancel each other which can either help or destroy the intended signal. If however, the interfering signal hops onto any of the other M-1 receiver banks, the total accumulation of the other banks will increase resulting in a higher probability that a decision error may occur. But just as in the intended receiver bank, if two or more interferers hop onto the same tone at the same hop-time phase cancellation may occur and actually help the receiver make a correct decision. Thus, we assume that the *ith* interfering signals that hop onto the same tone have mutually independent random phase shifts which are Gaussian distributed with zero mean. The Gaussian assumption is justified due to the addition of many uniformly distributed phases of the interfering signals.

For any given received symbol, these possibilities can be represented as a pattern in an L*M time-frequency matrix, so after L hops the state of the receiver's M banks can be described as shown in Figure (3.4).

	HOP#1	...	HOP#J	...	HOP#L
BANK#1	i_{11}	...	i_{j1}	...	i_{L1}
BANK#2	i_{12}	...	i_{j2}	...	i_{L2}
...	...	...	...	...	...
BANK#l	i_{1l}		i_{jl}	...	i_{Ll}
...	...	...	...	...	...
BANK#M	i_{1M}	...	i_{jM}	...	i_{LM}

Figure (3.4) Time-Frequency Matrix.

Each row in the matrix represents the interference status of one of the receiver energy detectors for the baseband MFSK receiver and the columns represent the L hops of the received symbol. The matrix elements i_{jl} denote the number of interferers that are present in bank l and hop j where $l=1,2,3,...M$ and $j=1,2,...L$. If we assume that the intended signal is in bank 1 without loosing generality, then the maximum number of possible low power interferers including the intended signal is U_t. Where as in the other banks the maximum number of possible interferers is U_t-1. The probability that at the intended receiver there are i_{jl} interferers in bank l at a specific hop j is represented by the binomial distribution given by.

$$\binom{U_t}{i_{jl}}(1/Q)^{i_{jl}}(1-1/Q)^{U_t-i_{jl}} \tag{3.1}$$

Where Q is the total number of equiprobable tones in the spread-spectrum

bandwidth W_{ss}. The probability of obtaining a particular pattern of interfence over all banks at a specific hop is the product of the binomial distributions for each bank denoted as $P(i_{j1}, i_{j2}, \ldots, i_{jM})$ is given by.

$$P(i_{j1}, i_{j2}, \ldots, i_{jM}) = \left[\binom{U_t - 1}{i_{j1}}(1/Q)^{i_{j1}}(1-1/Q)^{U_t - i_{j1}}\right]$$

$$\left[\binom{U_t - i_{j1} - 1}{i_{j2}}(1/Q)^{i_{j2}}(1-1/Q)^{U_t - [i_{j1} + i_{j2}]}\right] * \ldots * \left[\binom{U_t - \sum_{k=1}^{t-1} i_{jk} - 1}{i_{jt}}(1/Q)^{i_{jt}}(1-1/Q)^{U_t - [\sum_{k=1}^{t} i_{jk}]}\right]$$

$$\ldots * \left[\binom{U_t - \sum_{k=1}^{M-1} i_{jk} - 1}{i_{jL}}(1/Q)^{i_{jM}}(1-1/Q)^{U_t - [\sum_{k=1}^{M} i_{jk}]}\right] \qquad (3.2)$$

Since the number of users in the system is fixed at U_t, to calculate the product of the binomial distributions the number of interferers in the previous bank is subtracted from the total number of possible interferers left in the system.

In the following analysis we consider the worst case condition, and we do not subtract the interfere that hopped onto the previous bank from the total number of users (potential interferers in the system). Now the probability distributions of interferers hitting each bank in any given hop can be expressed as a multinomial distribution. But in keeping with our computational algorithm we will express the multinomial distribution as a product of M binomial distributions. We can write equation (3.2) as

$$P(i_{j1}, i_{j2}, \ldots, i_{jM}) = \left[\binom{U_t-1}{i_{j1}}(1/Q)^{i_{j1}}(1-1/Q)^{U_t-i_{j1}}\right]$$

$$\left[\binom{U_t-1}{i_{j2}}(1/Q)^{i_{j2}}(1-1/Q)^{U_t-i_{j2}}\right]\ldots\left[\binom{U_t-1}{i_{jl}}(1/Q)^{i_{jl}}(1-1/Q)^{U_t-i_{jl}}\right]$$

$$\ldots\left[\binom{U_t-1}{jM}(1/Q)^{i_{jM}}(1-1/Q)^{U_t-i_{jM}}\right] \qquad (3.3)$$

This can be put into the product form

$$P(i_{j1}, i_{j2}, \ldots, i_{jM}) = \prod_{k=1}^{M}\left[\binom{U_t-1}{i_{jk}}(1/Q)^{i_{jk}}(1-1/Q)^{U_t-i_{jk}}\right] \qquad (3.4)$$

The strong interfering signals (users near the intended base station in a mobile network) follow a format similar to the one used for the low-power users, both must hop in the same MFSK band as the intended signal to be considered in the analysis. The same time-frequency matrix described for the weak users is also applicable here. The total number of strong users in the system is fixed at U_{st} and is less then the number of weak users. Thus the probability that k_{jl} strong users will hop on bank l at hop j is again binomial distributed and denoted as $P(k_{jl})$ is given by

$$P(k_{jl}) = \binom{U_{st}}{k_{jl}}(1/Q)^{k_{jl}}(1-1/Q)^{U_{st}-k_{jl}} \qquad (3.5)$$

As before, for the j th hop the product of the binomial probabilities over the banks of the receiver becomes.

$$P(k_{j1},k_{j2},\cdots,k_{jM}) = \prod_{l=1}^{M}\left[\binom{U_{st}}{k_{jl}}(1/Q)^{k_{jl}}(1-1/Q)^{U_{st}-k_{jl}}\right] \tag{3.6}$$

The probability of correct symbol detection P_c is determined by assigning a certain outcome for the time - frequency matrix with some pattern of strong and weak users. Then, averaging over all possible outcomes over all L hops and all M receiver banks. This involves two step averaging (with respect to combinations of strong and weak users). We remove first the condition on the status of strong users in the system, thus obtaining

$$P_c = \sum_{k_{11}}^{U_{st}} \cdots \sum_{k_{jl}}^{U_{st}} \cdots \sum_{k_{LM}}^{U_{st}} \cdots (P_c/k_{11},\ldots, k_{jl},\ldots, k_{LM})$$

$$* P(k_{11},\cdots,k_{1M}) *\ldots * P(k_{L1},\cdots,k_{LM}) \tag{3.7}$$

where $P(k_{11},\ldots,k_{1M}) *\ldots * P(k_{L1},\ldots,k_{LM})$ are the product of binomial distributions corresponding to each hop (eg. j=1,2,..,L).

and $P(c/k_{11},\cdots,k_{jl},k_{LM})$ is the conditional correct symbol detection probability after summing the results of L hops and comparing M receiver banks. This is in turn is calculated by averaging over all weak users interference contributions (within the L*M matrix previously shown), ie.

$$P(P_c/k_{11},\cdots k_{jl},\cdots,k_{LM}) = \sum_{i_{11}}^{U_t-1} \cdots \sum_{i_{jl}}^{U_t-1} \cdots \sum_{i_{LM}}^{U_t-1} P(P_c/k_{11},\cdots,k_{LM},i_{11},\cdots,i_{LM})$$

$$P(i_{11},\cdots,i_{1M}) *\ldots * P(i_{L1},\cdots,i_{LM}) \tag{3.8}$$

Combining (3.7) and (3.8) we get

$$P_c = \sum_{k_{11}}^{U_{st}} \cdots \sum_{k_{jl}}^{U_{st}} \cdots \sum_{k_{LM}}^{U_{st}} \sum_{i_{11}}^{U_{t-1}} \cdots \sum_{i_{jl}}^{U_{t-1}} \cdots \sum_{i_{LM}}^{U_{t-1}}$$

$$Pr(c/k_{11}, \ldots, k_{LM}, i_{11}, \ldots, i_{LM}) P(k_{11}, \ldots, k_{1M}) * \ldots * P(k_{L1}, \ldots, k_{LM}) * \ldots$$

$$\ldots * P(i_{11}, \ldots, i_{1M}) * \ldots * P(i_{L1}, \ldots, i_{LM}) \qquad (3.9)$$

For moderate and high processing gains it has been typical to assume a ceiling on the number of interferers per hop at any given time (3 in our case). This is supported by the fact that presence of one interferer in another receiver bank at a certain hop means it will not be in the other (M-1) banks. Also, presence of one interferer in one hop means that the probability it will also hit the next hop is minimal.

Limiting the interference this way reduces the huge enumeration of (3.9) and makes it amenable to computation. Even after these limiting few steps, certain programming techniques to remove many of the combinational redundancies in the Time-Frequency matrix (Appendix A) had to be employed to make the computations feasible using a VAX 780.

To find the conditional probability of symbol detection after accumulating the envelopes of the symbol's L hops, namely the value of $P(c/k_{11}, \cdots, k_{LM}, i_{11}, \cdots, i_{LM})$ for a fixed pattern of all i_{jl} and k_{jl} a closer look at the received signal is in order.

The received signal from the desired transmitter entering the noncoherent MFSK receiver in the absence of other user interference, and assuming without loosing generality that the symbol corresponding to the first MFSK bank was transmitted is given by

$$r_l(j) = \sqrt{2}A\cos\left[(\omega_{hj1}+\omega_{j1})t+\Theta_{j1}\right] \quad 0\le t<T_h \tag{3.10}$$

where ω_{hj1} is the hopping frequency of the intended user during hop i and ω_{j1} is the MFSK frequency tone of the intended user during the intended symbol.

The rms power is then A^2 and the received signal energy for a single hop is $E_h = A^2 T_h$ joules. The intended signal is considered to have the same power level as the low power interferers. The phase angle Θ_{jl} of all received signals are uniformly distributed between 0 and 2Π.

The interfering waveforms for strong and weak users entering the receiver's filter bank with independent random phase shifts Θ_{jl} during the *jth* hop and for the *lth* receiver bank can be described by,

$$I_j(t) = (\sqrt{2}A)^{\gamma_w}(\sqrt{2}B)^{\gamma_s}\cos[(\omega_{hjl}+\omega_{jl})t+\Theta_{jl}] \tag{3.11}$$

where $\gamma_w = 1$ and $\gamma_s = 0$ for weak interferers

and $\gamma_w = 0$ and $\gamma_s = 1$ for strong interferers.

As before A^2 is the rms power for weak signals and B^2 is the power level for strong signals.

Following dehopping of the *jth* hop the 1*st* energy detector output containing the intended received signal is given by,

$$R_{j1} = X_{j1}^2 + Y_{j1}^2 \tag{3.12a}$$

$$X_{j1}^2 = \left[1 + \left\{\sum_{I=1}^{i_{j1}+1} A_{j1I}^{\gamma_w} + \sum_{I=1}^{k_{j1}} B_{j1I}^{\gamma_s}\right\} + n_c\right]^2 \tag{3.12b}$$

$$Y_{j1}^2 = \left[\left\{\sum_{Q=1}^{i_{j1}+1} A_{j1Q}^{\gamma_w} + \sum_{Q=1}^{k_{j1}} B_{j1Q}^{\gamma_s}\right\} + n_s\right]^2 \tag{3.12c}$$

Where n_c and n_s are the inphase and quadrature noise components respectively with variance $N_0/2E_c$. A_{j1I} and A_{j1Q} are the random variables expressing the inphase and quadrature values of the weak interfering signals in the receiver's first filter bank and B_{j1I} and B_{j1Q} are the random variables expressing the inphase and quadrature values of the strong interferering signals in the first receiver bank during the j*th* hop.

For the purpose of analysis, we assume that the i_{jl} interferers are statistically independent Gaussian random variables with zero mean. The transformation of the Gaussian random variables that takes place at the energy detector leads to the noncentralized chi-squared distributed random variable with two degrees of freedom and noncentrality parameter $s^2 = m_1^2 + m_2^2$. Where m_1 and m_2 are the means of the X_{jl} and Y_{jl} random variables. If variable $r = \sqrt{X_{j1}^2 + Y_{j1}^2}$ is used, then the PDF of the independent random variables of R_{jl} can be expressed as a PDF of a Ricean-distributed random variable.

$$P_{R_{j1}}(r) = \frac{r}{\sigma^2} e^{-(r^2 + s^2)/2\sigma^2} I_0\left[\frac{rs}{\sigma^2}\right] \quad x \geq 0 \tag{3.13}$$

Where $r = \sqrt{x^2 + y^2}$

and the variance is $\sigma^2 = (\sigma_n^2 + \gamma_w(i_{jl})A + \gamma_s(k_{jl})B)^2$

I_0 is the 0*th*-order Bessel function of the first kind which can be expressed as an infinite series

$$I_0(x) = \sum_{k=0}^{\infty} \frac{(x/2)^{2k}}{k!\Gamma(k+1)} \tag{3.14}$$

The remaining M-1 energy detectors not containing the intended signal form the output random variable at the end of the jth hop.

$$R_{jl} = X_{jl}^2 + Y_{jl}^2 \qquad 2 \leq l \leq M \tag{3.15a}$$

$$R_{jl} = \left\{ \left\{ \sum_{I=1}^{i_j} (A_{jlI})^{\gamma_w} + \sum_{I=1}^{k_j} (B_{jlI})^{\gamma_s} \right\} + n_c \right\}^2 \tag{3.15b}$$

$$+ \left\{ \left\{ \sum_{Q=1}^{i_j} (A_{jlQ})^{\gamma_w} + \sum_{Q=1}^{k_j} (B_{jlQ})^{\gamma_s} \right\} + n_s \right\}^2 \tag{3.15c}$$

with means X_{jl} and $Y_{jl} = 0$

and variance $\sigma^2 = (\sigma_n^2 + \gamma_w(i_{jl})A + \gamma_s(k_{jl})B)^2$

In this case the PDF can be described as the PDF of a Rayleigh distributed random variable, where $r = \sqrt{X_{jl}^2 + Y_{jl}^2}$ as described below.

$$P_{R_{jl}}(r) = \frac{r}{\sigma^2} e^{-(r^2/2\sigma^2)} \tag{3.16}$$

Equations (3.13) and (3.16) are the probability density functions of the output of the energy detector at each hop in presence of many possible interfering signals.

3.4 Soft Limiter Transformation

To reduce the effect of the i_{jl} users hopping onto the intended MFSK receiver banks during L hops, the sampled output of the energy detector is weighted at the end of each hop by a soft-limiter prior to being accumulated in the combiner circuit. The soft-limiter threshold is set at the intended signal received amplitude and thus will clip any powerful interference and bring it to the same level as that of the intended signal.

The PDF's representing the signal amplitude out of the energy detectors, $P_{r_{j1}}$ and $P_{r_{jl}}$, undergo a transformation by the soft-limiter weighting. The limiter characteristics is shown in Figure (3.5).

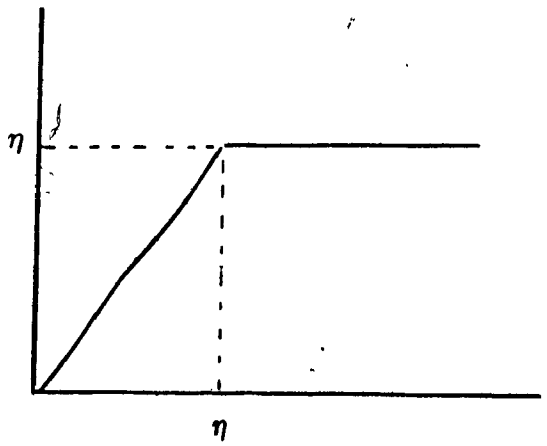

Figure (3.5). Soft limiter Threshold curve.

The limiter passes all input amplitudes less then η with unity gain and limits the values greater then η to unity (normalized with respect to the intended signal envelope). Thus, any larger contribution from other users either due to multiple hits or large signal interference will be nulled at the limiter and effectively decreasing the probability of bit error.

Following the envelope detection and soft-limiting, the PDF of the outcome corresponding to the first bank (containing the signal) for each hop is given by,

$$\chi_{j1}(r) = \frac{r}{\sigma^2} e^{-(r^2+s^2)/2\sigma^2} I_0\left(\frac{rs}{\sigma^2}\right) + \delta(\eta) \int_{\eta}^{\infty} \frac{r}{\sigma^2} e^{-(r^2+s^2)/2\sigma^2} I_0\left(\frac{rs}{\sigma^2}\right) dr \quad (3.17)$$

where η is the limiter threshold (Figure (3.5)) σ, s, x, y carry the same meaning previously defined and $\delta(\eta)$ is the unit impulse function.

The remaining M-1 filter banks obtain a PDF at each hop following envelope detection and soft-limiting and can be expressed as

$$\chi_{jl}(r) = \frac{r}{\sigma^2} e^{-(r^2)/2\sigma^2} + \delta(\eta) \int_{\eta}^{\infty} \frac{r}{\sigma^2} e^{-(r^2)/2\sigma^2} dr \qquad 2 \leq l \leq M \qquad (3.18)$$

An example of the above $\chi_{jl}(r)$ PDF is plotted in Figure (3.6), the impulse has a height equal to that of the probability that the random variable exceeds the threshold setting of the limiter.

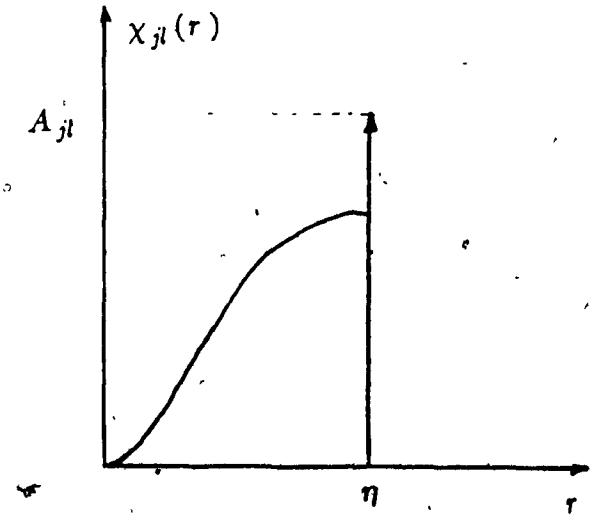

Figure (3.6). PDF of Output of Soft-Limiter.

3.5 The Combiner Circuit

The *lth* combiner circuit adds the soft limited contributions from the L hops of the *lth* receiver bank generating the new random variable Z_l and is described by

$$Z_l = \sum_{j=1}^{L} \chi_{jl} \qquad (3.19)$$

The summation of L random variables Z_l can be considered as an L-fold convolution of the PDF's and therefore creating a random variable. Performing the L-fold convolution to obtain the PDF of Z_l is very time consuming and difficult when the PDF's to be convolved contain impulse function contributions. An alternative approach for determining the PDF of the sum of random variables is the well known characteristic functions, ie.

$$\Psi_{\chi_{jl}}(\omega) = \int_{-\infty}^{\infty} P_{\chi_{jl}}(x) e^{j\omega x} dx \tag{3.20}$$

where χ_{jl} is the limiter output random variable corresponding to the *jth* hop and *lth* filter bank and assuming independence of the conditions of interference in the L hops.

Since the above random variables are statistically independent, we can state that the L-fold convolution can be replaced by

$$\Psi_{Z_l}(\omega) = \prod_{j=1}^{L} \Psi_{\chi_{jl}}(x) \tag{3.21}$$

Unfortunately, there is no closed form for the characteristic functions we are considering here. Alternatively the Discrete Fourier Transform (DFT) can be employed to replace the characteristic functions of (3.21). This will allow for a simple calculation of the L-fold PDF. As long as the sample size is large, there will be little inaccuracies introduced into the calculation.

$$\Psi_{\chi_{jl}}(\omega) = \sum_{n=-\infty}^{\infty} P_{\chi_{jln}} e^{j\omega n} \tag{3.22}$$

In the analysis to follow we use both convolution and the DFT algorithm to derive the probability density function of Z_l. It was found that by operating on two χ_{jl} (soft-limited output variables) PDF's at a time for a given bank instead of convolving all L hops, the analysis is facilitated. Since convolution is a linear function, any order of which L functions are convolved will always lead to the same result. So taking the random variables obtained in the first two hops we have.

$$P_{Z_{l12}}(x) = P_{\chi_{1l}} * P_{\chi_{2l}} \tag{3.23}$$

Noting that each $P_{\chi_{jl}}$ has a delta operator and must be treated separately, we can then write

$$P_{Z_{l_{12}}}(x) = \left[P_{\chi_{1l}}(x) + A_{1l}\delta(x - \eta)\right] * \left[P_{\chi_{2l}}(x) + A_{2l}\delta(x - \eta)\right] \tag{3.24}$$

where A_{1l} and A_{2l} are the heights of the delta function δ given by

$$A_{jl} = \int_{\eta}^{\infty} \chi_{jl}(x)\,dx \tag{3.25}$$

Expanding Equation (3.24) we get

$$P_{Z_{l_{12}}}(x) = P_{\chi_{1l}}(Y_1) * P_{\chi_{2l}}(Y_2) + A_{1l}P_{\chi_{2l}}\delta(x - \eta)$$

$$+ A_{2l}P_{\chi_{1l}}(x - \eta) + A_{1l}A_{2l}\delta(x - 2\eta) \tag{3.26}$$

The first term of (3.26), namely $P_{\chi_{1l}} * P_{\chi_{2l}}$, is determined by taking the inverse Fourier Transform of the product of the involved characteristic func-

tions. Using equations (3.23) and (3.25) the convolution denoted $P_{\chi_{12l}}$ becomes.

$$P_{\chi_{12l}} = P_{\chi_{jl}}(Y_1) \; * \; P_{\chi_{(j+1)l}}(Y_2) = F^{-1}\left\{ \left(\Psi_{\chi_{jl}}(\omega) \right)\left(\Psi_{\chi_{(j+1)l}}(\omega) \right) \right\}$$

$$0 \leq \omega \leq N-1 \qquad (3.27)$$

where N is the point size of the DFT.

The probability distribution of the accumulated signal amplitude after two hops $P_{Z_{12}}$ can now be written

$$P_{Z_{12l}}(x) = P_{\chi_{12l}}(x) + \left[A_{1l} P_{\chi_{2l}} + A_{2l} P_{\chi_{1l}} \right] \delta(x-\eta) + A_{1l} A_{2l} \delta(x-2\eta) \qquad (3.28)$$

If L = 2 then the PDF for each bank at the combiner is known. When there more then two hops (ie. 4 hops/symbol), the PDF can still be determined fairly easily by repeated application of the above procedure for the last two hops. Now we are left with the last two PDF's to convolve in a single receiver bank. The final convolution between $P_{Z_{jl_{12}}}$ and $P_{Z_{jl_{34}}}$ is denoted as P_{Z_l}. Thus we have

$$P_{Z_l} = P_{\chi_{jl_{12}}}(Y_3) * P_{\chi_{jl_{34}}}(Y_4) \qquad (3.29)$$

The convolution denoted as $P_{\chi_{12l}} * P_{\chi_{34l}}$ is done in the same fashion as equation (3.27), but now with double the sample size. Expanding $P_{Z_{jl_{12}}}$ and $P_{Z_{jl_{34}}}$ and using equation (3.28) we get.

$$P_{Z_l}(x) = P_{\chi_{jl_{12}}}(x) * P_{\chi_{jl_{34}}}(x) + P_{\chi_{jl_{12}}} A_{3l} A_{4l} \delta(x-2\eta) +$$

$$P_{\chi_{jl_{34}}}(x) Al_1 Al_2 \delta(x-2\eta) + A_{1l} A_{2l} A_{3l} A_{4l} \delta(x-4\eta) \qquad (3.30)$$

and now $P_{\chi 12l}(Y_3) * P_{\chi_{34l}}(Y_4)$ is determined from

$$P_{\chi_{1234l}} = F^{-1}\left\{\Psi_{\chi_{12}}(\omega)\Psi_{\chi_{34}}(\omega)\right\} \qquad 0 \leq \omega \leq 2N-1 \qquad (3.31)$$

Each bank of the M bank receiver banks is operated in the same fashion. The output of the M combiners is fed into the decision circuit where the bank that has the largest value after L hops is chosen.

The probability of error can be found by first deriving the probability that the receiver makes a correct decision. This is the probability that Z_1 exceeds all other decision variables $Z_2, Z_3, \cdots Z_M$ and may be expressed as

$$P_c = \int_{-\infty}^{\infty} P_r(Z_2<Z_1, Z_3<Z_1, \cdots, Z_M<Z_1/Z_1)\, P_r(Z_1)dZ_1 \qquad (3.32)$$

where $P_r(Z_2<Z_1, Z_3<Z_1, \cdots, Z_M<Z_1/Z_1)$ denotes the joint probability that $Z_2, Z_3, \cdots, Z_M$ are all less then Z_1 conditioned on Z_1. Since the Z_l are statistically independent, this joint probability factors into a product of M-1 marginal probabilities of the form

$$Pr(Z_m<Z_1/Z_1) = \int_{-\infty}^{Z_1} P_{Z_m}(Z_m)dZ_m \qquad m = 2,3,\ldots.M \qquad (3.33)$$

Which can be expressed as

$$P_c = \int_0^{\infty} \left\{\int_0^{Z_1} P_{Z_2}(Z_2)dZ_2\right\}\left\{\int_0^{Z_1} P_{Z_3}(Z_3)dZ_3\right\}\ldots.\left\{\int_0^{Z_1} P_{Z_M}(Z_M)dZ_M\right\}P_{Z_1}dZ_1 \qquad (3.34)$$

Now that the probability of correct symbol decision is known the probability of symbol error is $P_m = 1 - P_c$

The probability of bit error can be determined for equiprobable orthogonal signals, we state that all symbol errors are equiprobable and occur with probability

$$\frac{P_M}{M-1} = \frac{P_M}{2^k - 1} \tag{3.35}$$

where $k = \log_2 M$ is the number of bits per symbol

The probability of bit error is then

$$P_b = \frac{2^{k-1}}{2^k - 1} P_M \tag{3.36}$$

Thus from (3.9) and (3.34) the probability of bit error for the noncoherent FH/FMSK system with strong and weak users becomes

$$P_s = \sum_{k_{11}}^{U_{s1}} \cdots \sum_{K_{jl}}^{U_{sl}} \cdots \sum_{K_{LM}}^{U_{sl}} \cdots \sum_{i_{11}}^{U_t} \cdots \sum_{i_{jl}}^{U_t} \cdots \sum_{i_{LM}}^{U_t} P_b$$

$$P(k_{11}, \ldots, k_{L1}), \ldots, P(k_{1M}, \ldots, k_{LM})$$

$$, \ldots, P(i_{11}, \ldots, i_{L1}), \ldots, (i_{1M}, \ldots, i_{LM}) \tag{3.37}$$

For each set of system parameters, such as the number of receiver banks, hops/symbol, the total number of tones in W_{ss}, and number of active users in the network, equation (3.37) must be evaluated for all possible combinations of weak and strong interferers. For each combination of weak and strong interferes all the characteristic functions and DFT's in (3.22) to (3.35) are evaluated and finally the P_b is obtained from (3.37).

3.6 Performance of The FH/MFSK Systems Considered

In this section, we compare the responses of many SS systems with parameters of 2,4,8-FSK and 2,4 Hops/Symbol. The receiver SNR was set at 10 dB for the weak users and 20 dB for strong users. We first observe the performance of different FHMA systems for 2 hop/symbol and 4 hop/symbol diversity as illustrated in Figure (3.7). The graphs depict different M-ary FSK systems all with the same processing gain. However, the resulting spread-spectrum bandwidth W_{ss} corresponding to the curves figures are not all the same. Rather we only compare the performance of these systems having a processing gain of P.G.=128.

It is easily seen that the best performance is obtained for the system having parameters of L=4 and M=8 with 1024 tones in the SS bandwidth which is quite larger than the other SS systems. However, this implies using a large W_{ss}, if we assume that the information rates for all systems are the same.

The case of M=2 and L=4 deserves special attention. Contrary to the expectation that increasing the number of hops leads to performance improvements , this system behaves quite differently especially for large number of users. The system performance in this case is similar to the 2 bank 2 hop/symbol system. As seen from Table (3.1), the M=2 L=4 system needs only 256 tones within the SS bandwidth to achieve a processing gain of 128 which does not leave much margin for improvement gained from frequency diversity (compared to the remaining curves). Generally, the best P_e performance of the various SS designs results from increasing the number of hops per symbol.

When the various combinations of the spread-spectrum parameters are compared on a fair basis the outcome is quite different as shown in Figure (3.8). To compare the cases on a fair basis, we set the spread-spectrum bandwidth W_{ss} to 8.192 MHz and confine the data rate to 8 Kb/s. Thus, when the values of L and

M are changed corresponding to each of the cases the processing-gain and the total number of tones will change accordingly.

As an example, consider a BFSK receiver with 4 hops/symbol, the number of bits in a symbol is one, thus the number of bits/hop =0.25. The data rate is fixed for all cases at $R_b = 8Kb/s$. It follows that the hopping rate must be such that $R_b = (.25\ Bits/hop) * R_h = 8Kb/s$, and the processing gain is determined by $W_{ss}/W_d = W_{ss}/M*R_h$ which depends on the system parameters L and M in an evident fashion.

Fixing W_{ss} to 8.192 MHz we see that the best system, Figure (3.8), is the 8 bank 4 hop/symbol (8B4H). It is expected that a 4 hop/symbol diversity will perform better than the 2 hop/symbol diversity systems. This of course, is what is obtained in the results for the 4 and 8 bank 4 hop/symbol receivers. However, the 2B4H receiver performance degrades significantly for large number of users in the system, even worst than the 2 hop/symbol receivers. This occurs since the number of tones in the 2B4H system is much less than the 2 hop/symbol systems as seen in Table (3.2). Even though the processing gain for the 8B4H system is the least out of all the systems compared, the number of tones is the largest for all the 4 hop/symbol systems. Thus, frequency diversity and a large tone set provides for much better performance curves.

Changing the spread-spectrum bandwidth to 4.096 MHz, a fair basis analysis can be performed on a system with less bandwidth. Now as seen from Table (3.3) the processing gains of the spread-spectrum systems are one half of the processing gains used in Figure (3.9) for the 8.192 MHz bandwidth. The overall shape of the curves in the two figures are similar, but the spacing between curves in the 4.096 MHz bandwidth case are not as great. Again the 8B4H system provides better performance characteristics. We can say that as the spread-spectrum bandwidth

increases, the choice of a better system design gives much better results. When very large spread-spectrum bandwidths are involved, the selection of good parameters are even more critical.

In Figure (3.10) spread-spectrum systems with the same number of receiver banks are compared. Curves 1 and 2 show the difference for 2 bank systems using 2 and 4 hops/symbol and curves 3 and 4 show the difference for 4 bank receiver systems using 2 and 4 hops/symbol. Examining the 2 bank receiver designs, we see that the P_e performance improves as the number of hops/symbol increases. As expected, frequency diversity augments the system performance. Similarly, the 4 bank receiver design performs much better as the number of hops/symbol increase. However, in this case, the amount of increase in performance is better than the 2 bank receiver.

So far we have discussed the P_e performances for different receiver designs. Now, we shall examine a specific design and compare the P_e curves as the number of hopping tones in the spread-spectrum bandwidth vary. The performance curves for the 2B2H receiver and various number of hopping tones are illustrated in Figure (3.11). As expected, by increasing the number of tones the system improves. However, it is seen that the best improvement occurs when the number of hopping tones is low. The same results were obtained in Figure (3.12) for a 4B4H system. In this case the difference between the curves as the number of tones increase is not as great.

In all of the above comparisons, the performance curves were obtained with a Ricean system model for the bank containing the intended signal and a Rayleigh distribution model for all other M-1 receiver banks. In the absence of line of sight communications, all receiver banks will have the Rayleigh distribution in each of the hops. Figure (3.13) shows a sample of the obtained results for Ray-

leigh fading and line of sight Ricean models. For comparison purposes, curves for parameter settings of L=2,4 and M=8 with a total of 1024 tones in the spread spectrum bandwidth are employed.

The small difference in the performance is due to the diversity effect of like user interference which outweighs the fading of the signal especially under soft-limiting.

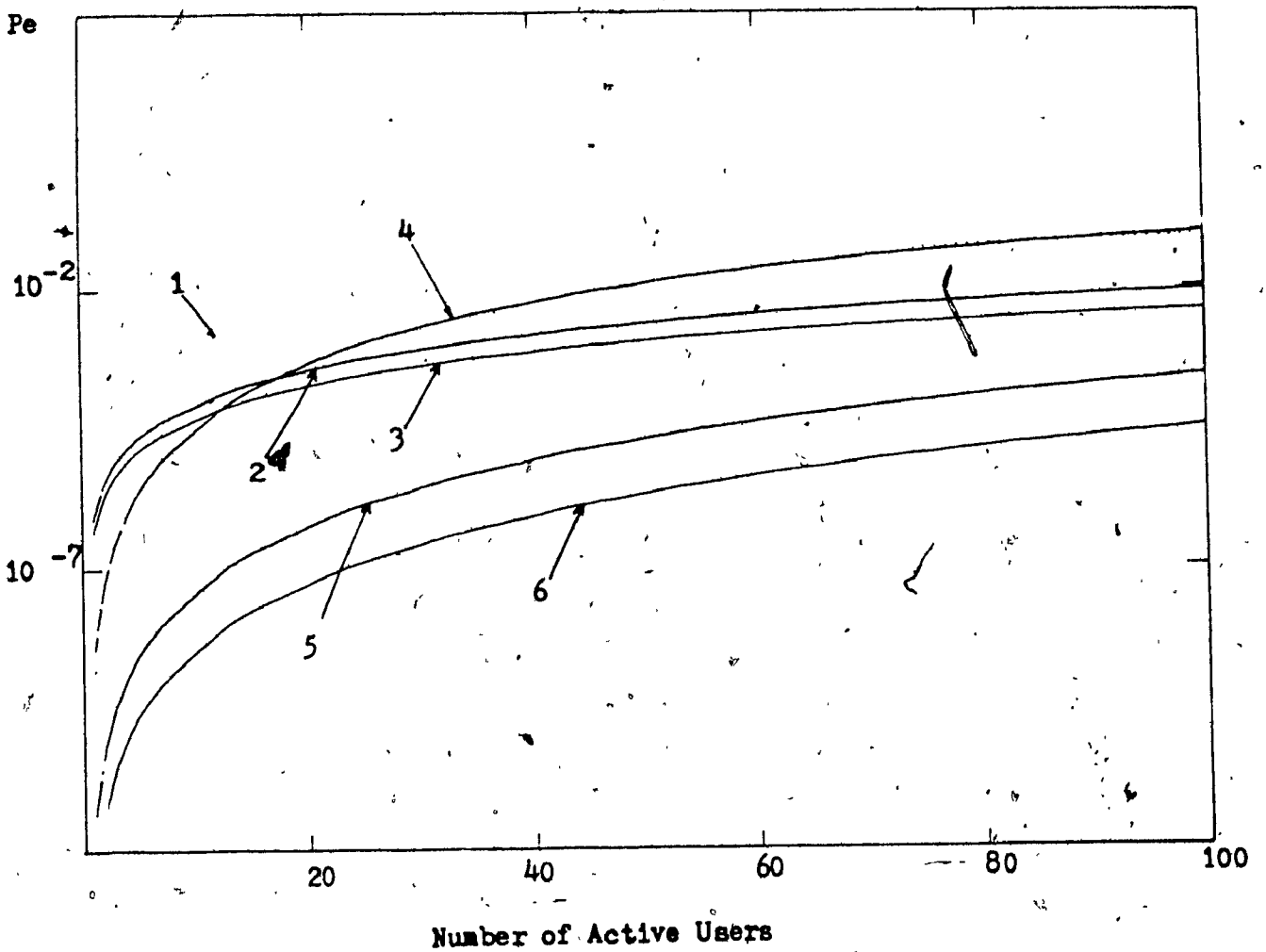

Figure (3.7) Performance of FHMA Spread-Spectrum Systems With Equal Processing Gains.

Table (3.1) System Parameters For Figure (3.7).

Graph #	Bank #	Hops/Symbol	# of Tones	Processing Gain
1	2	2	256	128
2	4	2	512	128
3	8	2	1024	128
4	2	4	256	128
5	4	4	512	128
6	8	4	1024	128

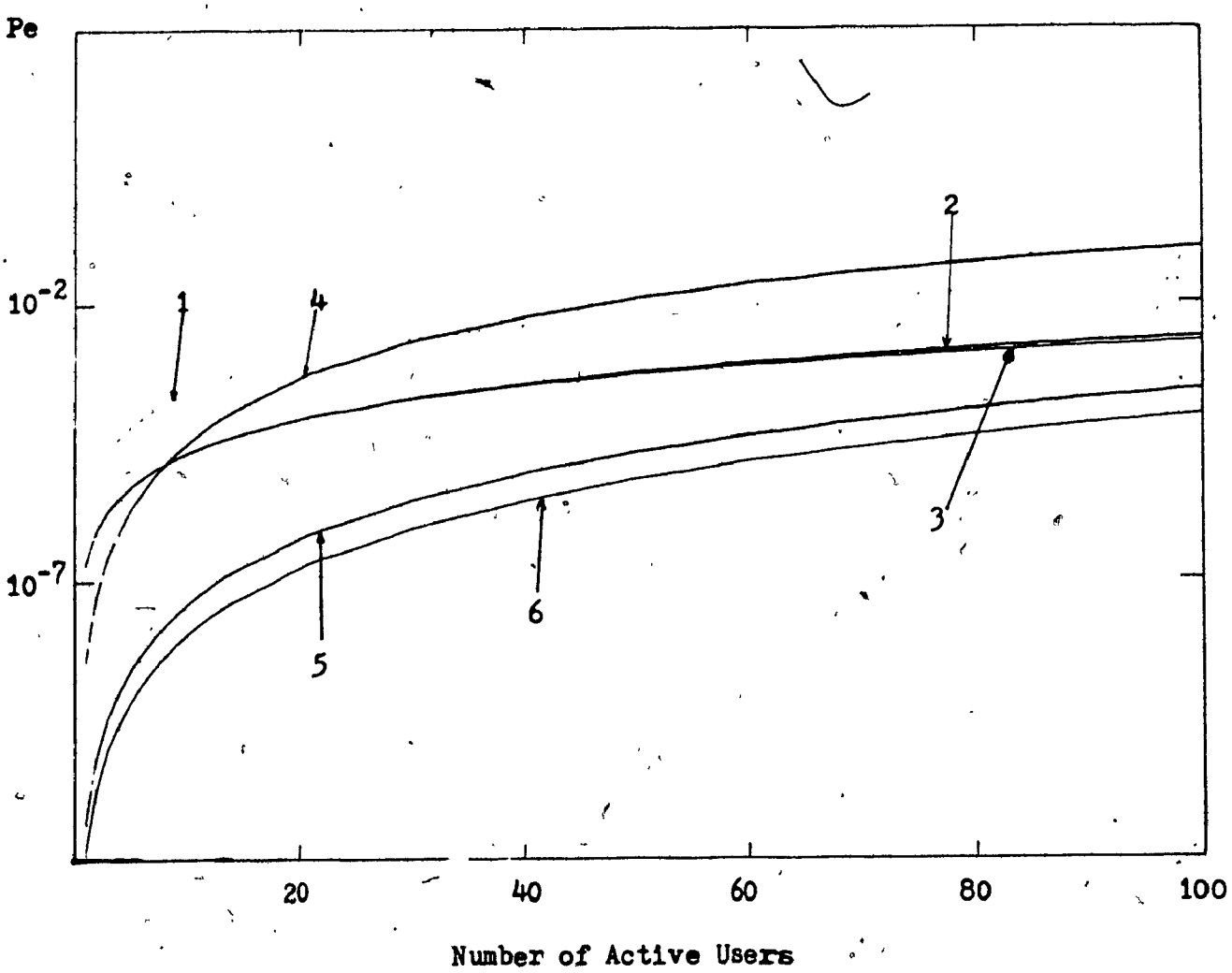

Figure (3.8) Comparisons of Spread-Spectrum Systems on Fair Basis With same $W_{ss} = 8.124\ Mhz$ and $R_d = 8\ Kb/s$.

Table (3.2) Systme Parameters For Figure (3.8).

Graph #	Bank #	Hops/Symbol	# of Tones	Processing Gain
1	2	2	512	256
2	4	2	1024	256
3	8	2	1536	192
4	2	4	256	128
5	4	4	512	128
6	8	4	768	96

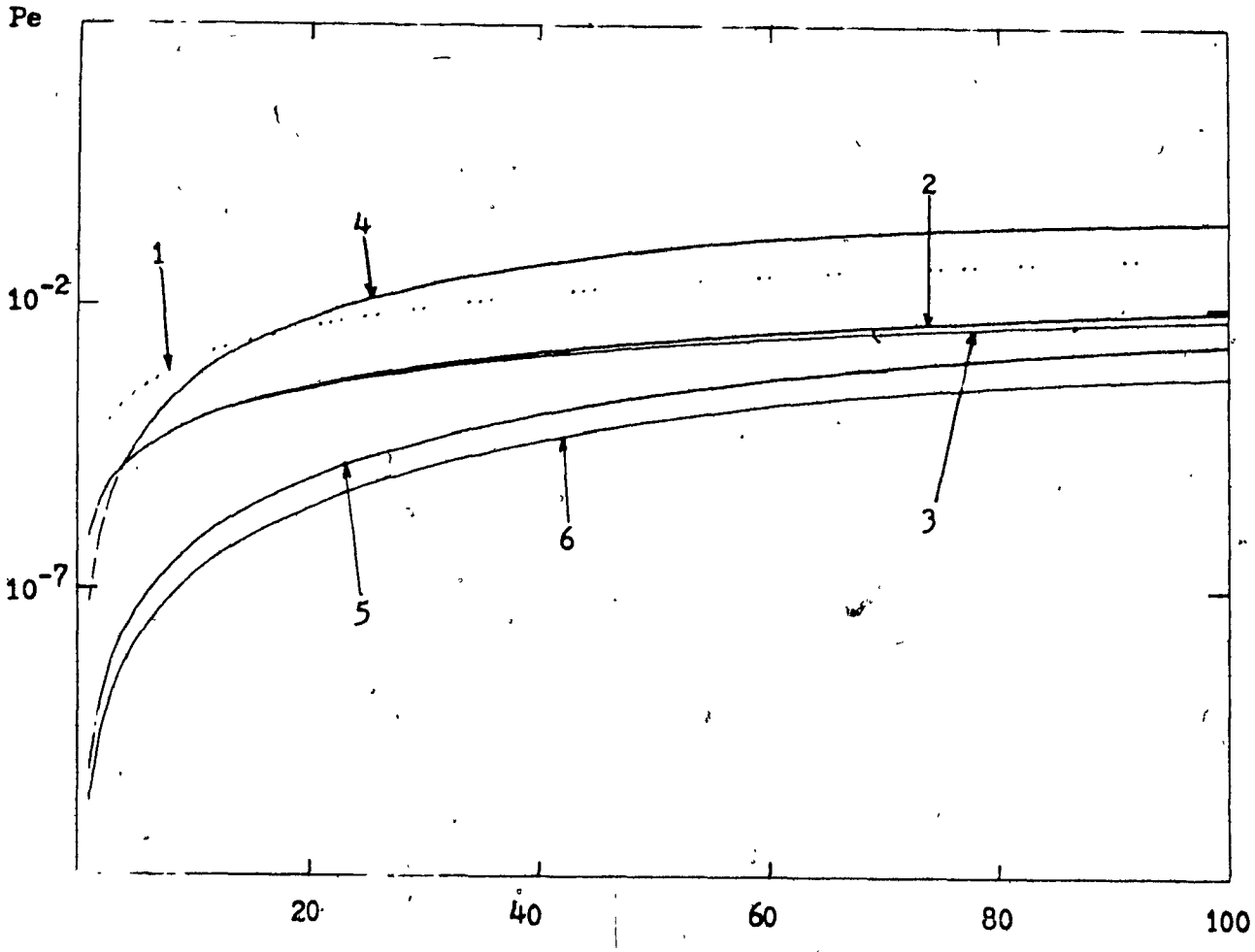

Figure (3.9) Comparison of Spread-Spectrum Systems on Fair Basis With Same $W_{ss} = 4.096\ Mhz$ and $R_d = 8\ Kb/s$.

Table (3.3) Parameters for Figure (3.9).

Graph #	Bank #	Hops/Symbol	# of Tones	Processing Gain
1	2	2	256	128
2	4	2	512	128
3	8	2	768	96
4	2	4	128	64
5	4	4	256	64
6	8	4	384	48

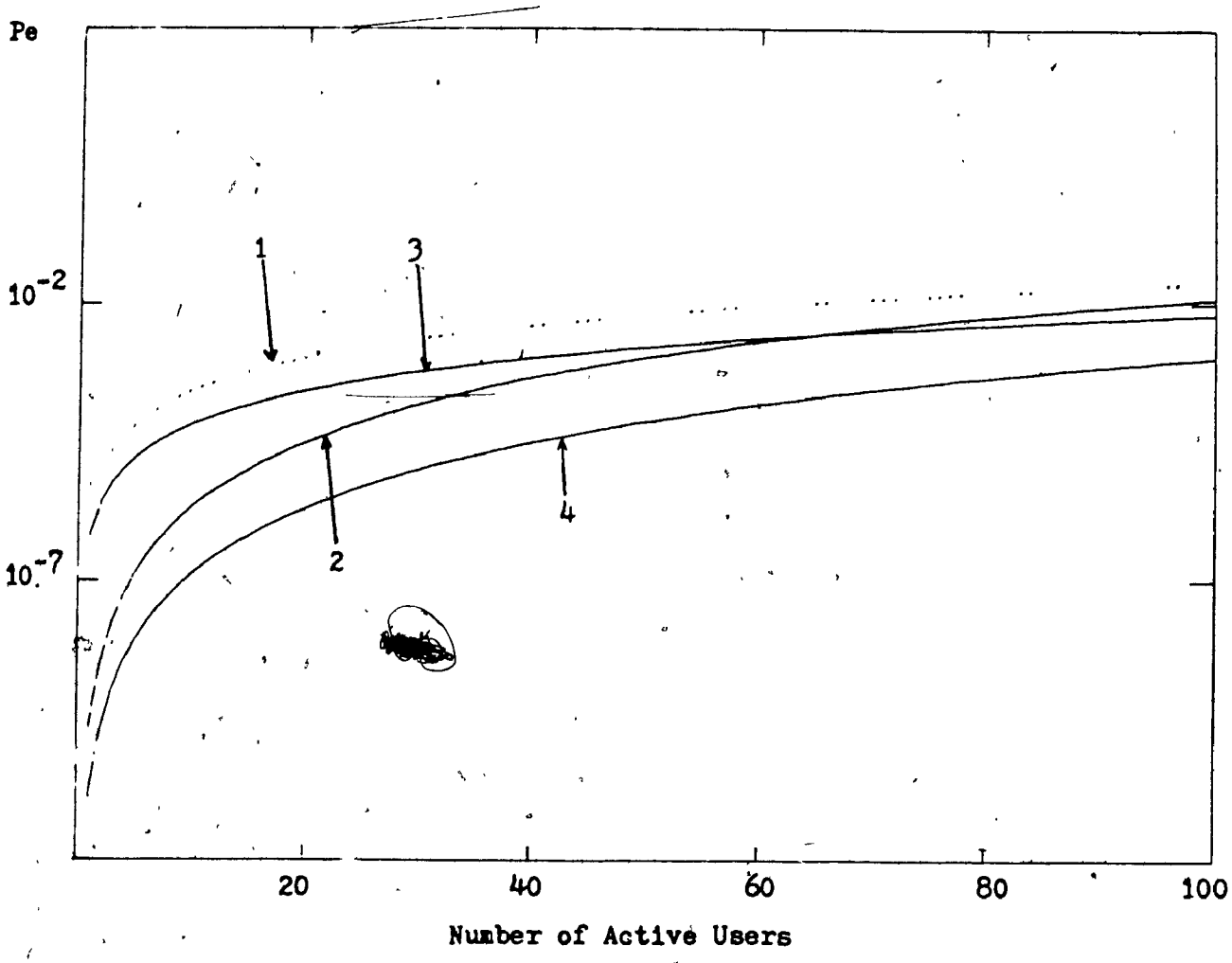

Figure (3.10) Spread-Spectrum Systems With The Same Number of Banks.

Table (3.4) Parameters for Systems Figure (3.10).

Graph #	Bank #	Hops/Symbol	# of Tones	Processing Gain
1	2	2	512	256
2	2	4	512	128
3	4	2	1024	256
4	4	4	1024	256

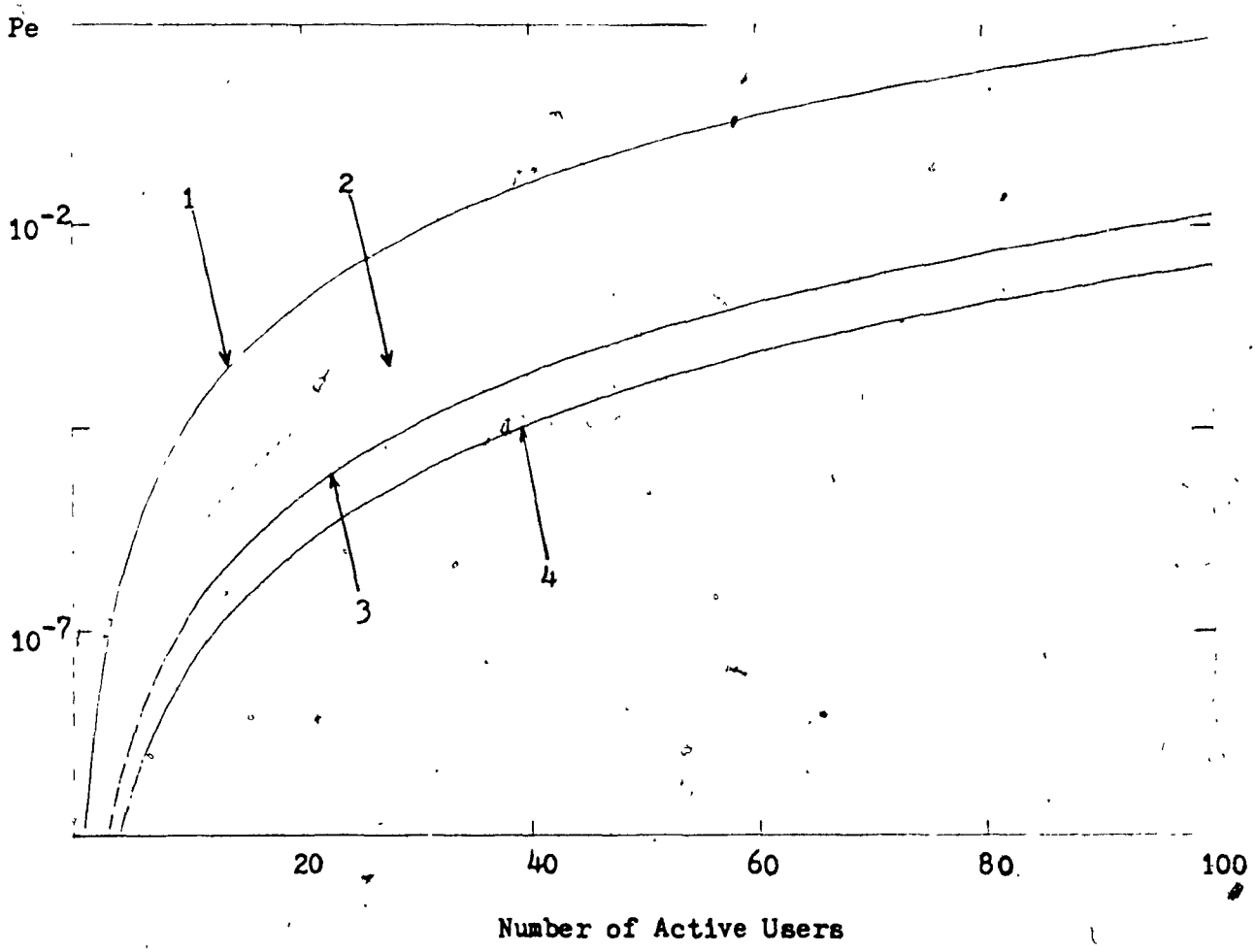

Figure (3.11) Comparisons of 2 bank 2 Hops/Symbol System With Different Number of Tones.

Table (3.5) Parameters for Figure (3.11).

Graph #	Bank #	Hops/Symbol	# of Tones	Processing Gains
1	2	2	256	128
2	2	2	512	256
3	2	2	768	384
4	2	2	1024	512

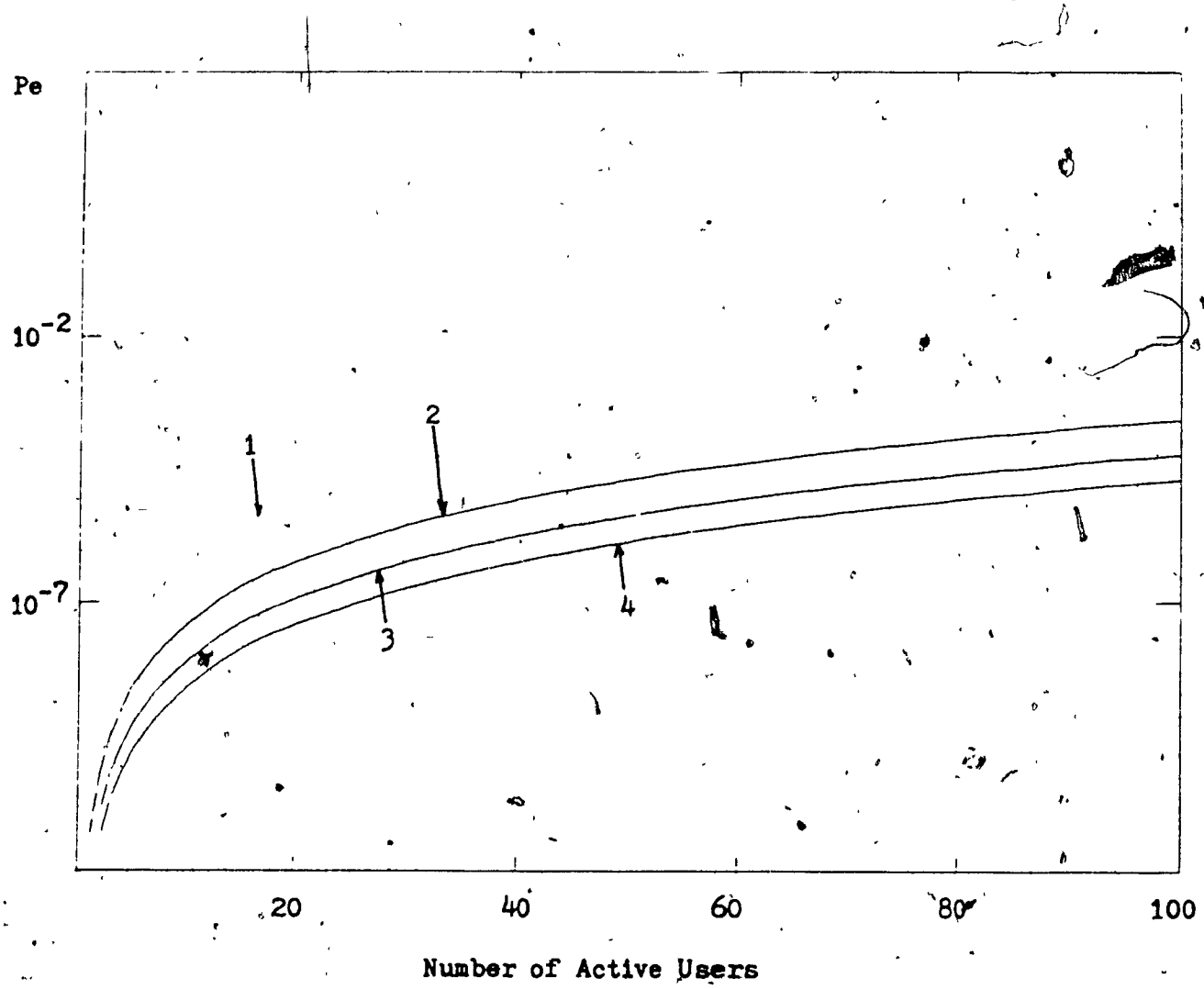

Figure (3.12) Comparisons of 4 Bank 4 Hops/Symbol System With Different Number of Tones.

Table (3.6) System Parameters for Figure (3.12).

Graph #	Bank #	Hops/Symbol	# of Tones	Processing Gain
1	4	4	256	64
2	4	4	512	128
3	4	4	768	196
4	4	4	1024	256

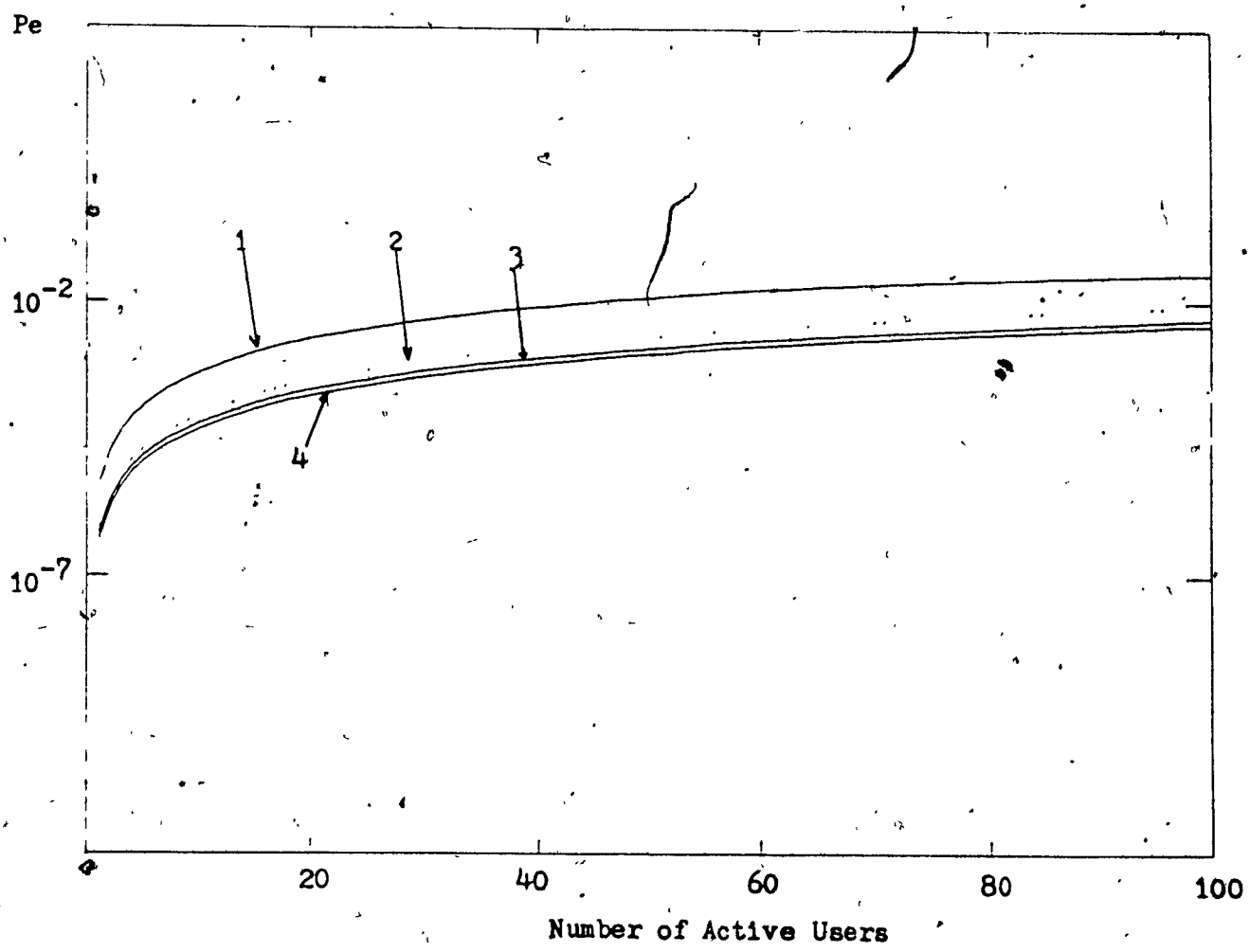

Figure (3.13) Spread-Spectrum Systems In Rayleigh Fading and Riclen Specular Components.

Table (3.7) System Parameters For Figure (3.13).

Graph #	Bank #	Hops/Symbol	# of Tones	Processing Gain	Type
1	4	2	256	64	Rayleigh
2	4	2	256	64	Riclen
3	4	4	256	64	Rayleigh
4	4	4	256	64	Riclen

CHAPTER FOUR

MOBILE CELLULAR RADIO SYSTEMS

4.1 Introduction

Communications between mobile stations has always been a difficult problem to solve. This communications field, as well as others is not without its limitations and mobile radio communications must overcome some extremely difficult transmission and reception problems. Such as multipath propagation conditions, which can cause the received signal to exhibit rapid and severe amplitude and frequency variations. Also man-made interference sources cause mobile radio systems to encounter many difficulties thus limiting reliable communications.

Adding to the troublesome task of designing a reliable mobile radio system, the demand for more mobile radio licenses is increasing at an ever increasing rate. Much work is required to develop spectrally efficient mobile systems capable of handling the growing traffic demands. The number of channels allocated in present mobile radio systems does not seem to be adequate in providing for such a large demand.

In the past, mobile radio systems tried to cover the largest area possible by placing the base station antennas on the highest structures in the area, such as mountains or tall buildings. Because of the vast area covered, secondary antenna systems were placed in regions where the signal strength was low, due to hills or tunnels. Problems arose with this diversity solution because of the multipath delay in the baseband signals and the complexity of the mobile base stations design increased to keep the distortions at acceptable levels.

Instead of covering an entire local area from one high powered land

transmitter site, a system can be employed where many moderate powered sites are placed throughout the coverage area. This will also overcome the scarcity problem of available radio channels in a high traffic density area such as in metropolitan regions, where smaller coverage areas or cells can be employed. The number of available channels are increased by simultaneously using channels in different cells that are spatially separated enough to prevent co-channel interference.

The cellular concept emerged when system designers needed a more efficient method for planning the layout of cellular systems. The shape of the cell which has been accepted by system designers is the hexagonal grid pattern. Although, the propagation of radio fields would suggest a circular cell structure, there are ambiguous areas where overlapping or no cell regions exits. Other cell shapes, such as equilateral triangles and squares have no ambiguous regions but do not accurately cover the general radiation pattern of a cell base station as well as the hexagonal pattern.

The determination of the distance between cells which use the same frequency channels is of great importance. Choosing a distance to small will cause unacceptable co-channel interference and a distance which is too large will demand more frequency channels in the network but, due to the fixed spectrum allocated for mobile use it will ultimately reduce the number of channels per cell. We shall examine the concepts of determining the distance required for reusing the same channels in various cells within a mobile network.

If we consider two base stations A and B separated by distance D and each within a cell of radius R, the power received at point P from base station A is proportional to R^{-n}, where n is the propagation law based on the terrain environment as illustrated in Figure (4.1) Where as is the power received at point

P from other base station transmitting on the same frequency at distance D is D^{-n}. In a hexagonal testellation there will be always six effective interfering cells located in the first tier or level. Other effective interfering cells further away are assumed to have a negligible effect. Thus the signal-to-interference ratio can be written as

$$S/I = \frac{R^{-n}}{\sum_{k=1}^{6} D_k^{-n}} = Q^{-n}/6 \qquad (4.1)$$

where Q is the co-channel interference reduction factor. As long as the cell size is fixed, co-channel interference is independent of the transmitted power of each cell, but instead is a function of the parameter $Q = D/R$. When the ratio Q increases, the co-channel interference decreases.

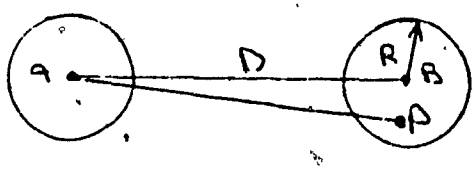

Figure (4.1) Cell Structure.

If we consider that the distance between adjacent cells as being unity, then the length cell radius R is $1/\sqrt{3}$. The number of cells per basic pattern (C) is related to the values of D and R namely, $D/R = \sqrt{3C}$. Thus the minimum number of channels sets required to fully cover any planer region using hexagon

patterns is

$$C = 1/2(D/R)^2 \qquad (4.2)$$

The co-channel reuse ratio (D/R) also has an impact on both the transmission quality because it effects the co-channel interference statistics. If D/R is made as small as possible a low cost and large capacity system can be designed. On the other hand, making D/R as large as possible benefits the transmission quality.

4.2 Channel Assignment Techniques

In cellular systems, initial call setup must be accomplished from the information transmitted to the base station from the mobile user through " Idle Channels ". After a base station has been assigned to serve a call request from a mobile user, a channel assignment procedure must be followed. This will allow the base station to determine if a channel is available to serve the call. One such method of channel assignment is known as "Fixed Channel Assignment". In a Fixed Channel Assignment system, a subset of the total channels available in the mobile network is permanently reserved for use within each cell. The channel subsets are reused in other cells which are geographically separated by a distance determined by the system criteria. The channel search for an available channel in a particular cell only involves searching for a channel in the reserved subset that is not in use. However, if all channels in the reserved subset are in use, service will not be provided to the requesting mobile user. The denial of an assignment can occur even though there may exist vacant channels in the adjacent cells.

The problems caused by this assignment scheme is due to the nonuniform traffic requirements of mobile networks. Some cell areas might be congested with high traffic loads while others can be totally vacant or with many free channels. This leads to message blocking and deteriorates the network capacity in high load regions.

To overcome this problem of high blocking areas, a "Dynamic Channel Assignment" scheme can be employed. The most general form of a Dynamic Channel Assignment scheme has all channels in the entire network available to any particular cell. Now the channel search for a requesting mobile user involves searching through all channels allocated to the mobile network to find an available channel. Available channels are defined as those not being used closer than the permitted D/R ratio from the cell. The use of a central processor to keep track of all channels being used at any given moment is required along with an optimizing strategy of selecting an available channel if more than one is free. Updates to the data storage memory must be made for all call request terminations and cell boundary crossings. The complexity of the cell base station is increased due to the requirement that all cell base stations must be switchable from channel to channel as the assignment changes.

A channel assignment scheme proposed by Elnoubi [9] employs a fixed channel channel assignment strategy with a slight modification to achieve better waiting time responses. The cell structure was formed by combining a repeating pattern of 7 cells each with 10 different channels to make a total of 70 channels in the basic cell pattern.

A group of 10 channels are initially allocated to every cell in the system according to the fixed channel assignment. When a mobile user requests a call the first free channel is assigned. If all the initial allocated channels are busy, a chan-

nel is borrowed from another cell. This is done by first counting the number of available channels for borrowing in the remaining 6 cells. A channel is available for borrowing if it is free in the adjacent cell and the other two interfering cells. Where an interfering cell is a cell that is located between the borrowing cell and the cell the channel is borrowed from. The algorithm is processed over all cells and the channel is borrowed from a cell that contains the most available channels for borrowing. When a cell has borrowed a channel and obtains a newly terminated call in one of the initially allocated channels, the borrowed channel is set free and the call is switched to the fixed channel. Thus keeping the number of borrowed channels to a minimum.

4.3 Next Generation Mobile Services

The rapid rate of growth of land mobile radios and the introduction of many more types of services such as, computer aided dispatch and specialized data bases, are over burdening the existing mobile radio services. There is a great need to develop the next generation of mobile systems to be more efficient and diversified. [33] has proposed a land mobile service that employs a microcell concept and has the ability to integrate both voice and data users.

The microcell concept employs many low-power base stations positioned along streets and highways. In metropolitan areas where traffic is high, the base stations can be located at every street corner if required as shown in Figure (4.2). Two PSK/TDMA channels operating at a bit rate of 1.6 mHz are used as the modulation scheme between the mobile users and the base stations. One channel is used for base station to mobile signaling, and the other for mobile to base station communications. The time slots of each TDMA channel are equally divided into 2.5 msec duration with a 10μsec interframe guard-time to avoid packet overlaps.

Control and identification data are transmitted between the base station and the mobile units in specific frames. Every 2 seconds each base station transmits a 40 bit location frame containing the base station's ID. The mobile unit that receives the location frame of the base station stores this information for future call requests.

During a call set-up, either for voice or data, the mobile units send a 72 bit interrogation frame to the base station. The frame consists of transmission request commands, the mobile's ID, and the stored ID received from the location frame. A similar interrogation frame is sent from the base station to the mobile units for acknowledgments and control signaling.

The system hierarchy structure, illustrated in Figure (4.3), employs a distributed control approach where each level provides a certain control function. The heavily traffic plagued centers of a city are divided into blocks of 16 base stations set in a matrix of 4 by 4, and are called subgroups. Each subgroup consists of a subgroup collector which is responsible for keeping a file on all mobile units within its control and is also a link between its block base stations and the rest of the network.

The second hierarchical level contains the group collector which is responsible for 16 subgroups. The group collector must also keep a file of all the units under its control while providing communication links between its subgroups and the rest of the network. Going one level higher, the highest network level is the sector level and is responsible to maintain files on all units. The sector controllers are connected to each other through a ring network to connect the entire system.

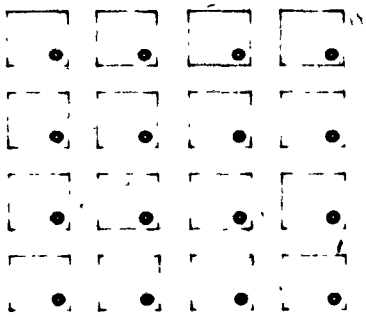

Figure (4.2) Base Station Locations in Microcell Design.

In this system format, the close proximity of the base stations allow for line-of-sight communications over short paths allowing the use of low-power mobile and base station transmitters. Thus, the problems of multipath fading that corrupt existing mobile services are overcome by this design. Another important attribute in the microcell design is the large handling capacity because of the large number of base stations in the network.

The maximum number of units that are under the control of a base station at any given time is 452, including vehicles, portable units, and paging equipment. A summary of the system handling capacity at all hierarchical levels is shown below in Table (4.1).

Table (4.1) Capacity of Microcell Network.

Level	Number of Units	Number of Base Stations
Base Station	452	1
Sub-Group	7232	16
Group	115712	256
Sector	1.851392 M	4096
System	14.811 M	32768

The above proposed Microcell design is but one solution to the spectral efficient system problem. In the next section, we propose a spectral efficient mobile network with the capability of handling different information types.

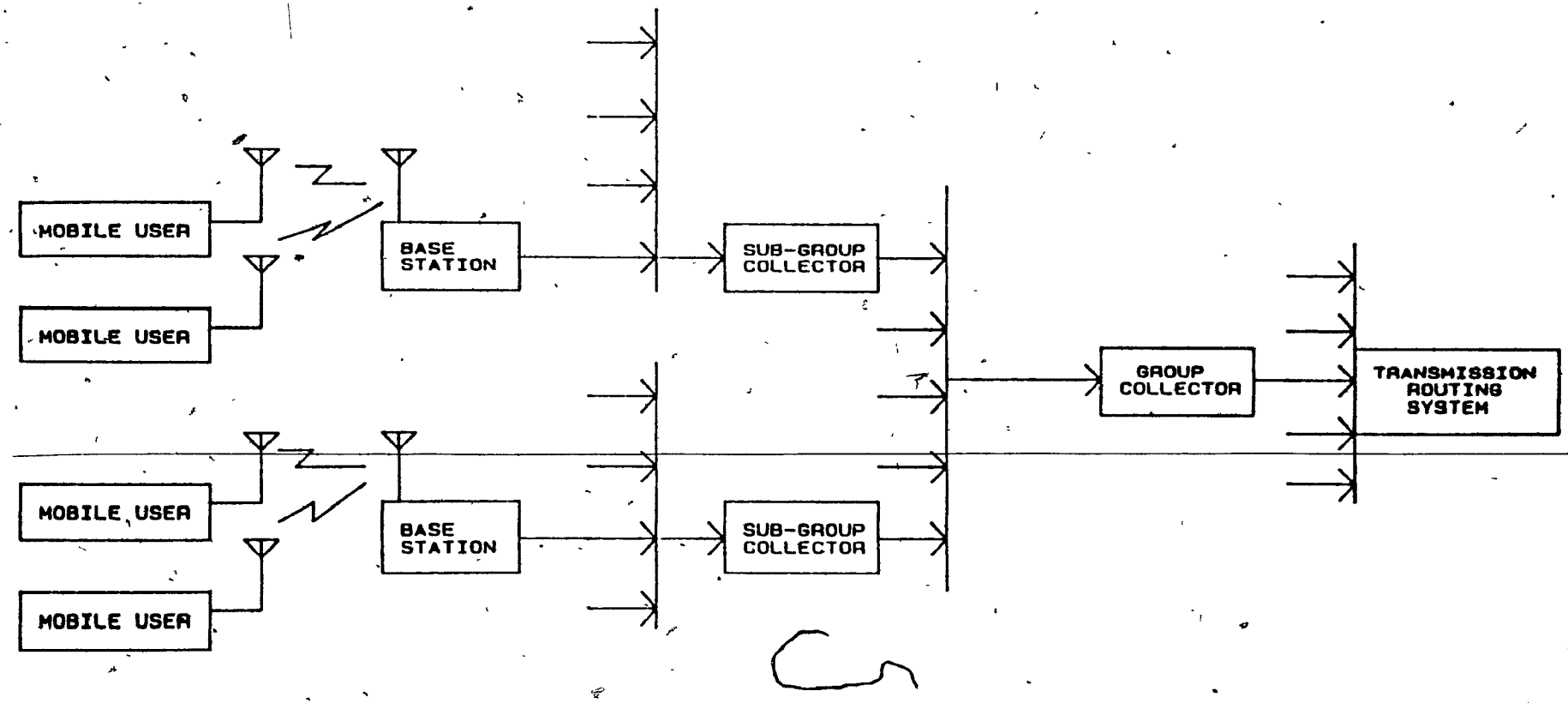

Figure (4.3) System Hierarchy Structure.

CHAPTER FIVE

PERFORMANCE CHARACTERISTICS OF A FH/CDMA MOBILE COMMUNICATION SYSTEM

5.1 Introduction

Traditional modulation techniques for mobile communications have been narrowband FM, and PSK modulation. In this study, we consider a cellular FH/MFSK spread-spectrum mobile network with a total bandwidth in each cell of $2*W_{ss}$. There are two nonoverlapping channels within each cell, uplink and downlink, each with a bandwidth of W_{ss}. The uplink channel handles information from the mobile units to the cell base station and the downlink channel directs information from the cell base station to the mobile users. To avoid any interference from adjacent cells, each of the neighboring cells has a different center frequency for the uplink and downlink channels than the adjacent cells as shown in Figure (5.1). We assume that the number of cells with different center frequencies in a cellular network is C.

However, in practical cellular systems there are many such cells and network expansion is possible as the system expands. Thus it is very easy to diminish the total mobile spectrum (400-900MHz) allocated to a specific system. To enhance the frequency efficiency, the same group of center frequencies will be reused at a different geographical distance away from each other. This process is called frequency reuse.

Frequency reuse can most easily be managed by regular channel assignment, where N channel sets are assigned in a regular pattern as a uniform hexagonal cell grid as shown in Figure (5.2). The proposed basic pattern is made up of 7 such cell grids, thus the reuse is far enough from a cell with the same center fre-

quencies. Figure (5.3) depicts the frequency allocation spectrum of the basic patterns within a network. Any interference due to the use of the same center frequency from different cells is call co-channel interference. Many schemes to reduce co-channel interference, such as directional antennas, have been developed to suppress the major problem co-channel interference causes. As opposed to typical modulation techniques, spread- spectrum modulation can smooth out most of the co-channel interference as will be discussed later in this section.

By increasing the number of cells in a basic pattern of different center frequencies (increasing C) while keeping the total network bandwidth ($2*C*W_{ss}$) constant the adjacent cell interference will of course, be reduced due to the increase in distance between similar cell center frequencies. But the W_{ss} of each cell must then decrease and with it the processing gain. Now each cell is subjected to more interference from Spread-Spectrum users within the cell itself and defeating the purpose of eliminating interference. The tradeoff between the SS interference from within a cell and the SS interference from neighboring cells becomes evident.

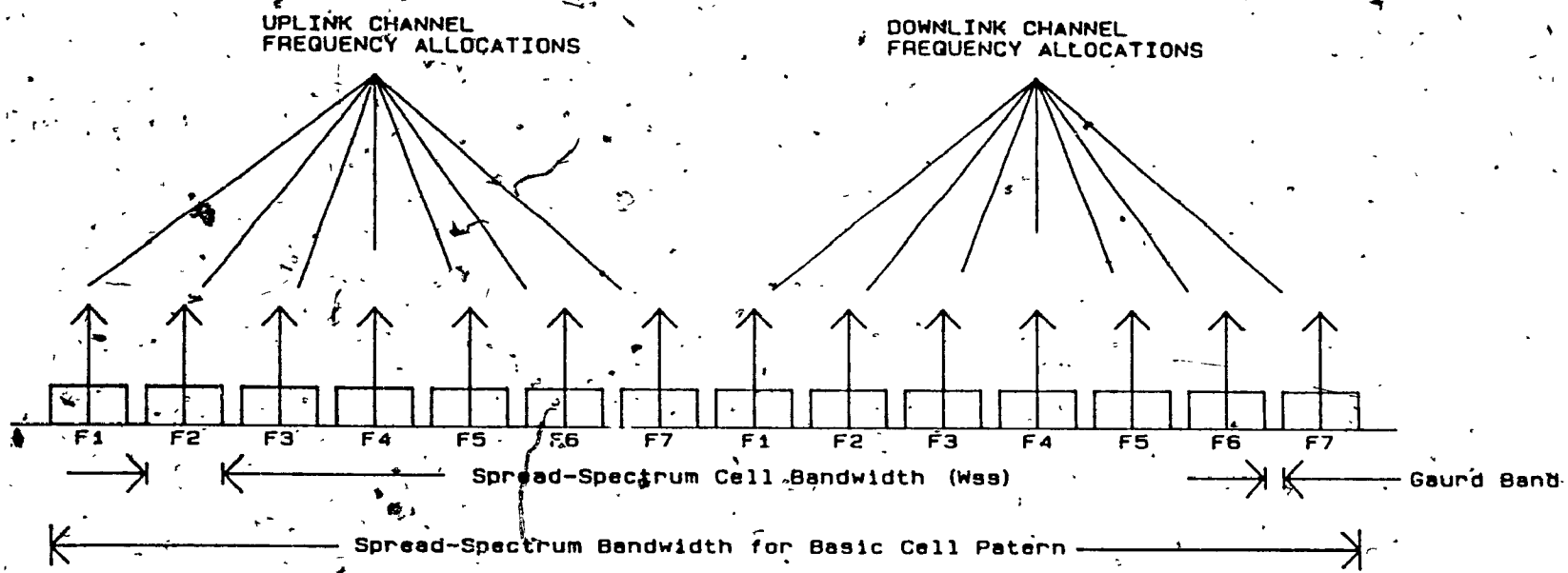

Figure (5.1) Frequency Spectrum of Non-Overlapping Uplink And Downlink Channels.

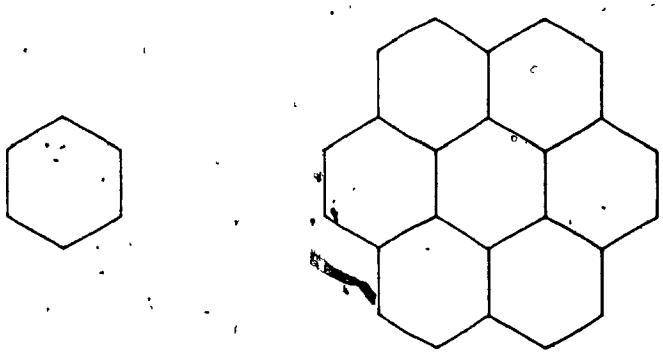

Figure (5.2) Hexigonal Cell Grid And Basic Cell Pattern.

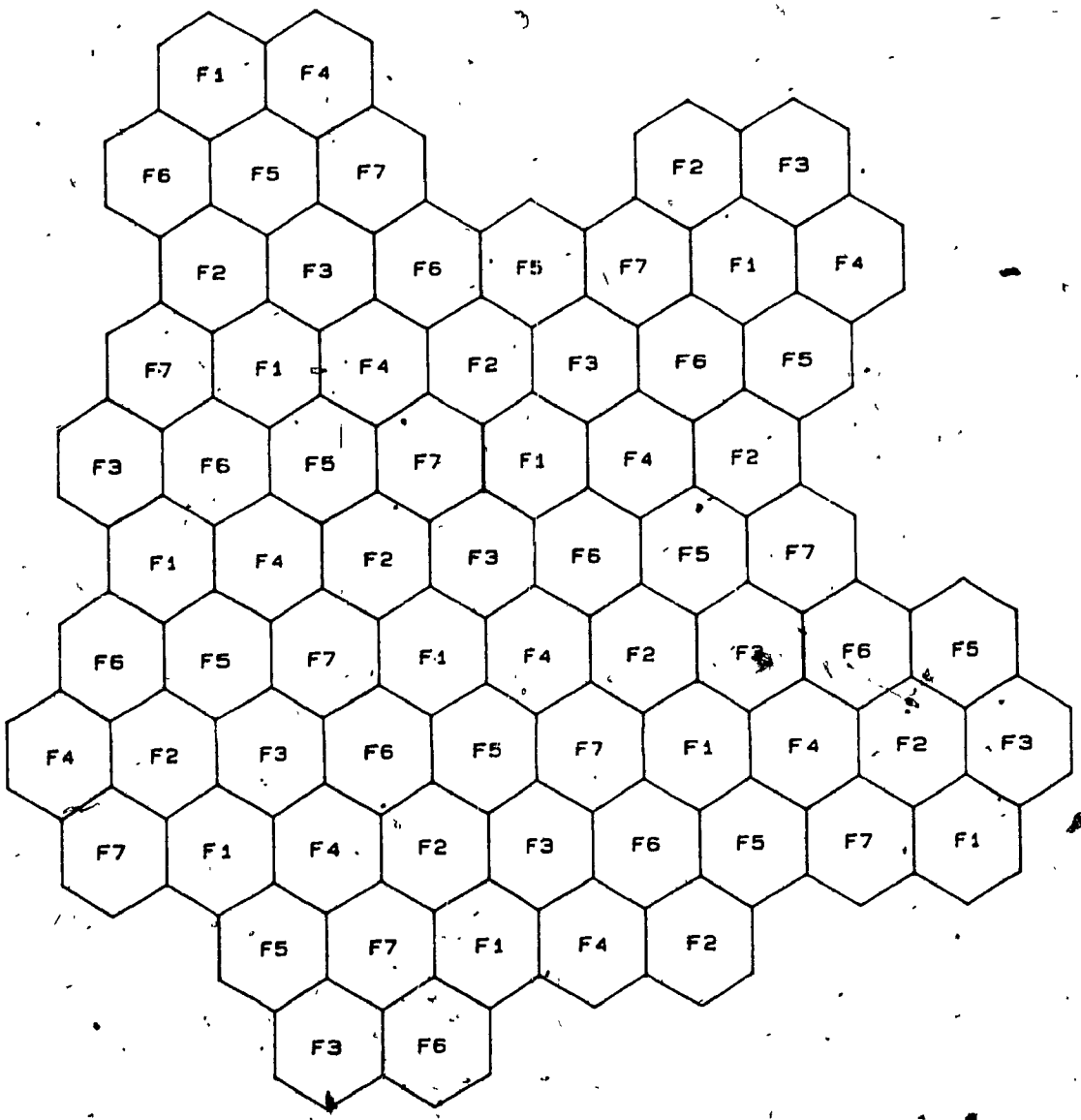

Figure (5.3) Frequency Allocation Spectrum of Basic Patterns.

5.2 Traffic Control

Traffic control of the mobile system takes place via the downlink channel of each cell. Each user is informed of various system status parameters from the cell base station and is addressed by its unique pseudo-random code.

Once the subscriber unit has been switched on, all base stations which can be reached are received via the organizational channel (downlink channel). The mobile unit then automatically selects the base station giving the strongest signal at the receiver and identifies itself. The base station can now update its file of present mobile units available in its cell. After which, the mobile unit continues to check the availability of its own base station as compared to the neighboring base stations. If another cell (neighboring) base station has a stronger signal at the mobile's receiver, then the mobile unit automatically reports to the new base station and an update takes place at the new base station. This gives the mobile user communicating in sever fading conditions the ability to select the appropriate base stations to tune to and reduces the problems of zone crossing apparent in cellular radio systems. The same can be said for the HANDOFF technique. While the mobile user transmits its information packets the mobile receiver will continue to receive the base stations identification signals (at 7 different frequencies). Again if the neighboring cell base station presents a stronger signal or if the mobile moves into another, cell the base station switching can be smoothly performed during packet transmissions.

Voice traffic consists of thousands of information packets and cannot afford long delays. Thus, voice traffic will be a priority type traffic in the cell. However, as the voice user sets up his call, it is considered as a data user (called "data like user"). Permission to start transmission signal is sent by the voice users transmitter to the best available base station. This request continues until an

acknowledgement signal is received, which can be either in the form of "READY FOR TRANSMISSION" or "STATION OVER CROWDED" depending on the availability of the base station's buffer and if the number on going voice calls and data traffic permits. If the voice user is denied access into the desired base station, it automatically switches to another base station and trys again to set up a voice call. When the destination voice user and the destination base station are both free the call will then be granted otherwise a "Trunk Busy" signal is sent from the destination base station through the backbone network to the source base station and finally transmitted on the downlink channel.

Data users can transmit their packets without a setup call since the nature of data transmissions are bursty and can sustain relatively long delays compared to voice traffic. The data users may also be blocked when the base station has reached a certain limit depending on the combination of on going voice calls and an average level of data user traffic. The base station will respond to the above circumstance by transmitting a "NO STATION AVAILABLE" message to the mobile data user. This will result in the data user to backoff for a random time upto K_d time slots. By intentionally delaying the retransmission helps to avoid future packet overlap.

5.3 Error Correction Techniques

Backoff can also occur when the data packet is not received by the base station or when there are an appreciatable number of errors within the data packet. Since data cannot withstand any errors it is vital that the data packet is retransmitted. For this reason, error control techniques are employed in the system.

Basically there are two categories of techniques for controlling transmission

errors in data communication systems. They are automatic-repeat-request (ARQ) scheme and forward-error-control schemes. In an ARQ system the receiver checks the parity of the transmitted codeword. If the parity checking is successful, the received codeword is assumed error free and sent to the appropriate destination base station. The cellular base station then notifies the mobile unit, via the downlink channel, that the packet has been successfully received. If however there is an error in the reception of the data packet, the base station will notify the mobile user to retransmit the packet. Retransmission continues until the packet is successfully received. Since ARQ schemes alone diminish the channel throughput as the error rate increases, the number of users in a given cell will always be forced to a relatively low level.

In a Forward-Error-Control (FEC) communication system, an error correcting code is used for controlling transmission errors. With this method, any received packets containing errors can be corrected up to a certain number of bits in error. The maximum number of correctable bits (t) in a given packet depends on the code and the number of parity bits used. In a system using only FEC techniques, the packet is sent to the appropriate destination even if the receiver could not correct all the errors.

As stated before, data packets must be successfully received, thus a high system reliability is needed. To do this using FEC techniques, powerful codes must be employed to correct a large number of errors (increasing t). This will effectively decrease the information rate and force the system to be designed with a smaller W_{ss} for each cell or decrease the processing gain of each cell. Either of which will also decrease the the maximum number of users that will be effectively transmitting in a given cell.

When ARQ and FEC systems are combined, the drawbacks of both can be

overcome. The combination of the two schemes is known as Hybrid ARQ. When FEC is used with ARQ, the frequency of retransmission is decreased by the ability of correcting error patterns. This increases the system throughput over an ARQ system alone. If a pattern of errors occur which cannot be corrected the receiver requests a retransmission. Thus, combining ARQ and FEC the transmission reliability is enhanced compared to FEC alone and the throughput is greater than having ARQ alone.

The ARQ scheme employed in this mobile cellular system is the "Stop And Wait" technique Figure (5.4). Using this technique, when a block of data is received with errors, the decoder tries to correct it. If the number of errors is within the maximum number of correctable errors of the code (distance t) the errors will be corrected and the packet is sent to the destination base station. When a received block contains more than t errors, the base station receiver will request a retransmission. Upon receiving a retransmitted packet, the receiver will try to correct the errors if any exist. If there are again, more than t errors another retransmission signal is sent. This continues until every block in a packet is received correctly. Thus a packet is in error if one out of the M blocks cannot be decoded. However, the receiver does not wait for every block in the packet to be received before it issues a retransmission signal to the mobile transmitter. If any of the blocks have uncorrectable errors the base station will automatically send a retransmission signal at the end of the block.

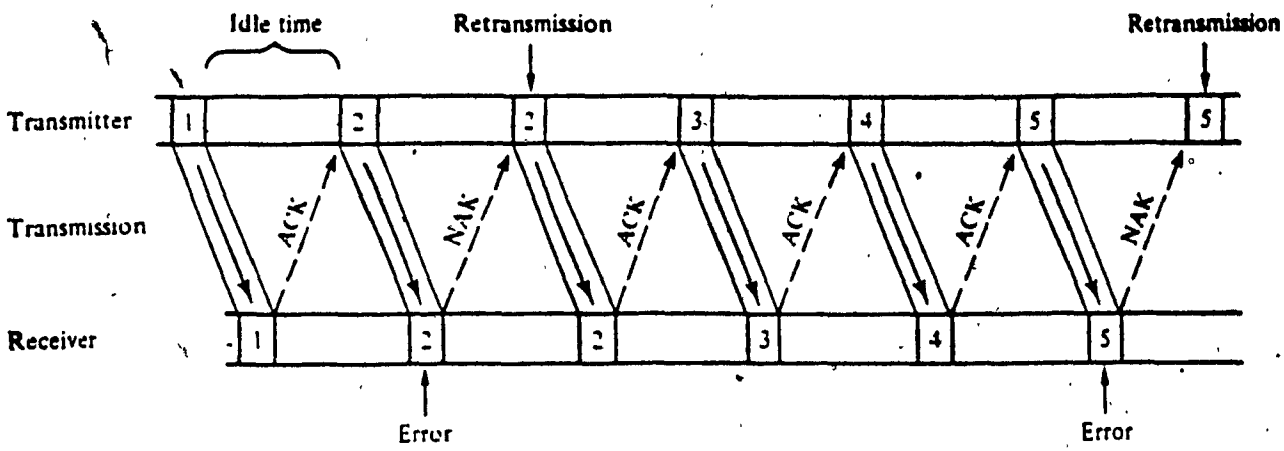

Figure (5.4) The ARQ "Stop And Wait" Scheme.

The hybrid scheme is very useful when there are many users with ongoing calls within a given cell since the occassional unintentional jamming signals (mutual interference) will increase the error rate. The algorithm of the above sequence of events can be seen in Figure (5.5).

Using spread-spectrum techniques, the overlap of data and voice packets will be in time and frequency. Because of the unique pseudo-random nature of the hopping frequencies for each transmitter, it is very unlikly that another transmitter will hop onto the same frequency tone at the same time and overlap the packet for one more then one time hop. As the number of ongoing calls are inceases, the probability of overlap due to many users is also increased to a point where the gain of FEC becomes apperant.

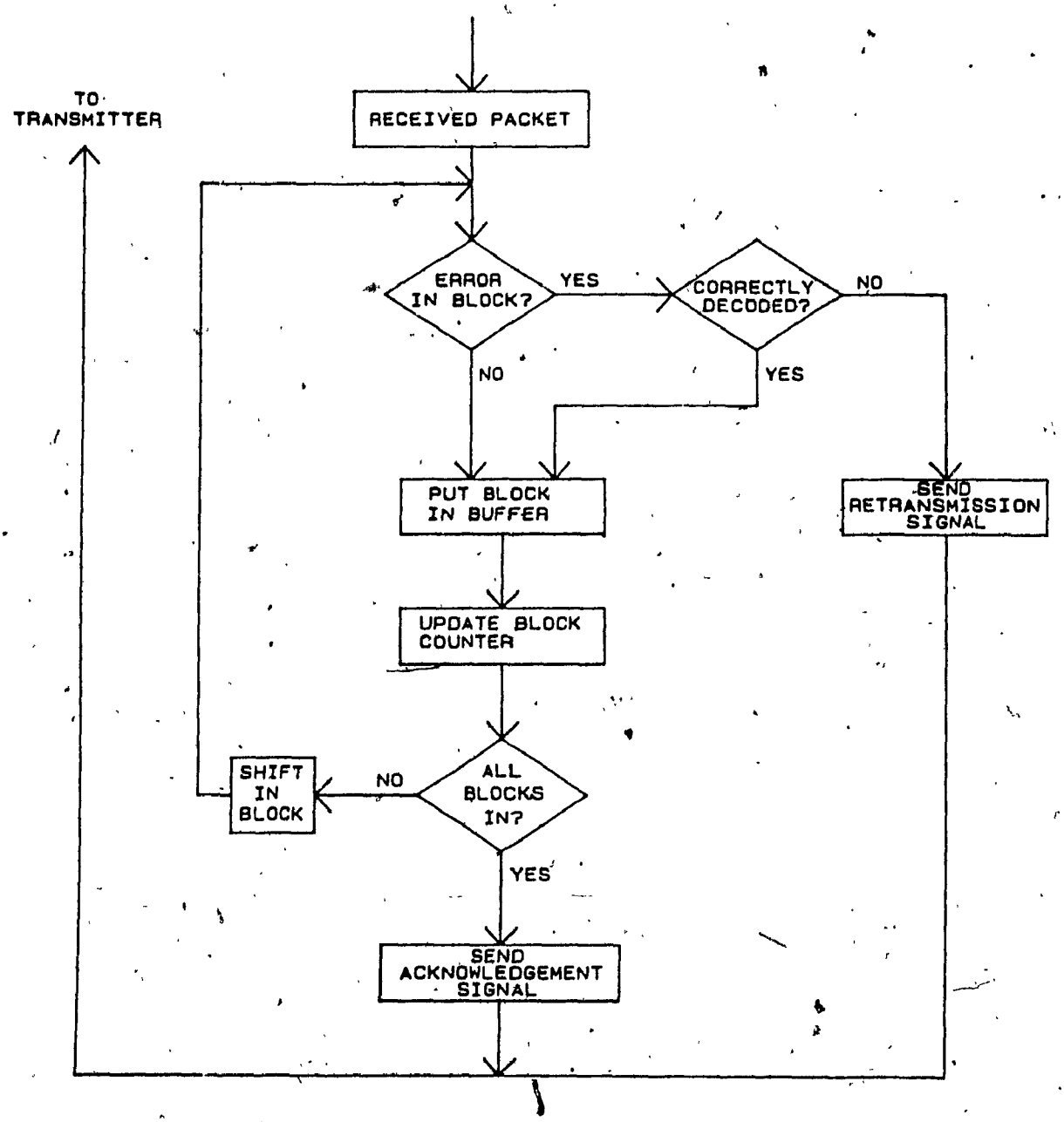

Figure (5.5) Algorithm of The Hybrid ARQ Scheme.

The error correcting codes considered in this cellular network are block codes. The encoder for the block codes breaks the continuous sequence of information bits into sections or blocks of n bits. The encoded blocks called "codewords" contain k information bit used for coding. The code rate or amount of redundancy introduced by the encoder is the ratio k/n and is denoted as the Code Rate (R_c). However, if we choose to fix the channel rate at R_d, the effective bit rate reduces to $R_d * R_c$.

The voice and data information packets that we consider are fixed in length, thus, depending on the code being used the block size and the number of blocks (M) in a single packet will change. Different classes of block codes are used to determine the characteristics of the network under different load conditions as will be discussed in the performance section of this chapter. Among them are the BCH codes, Hamming codes, and Golay codes whose characteristics will be described below.

The Spread-Spectrum cellular network utilizes coding techniques to improve the system performance in jamming environments, such as in multiple access schemes. We shall briefly describe the three different types of linear block codes that will be encountered in our analysis and list their important parameters including block size, maximum number of correctable bit, and the minimum distance of a code. The minimum distance of a code can best be described by considering any two code words in an (n,k) block code. A measure of the difference between the code words is the number of corresponding elements or positions in which they differ, denoted B_d and is also known as the Hamming distance. The minimum distance d_{min} can be defined as the smallest value of B_d for the m code words, where $m = 2^k$ code words that form a block code.

Binary Hamming codes are the class of codes with property that

$(n, k) = (2^m - 1, 2^m - 1 - m)$ where m is any positive integer and a minimum distance of 3 providing an error capability of correcting all single errors. From this class of codes, a binary code with a minimum distance of 4 can be produced by adding one parity bit to a binary Hamming code. Now there will be $m+1$ parity check bits and $2^m - 1 - m$ information bits resulting in a total of $n = 2^m$ bits per block. The number of correctable bits/block for the $(2^m, 2^m - 1 - m)$ Hamming code is 2 bits in error.

For channels in which errors affect successive symbols independently BCH codes are the best suited. The cyclic BCH codes have the following parameters

Block length: $n = 2^m - 1, \; m = 3,4,5,\ldots$

Number of information bits: $k \geq n - mt$

Minimum distance: $d_{\min} => 2t + 1$

The last linear block to be described is the Golay (23,12) code. This code has the capability of correcting all patterns of three or fewer errors with a minimum distance of 7. There is an extended Golay code which is obtained by adding an overall parity bit to the (24,12) code and creating a minimum distance of 8 with the ability to correct 4 bits in error per block. Unfortunately, the Golay code does not generalize to other combinations of n and k.

5.4 Inter Station Communications

The communication network which handles the data from base station to base station traditionally has been the public network system or microwave radio links. In our proposed mobile network, a Fiber Optic Wide Area Network (WAN) can be employed to carry the data transmissions between cells or to the public trunks. The WAN is especially useful for carrying huge amounts of management and control data for integrated voice and data communications.

The fiber optic network is configured as a STAR topology enabling upto 16 User Access Nodes (UAN) to be connected to a central node (Central Switch). Each UAN is located at every cell base station that is connected to the optical network whereas the cell in the center of the cell group connected to the WAN contains both the CENTRAL SWITCH and the UAN. The backbone network allows for expansion and reliable dedicated routing in case of base station failure. This type of network may also be used in conjunction with the standard public utilities. When there are areas within the network that have low average traffic loads, the public utilities can carry the information to and from the cell base stations. However, under high load stresses (high-traffic times), the fiber optic backbone network will be needed to handle the traffic of voice and data users with a guaranteed dedicated path.

The optical network can be placed to cover only the network regions that contain the most traffic loads, Figure (5.6), other cells in the network can be connected to the public system through which a connection is made to the other base stations or to a base station's UAN if it requires one.

In an actual mobile network, most of the voice users communicate through the public telephone systems and not to other mobile stations alleviating some of the load through the backbone network. The data users, however, will

communicate possibly to other UANs at another base stations' data base or into a global network message system.

The WAN uses a demand assignment protocol for routing the packets to their correct destinations. When the base station receives a correct data packet it signals the UAN to request a time-slot to the destination cell. The central switch does the processing of the demand assignment requests and sends the "ACKNOWLEDGE" signals back to the requesting UAN and a "GET READY" signal to the destination UAN. Since the call set-up for the high-speed optical network is relatively faster than the packet reception at the cell base station receiver the packet is downloaded into the UAN's buffer as the base station signals the UAN.

The voice users, as stated before, will setup the call with the cell base station. In this case the base station will signal the UAN to request many time slots for transmission to the destination UAN. The time it takes to receive an acknowledge signal from the central switch is non-existed to the real-time voice user.

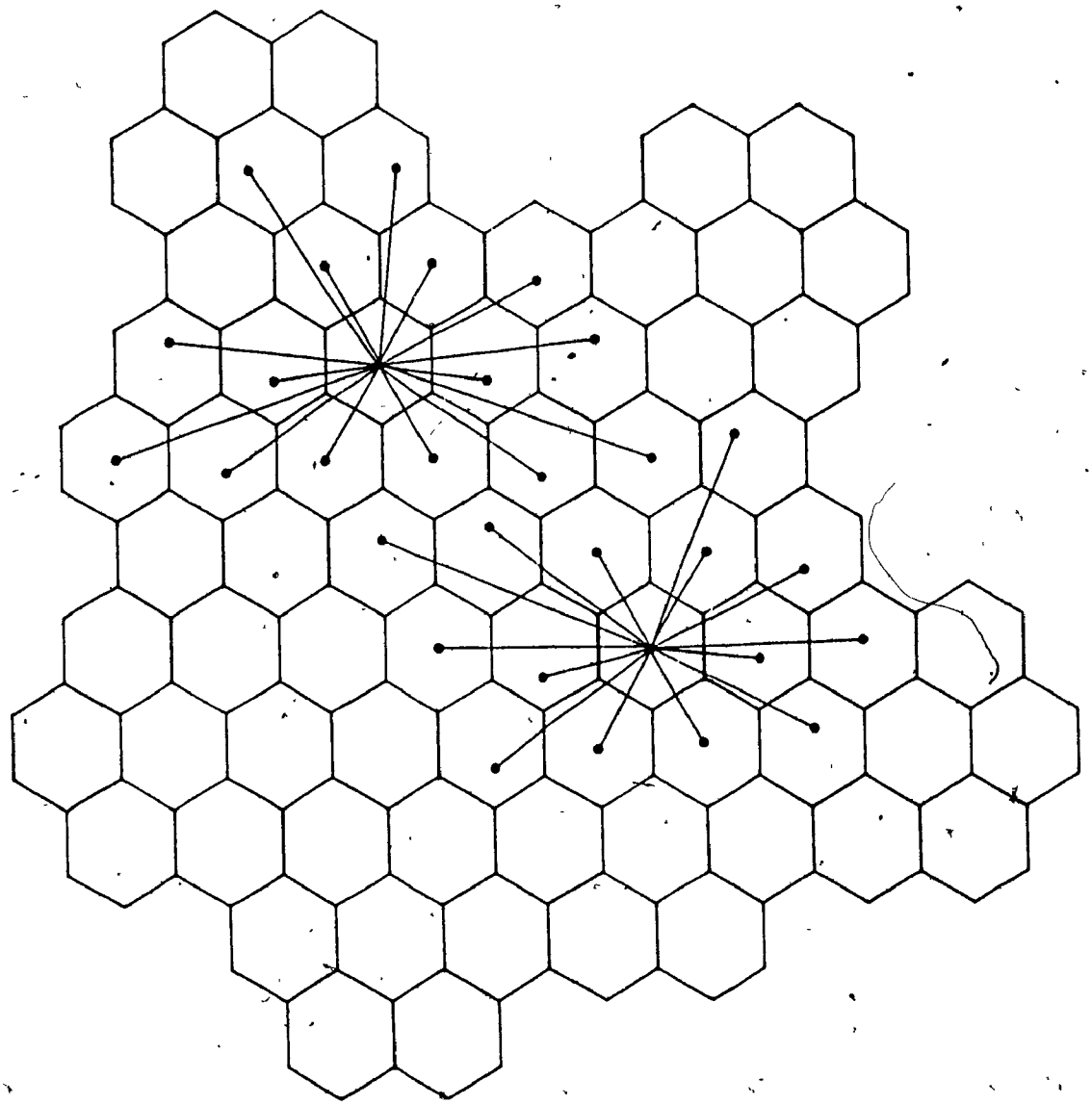

Figure (5.6) Potential Use of an Optical Backbone Network

In a Mobile Cellular System.

5.5 System Analysis

When designing a mobile radio network, many constraints must be considered such as information bit rate, maximum number of allowable stations in a cell, and radio spectrum utilization. The latter constraint is due to the limited number and width of frequency bands allocated to public mobile applications. It is necessary to make the proper tradeoffs in mobile radio systems to design the most economical and efficient network. The efficiency of a mobile network is primarily determined by the value of the throughput the network can achieve under certain loads and is influenced by a large variety of factors such as modulation scheme, coding, and network management protocols.

In this section, the efficiency of the mobile network will be analyzed for different modulation and receiver designs such as 2 & 4 hops/symbol and 2,4,8-FSK systems.

As we stated before, there are both uplink and downlink channels with a given cell structure. The downlink channel carries both information data (voice and data packets) and network management information from base station to the mobile users. Since the downlink channel source is from only one location there will be no overlap or collision between packets in this channel. There is no contention between channels in a cell since the downlink and uplink channels in a cell are nonoverlapping as well as the uplink and downlink channels in the neighboring cells. The cell base station transmits at much higher power levels than the mobile users limiting the error rate of transmission in the downlink channel.

However, the uplink channel carries information from many low-power sources to the centralized cell base station and is susceptible to interference between mobile users transmitting in the cell. Thus the measure of system performance such as, throughput, blocking, and delay is determined by the perfor-

mance of the uplink channel.

We consider an uplink channel with a spread-spectrum bandwidth of W_{ss}, the number of data and voice users in each cell is denoted as M_d and M_v respectively. For analysis, the number of bits in each data and voice packet is set to the same value N_P and the information bit rate equals R_d. Therefore the time to transmit one packet can be written as,

$$t_p = [1/R_d]\, N_p \tag{5.1}$$

This means that the actual packet transmission time on the spread-spectrum channel is given by

$$t_p = n\,/k * 1/R_d * N_p \tag{5.2}$$

C(N,K) denotes the FEC being used and t_p is the unit of the final delay.

The time between two embedded points in the Markov Chain are normalized to the time it takes to transmit a data packet t_p at data rate R_d. The generation (arrival) rate of arrival for data users is Poisson. With, the probability of generating a data packet per packet time equal to λ_d.

It has been determined that voice traffic contains both talking and silent periods. The voice signal arrives in Poisson fashion while the inter-arrival (silent period) times are exponentially distributed. We can write the exponential distribution of silent periods as

$$P(t) = a \exp(-at) \tag{5.3}$$

with a mean of $1/a$

The probability distribution of a talking period is written as

$$Q(t) = b \exp(-bt) \qquad t >= 0 \qquad t < 0 \tag{5.4}$$

The mutual independence of the talking and the silent periods allow the determination of the PDF of inter-time arrival of voice signals by convolution, that is

$$P_v(t) = P(t) * Q(t) = \left[ab/(b-a)\right](e^{-at} - e^{-bt}) \tag{5.5}$$

For a worst case assumption the arrival rate is Poisson distributed, and in the following we can assume that the M_v voice users in the cell generate new packets (talking plus silent period) during each packet time t_p with probability λ_v.

By normalizing the packet time t_p ($t_p = 1$) we can state that the probability of finding a talking packet is equal to the ratio of the talk period over the packet time. Thus we have

$$u. = (1/b)/(t_{p_{norm}}) \tag{5.6}$$

where $t_{p_{norm}}$ is the normalized packet time and u is the probability of having a voice packet.

For a silent period the probability is

$$P_{vd} = (1/a)/t_{p_{norm}} = 1/a \tag{5.7}$$

The voice user can be in three different states during a packet time t_p. They

are defined as packet transmission with probability ($P_{vs} = uP_{s}$), silent period (P_{vd}), and unsuccessful transmission with probability (P_{vf}). However, we say that the probability that a voice user transmits a packet during the packet time t_p is λ_d .

Now the total traffic entering the cell base station in the uplink channel is defined by

$$T_l = (M_d \lambda_d + M_v \lambda_v)/PG \tag{5.8}$$

where T_l is the average traffic load in the uplink channel and PG is the processing gain of the spread-spectrum system. Dividing the load ($M_d \lambda_d + M_v \lambda_v$) by the processing gain enables us to compare the results of several networks on a fair basis.

Before we go further with the throughput analysis a closer look at the mobile transmitter is required. Unlike voice user packets, data packets must contain no errors and thus require a Hybrid ARQ scheme. The mobile data transmitter then must be allowed to store the data packet in its buffer until it gets an acknowledgement from the cell base station upon successful transmission. In the case of a retransmission of the data users' packet, the mobile transmitter will backoff for a random length of time upto K_d packet transmission times. Thus, the effective average probability of retransmission in in one of the packet intervals is

$$q = 1/k_d \tag{5.9}$$

While the data mobile transmitter is delayed due to retransmission (backoff), a queue can be accumulating in its buffer due to the generation of other packets

from the data source. Theoretically, if the transmitter does not receive an acknowledgement signal from the base station, the queue may build up indefinitely. However, in keeping with the practice, the buffer size is limited to a finite level. The buffer is configured as a First-In-First-out (FIFO) memory device, when a queue builds up the transmitter will always try to transmit the packet first in line. Depending on the traffic load T_l, the probability of packet success P_s in the uplink channel will determine the state of the transmitters' buffer.

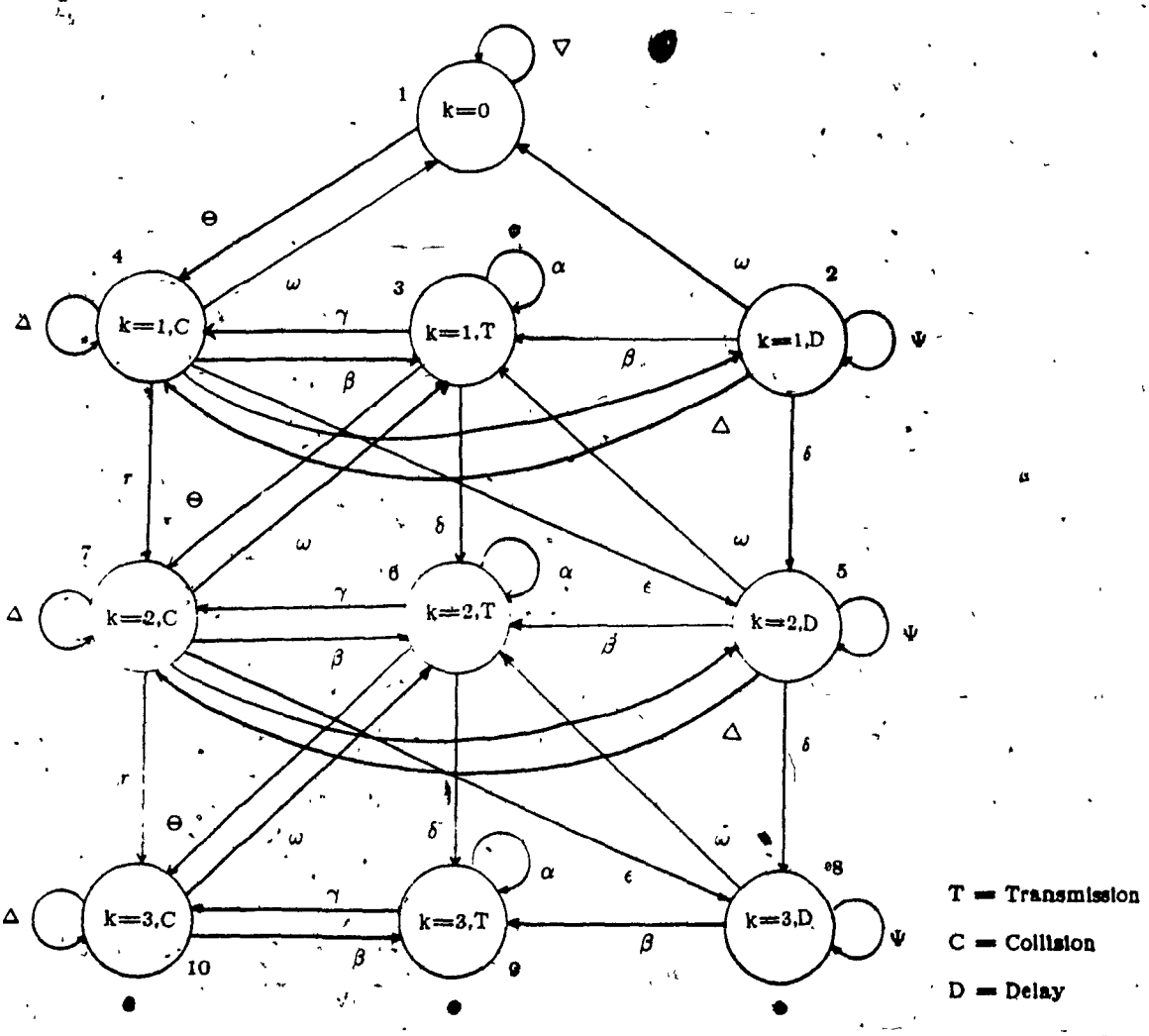

Figure (5.7) Markovian State Diagram of The Transmitter Buffer.

The behavior of the transmitter buffer can be analyzed through studying the Markovian state diagram of Figure (5.7). Each state of the buffer is observed at the packet departure time and can be defined by

$$S_l = S_l(i,j) \tag{5.10}$$

where $i = 1,2,3, \cdots, L$ represents the buffer contents in packets. and $j = 0,1,2$ represents the state of the transmitter, such as, transmitting, delayed, or colliding.

For analysis, the downlink signals from the base station to the mobile data transmitter indicating an acknowledgement or a collision is assumed to be instantaneous, thus permitting the existing link between states in Figure (5.7).

Many state trahsition possibilities can occur in the transmitter buffer during the packet time t_p and are described in the Table (5.1).

The queuing analysis leads to a set of multidimensional probability state equations that must be solved. First, we consider a general set of linear equations.

$$AX = B \tag{5.11}$$

where A is a given square matrix and B is a given vector and X is an unknown vector. In this case, the equilibrium state probabilities (the components of X) that are to be found is the set of equilibrium state equations.

EQUATIONS	PROBABILITY DESCRIPTION
$\Psi=(1-\lambda_d)(1-1/K_d)$	User will not generate a new packet and will backoff from transmitting the old packet
$\omega=1/K_d(1-\lambda_d)P_s$	User will try transmitting and will succeed without generating a new packet
$\Theta=\lambda_d(1-P_s)$	User will generate a new packet and not succeed in transmitting a packet
$\delta=P_s(1-\lambda_d)$	User succeeds in transmitting a packet with no new packets generated
$\alpha=\lambda_d P_s$	Packet transmission succeeds while a new packet generated
$\beta=\lambda_d(P_s/K_d)$	Packet transmission with new packet generated
$r=\lambda_d(1-P_s)/K_d$	Collision with the generation of a new packet
$\Delta=(1-P_s)(1-\lambda_d)/K_d$	Collision with no new packet generation
$\epsilon=\lambda_d(1-1/K_d)$	No transmission and new packet generation
$\gamma=(1-P_s)(1-\lambda_d)$	Packet collision with no new packet generated
$\nabla=(1-\lambda_d)$	Probability of no new packet generation state

Table (5.1). Description of The Probability State Transitions In The Transmitter Buffer.

The probability state transition matrix A of the buffer states (Figure (5.7)) can be presented as shown

$$\begin{bmatrix} Y_{l+1}(1) \\ Y_{l+1}(2) \\ Y_{l+1}(3) \\ \vdots \\ Y_{l+1}(B_l) \end{bmatrix} = \begin{bmatrix} \nabla & \Theta & 0 & 0 & 0 & 0 & 0 & 0 & 0 & \cdots \\ \omega & \Delta & \Psi & \beta & \tau & \epsilon & 0 & 0 & 0 & \cdots \\ \omega & \Delta & \Psi & \beta & \tau & \epsilon & 0 & 0 & 0 & \cdots \\ \delta & \gamma & 0 & \alpha & \Theta & 0 & 0 & 0 & 0 & \cdots \\ 0 & 0 & 0 & \omega & \Delta & \Psi & \beta & \tau & \epsilon & \cdots \\ 0 & 0 & 0 & \omega & \Delta & \Psi & \beta & \tau & \epsilon & \cdots \\ 0 & 0 & 0 & \delta & \gamma & 0 & \alpha & \Theta & 0 & \cdots \\ 0 & 0 & 0 & 0 & 0 & 0 & \omega & \Delta & \Psi & \cdots \\ \cdots & \cdots & \cdots & 0 & 0 & 0 & \omega & \Delta & \Psi & \cdots \\ \cdots & \cdots & \cdots & \cdots & \cdots & \cdots & \delta & \gamma & 0 & \cdots \\ \cdots & \cdots & \cdots & \cdots & \cdots & \cdots & 0 & 0 & 0 & \cdots \\ \cdots & \cdots & \cdots & \cdots & \cdots & \cdots & \cdots & \cdots & \cdots & \cdots \end{bmatrix} \begin{bmatrix} Y_l(1) \\ Y_l(2) \\ Y_l(3) \\ \vdots \\ Y_l(B_l) \end{bmatrix} \tag{5.11}$$

The two dimensional state $S_l(i,j)$ is now mapped to the single dimension state $Y(x)$ using

$$Y(3i+j-3) = S_l(i,j) \tag{5.12}$$

To solve the above state transition matrix we set the idle state $Y(1)=1$ and all other states of the buffer are initialized to zero. Thus we have

$$Y(1), \ldots, Y(B_l) = [1,0,0,\ldots,0] \tag{5.13}$$

Now we employ the Gauss-Seidel iteration method of solving linear systems This is based on the standard form of iteration method and can be performed by solving the first equation for $Y(1)$, the second for $Y(2)$, and so on. In general this method can be written as

$$Y(i) = (1/a_{ii})[b_i - a_{i1}Y(1) - a_{i2}Y(2) - \cdots$$
$$-a_{ii}Y(i-1)a_{i(i-1)}Y(i+1) - \cdots - a_{in}Y(n)] \tag{5.14}$$

We can write the Gauss-Sedal method in an iteratlye fashlon as

$$Y_{(l+1)}(i) = (1/a_{ii})[\beta_i - a_{i1}Y_{(l+1)}(1) - a_{i2}Y_{(l+1)}(2) -$$

$$\cdots - a_{i(i-1)}Y(i-1) - \cdots - a_{i1}Y_l(i+1) - a_{in}Y_l(n)] \qquad (5.15)$$

where l is the iteration number

The iteration continues until the values of Y(l) (where l=1,...,L) have converged to a predefined tolerance. Thus at equilibrium we can write

$$Y_{l+1}(j) = Y_l(j) \qquad (5.16)$$

The sum of the probabilities of all states in the transmitter buffer at equilibrium is equal to 1.

Now with each state of the buffer at equilibrium, we can determine various parameters of the queue. The delay or waiting time for a given packet can be calculated by summing the probabilities in the columns of Figure (5.7) and multiplying by a weighting factor (how far back in the queue) then summing over all buffer stages. This can be written as

$$D = \sum_{k=1}^{B_l} k\,(Y(3k-1) + Y(3k) + Y(3k+1)) \qquad (5.17)$$

where k is the buffer stage and L is the length of the buffer.

The probability of a data user transmitting a packet or colliding in the uplink channel is given by.

$$P_{dp} = 1 - Y(1) - \sum_{k=1}^{B_l} Y(3k-1) \qquad (5.18)$$

and the probability of a data user that has successfully transmitted is

$$P_{ds} = \sum_{k=1}^{B_l} Y(3k) \tag{5.19}$$

From the values for the probability of a data packet transmission (Pdp) and the probability of a voice packet transmission from equations (5.18) and (5.6) respectively, we can determine the probability of having N packets generated by $M_d + M_v$ users within a cell. This is given by

$$P(N) = \sum_{i=1}^{M_d} \sum_{j=1}^{M_v} \binom{M_d}{i} (P_{dp})^i (1-P_{dp})^{M_d-i} \binom{M_v}{j} (\lambda_{vp})^j (1-\lambda_{vp})^{M_v-j} \tag{5.20}$$

where $N = (i+j)$ and $N = 1,2,3,\ldots,(M_d + M_v)$

Now the effect of FEC coding is considered in the analysis. Given a FEC code defined as a (n,k) code, then the code rate is (k/n) and has a correctability of t bits. Thus, the probability of transmitting a packet by a mobile user and receiving the packet correctly with up to t bits in error is

$$P(correctpacket/n) = \sum_{k=0}^{t} \binom{l}{k} (P(e/n))^k (1-P(e/n))^{l-k} \tag{5.21}$$

where P(e/n) is the probability of bit error calculated in Chapter Three for n users and different FH/MFSK systems with various system parameters, (eg. 2 and 4 hops/symbol and 2,4,8 - FSK receiver designs) and l is the block length in bits.

Since the FEC code in the base station works on blocks only, and packets are constructed from m blocks then the probability of correct packet for a given number of users in the cell is

$$P(correct\ \ packet/n) = (P(correctblock/n))^m \qquad (5.22)$$

Averaging over the the probability of correct packet and the probability of transmitting a packet for all n (eqn (5.19) & (5.21)) we obtain the average probability of packet success, ie.,

$$P_s = \sum_{n=0}^{M_d+M_v} P(correctpacket/n)\, P(n) \qquad (5.23)$$

With this new value of P_s , we go back to the qualities in Figure (5.9) and substitute the new value. The entire procedure of determining the steady-state values of the data transmitters buffer and the average probability of packet success is repeated with the new value of P_s . This iterative procedure continues until P_s converges to less than the predescribed tolerance. The measure of convergence of P_s can be calculated be taking the value for two consecutive iterations as shown below

$$Tol > (P_{s_i} - P_{s_{i+1}})/P_{s_i} \qquad (5.24)$$

Once the probability of successful packet transmission P_s has converged from the initial estimate the throughput of the system can be calculated at the current load conditions (ie. $M_d\lambda_d + M_v\lambda_v$). and the FEC code by the equation given below.

$$THRO = (k/n)(P_s)(T_l) \qquad (5.25)$$

where (k/n) is the efficiency of the (n,k) code.

The blocking estimate is at this point determined from the probability of not having a successful packet transmission multiplied by the probability of trying to

transmit a packet or

$$B_l = P_{dp}(1-P_s) \tag{5.26}$$

The entire procedure must be done for every different input traffic load value and for various amounts of Backoff (transmitter waiting time). This enables us to view the cellular uplink channel capacity in many load environments and design features.

5.6 Performance

In this section the throughput, delay, and blocking characteristics of three different Spread-Spectrum systems will be examined for various FEC codes. The three systems selected are BFSK with 2 Hops/Symbol, BFSK with 4 Hops/Symbol, and 4-FSK with 2 Hops/Symbol. We compare the three systems on fair basis as shown in Figure (4.14) which requires that the total bandwidth (W_{ss}) and the bit rate R_d of each system be the same. For the analysis to follow, the spread-spectrum parameters were set at $W_{ss} = 2.048 Mhz$ and $R_d = 8 Kb/s$. Also the mobile transmitter's buffer is limited to 20 packets.

For convenience of notation, we will denote the Spread-Spectrum parameters for all three forms of network configurations as

System A: BFSK with 2 Hops/Symbol

System B: BFSK with 4 Hops/Symbol

System C: 4-FSK with 2 Hops/Symbol

In the first part of the analysis, a (63,45) BCH code with a correctability up to 3 bits in error/block and code rate of 0.714 was used on all three SS systems. To maintain fairness for all cases, the packet length is fixed at 504 bits, then with a (63,45) BCH code the number of blocks per packet is 8 each consisting of 63 bits. The extended Golay code consists of 24 bits/block, in keeping with a 504 bit packet a total of 21 Golay blocks (codewords) must be sent for each packet. The final error correcting code employed in this analysis is the (63,55) Hamming code which requires the same number of blocks/packet as the (63,45) BCH code. Depending on the code used the effective information rate is always less than 8 Kb/s due to the redundancy of the code. However, this is taken into consideration in the throughput analysis as in equation (5.22).

Figures (5.8) to (5.10) depict the throughput for System A , System B, and System C with various values of backoff (BO) possibilities (K_d =1,2,4,8,16). In this part of the analysis, the number of data users were confined to value of 10 with a probability of transmitting a packet during a packet time t_p of $\lambda_d = 8$. and only the $M_v \lambda_v$ component of the input load was allowed to vary enabling us to view the throughput performance of the cell as the voice users' load is increased. In Figure (5.8) (System A) it is clearly seen that as the value of K_d increases the throughput improves especially at higher loads. For lower load values (upto T_l =0.51), the amount of backoff given for the mobile transmitter did not have any effect since the throughputs followed the optimum load line up to a maximum throughput of 0.23. For backoff values of K_d = 1,2,4, the throughputs begin to decrease after diverging from the optimum load line whereas the throughputs for K_d = 8,16 increased slightly before sloping downward. The general consensus for all values of K_d is that the more backoff given to the transmitter the more gentle the degradation of the throughput.

System B in Figure (5.9) has similar performance characteristics to that of System A. For low loads, the load lines of Systems A&B have the same slope. Since System B has a higher bit error rate than System A, as expected, the maximum throughput of 0.18 for System B is less then system A. The value of the input network load corresponding to the throughput peak is at 0.22.

The best network capacity is achieved through System C in Figure (5.10) where the maximum throughput obtained is 0.78 at K_d = 16 and input load of 0.9. Comparing these figures, it is apparent that as the P_e decreases because of better SS design, the less steep the drop of the throughput becomes. It can also be said that as the channel error rate decreases, as we change the SS system parameters, less backoff will be required. So when a system is operating with a

high P_e more backoff is needed, but when the P_e is low (because of better SS system design), any additional backoff does not add much to the performance. Thus a tradeoff can be made between a transmitter with backoff or a more complicated receiver design.

The delay of the BFSK 2 Hops/Symbol system in Figure (5.11) portrays some quite interesting results. For low loads ($T_l = 0.38$) the delay is less for lower values of K_d. When the transmitter is permitted to backoff for less time the probability of packet delay is decreased for networks with longer backoff times. However, the opposite is true when the load increases ($T_l > 0.38$). In this case, when the transmitter backoffs for longer periods the delay actually decreases. The tapering of the delay curve to 18.68 as the load increases is due to the limitation of the buffer size of 20 stages.

System B delay characteristics in Figure (5.12) reacts quite similar to the delay characteristics of System A. Because of the larger P_e of system B, the benefits of BO are obvious. For low loads (less than $T_l = 0.28$), all curves respond in a similar manner with the lower valued K_d curves with slightly better response. After which curves for higher K_d values really show an improvement over the lesser ones.

Since System C has a relatively low P_e and backing off just seems to increase the probability of packet delay for all BO values shown in Figure (5.13). Now as K_d increases so does the delay. The nature of the delay curves leads us to deduce that BO is a burden for SS systems with low P_e and an asset for systems with high P_e or systems which operate under severe load conditions.

The delay of the network behaves as such because during low loads the probability of receiving a block in error after backing off is less than at higher loads, so any increase of BO just increases the delay. But as the traffic increases the low

BO transmitter will be jammed again with a high probability if it does not wait. This leads to retransmission of the entire packet and will be requested by the base receiver and will augment the uplink channel delays.

If the packet is delayed indefinitely it is considered to be blocked with no chance of being received by the base station. The probability of a blocked packet for systems A, B, and C are displayed in Figures (5.14), (5.15), and (5.16) respectively. The results of the packet blocking in the cell uplink channel are similar for all of the three SS systems. There is almost no packets blocked in System A until the load reaches 0.38, 0.28 for System B, and 0.75 for System C which are obtained when the throughput begins to slope downward. It is seen that blocking increases more rapidly as the probability of error increases.

Up to this point we have considered only the throughput, delay, and blocking characteristics of the Spread-Spectrum uplink channel as the voice users' contributions are increased. Due to the different methods of handling data and voice users, the cellular channel is some what dependent on the type of input traffic load present. To further examine how the SS cell operates, the $M_v \lambda_v$ component of the input load is held constant while the $M_d \lambda_d$ component is allowed to vary.

We first survey the results obtained for the throughput of system A, Figure (5.17). The number of voice users are confined to 20 with a probability of transmitting a packet during a packet time of 0.8. Throughput curves for $K_d = 1,2,4$ react similarly to what was obtained when only the $M_v \lambda_v$ component was varied for system A in Figure (5.8). But in this case, the maximum throughput is only 0.32 which is less than when only the voice users were varied. It is also seen that as the value of K_d increases the throughput curves tilt downward rather sharply.

System B however, portrays different results (Figure (5.9)) when the possibil-

lty of BO is 4 packet times and the load is determined mainly on the data user traffic. In this case the throughput performance is actually worse than it is for $K_d = 2$ (at high loads) which is contrary to the results obtained in System A. The throughput for $K_d = 4$ advances beyond the performance of the curves for $K_d = 1,2$ to a value of 0.32 after which it decreases rather sharply and eventually becomes less than the performance of $K_d = 2$. It is observed that the throughput suffers as the number of data users and the BO level increases. To explain this, we consider a uplink channel of a single cell with many data users backing-off for longer periods, but during retransmission they interfere with other data users once again. In a uplink channel with increasing number of voice users, the data users can retransmit their packet (upon request) with less chance of hitting a voice users.

The above performance trends are also observed in Figure (5.19) where System C is subjected to varying data users. The maximum throughput obtained is 0.78 which is much higher then the value obtained when the input load was determined many by the voice users (Figure (5.13)). But again the the performance decreases rapidly after obtaining its maximum level.

The delay characteristics for Systems A are shown in Figure (5.20). As expected the packet delays are longer for higher traffic load values and for uplink channels whose transmitters backoff for longer times. For lower loads we see that the least amount of packet delay occurs when BO is minimal. One interesting note for System A is when the input load is 0.36 all of the BO curves intersect at a delay value of 10 packet times. This behaves as a crosspoint where depending on the expected load value of the uplink channel, the choice of K_d is determined to select a suitable delay.

The delay characteristics for Systems B and C in Figures (5.21) and (5.22)

are similar to each other, since they show a dramatic response for low values of BO. Examining first the delay of the System B when $K_d = 1$ we see that the probability of packet delay is almost zero for load values less then 0.28 and shoots up to a delay of 17 when the load is slightly increased to 0.29. This gives an impression that higher BO waiting times are required when many data users are active on the uplink channel.

A dramatic increase in packet delay is also apparent in System C for $K_d = 1$. At the load value of 1, the delay begins to increase and continues to do so quite rapidly until it reaches a packet delay of 13.0 at an input load of 1.12.

In both of the latter cases, the delay curves for high BO possibilities increase smoothly.

Blocking characteristics for the three systems can be seen in figures (5.23), (5.24), and (5.25). The general behavior is equivalent to what we previously observed for the three systems as the $M_v \lambda_v$ component was varied. The larger the value of BO, the lesser the probability of unsuccessful packet transmission.

Upto this point we have discussed the cellular uplink channel throughput performance, delay, and blocking characteristics using a (63,45) BCH code with a correctability of 3 bits in error/block. Concentrating on the 2 Bank with 4 Hops/Symbol (System A) spread-spectrum uplink channel, we shall examine the system performance using differing error correcting codes.

The throughput performance of System A in Figure (5.26) is determined using a (63,55) Hamming error correcting code with a correctability of 1 bit/block. Even though the code rate for the (63,55) Hamming code of 0.846 is greater than the code rate of the (63,45) BCH code (0.78), the maximum throughput obtained using the BCH code is greater. When employing a Hamming code the throughput suffers because the number of correctable bits in error is

much less and more retransmissions of entire packets are requested lowering the effective throughput. The results for the Golay code in Figure (5.27) strengthens this argument further, with a maximum correctability of 4 bits in error per block and a code rate of only 0.5, the maximum throughput obtained is 0.30. Clearly, as the number of correctable bits per block increase the throughput performance improves regardless of the redundancy introduced.

Blocking curves shown in Figures (5.28) and (5.29) for the Hamming and Golay codes depict some interesting results. Using a (63,55) Hamming code the cross-over delay curves are obtained as we saw in Figure (5.12) using the (63,45) BCH code. But when we introduce a code that has a higher correctability such as the Golay code, the cross-over is less apparent but still exists. Now the delay for higher values of BO is worst for all load values except for higher load values where the lower values of K_d show less delay.

Finally we compare the packet blocking characteristics of system A using Hamming and Goley codes respectively. From examining the figures, a general consensus is made for the two graphs. As the correctability is reduced, the probability of packet blocking is lower for low values of K_d during small load values. However, the blocking increases for high K_d values during intense load conditions. When the error correcting code used is more powerful, the above consensus is less apparent.

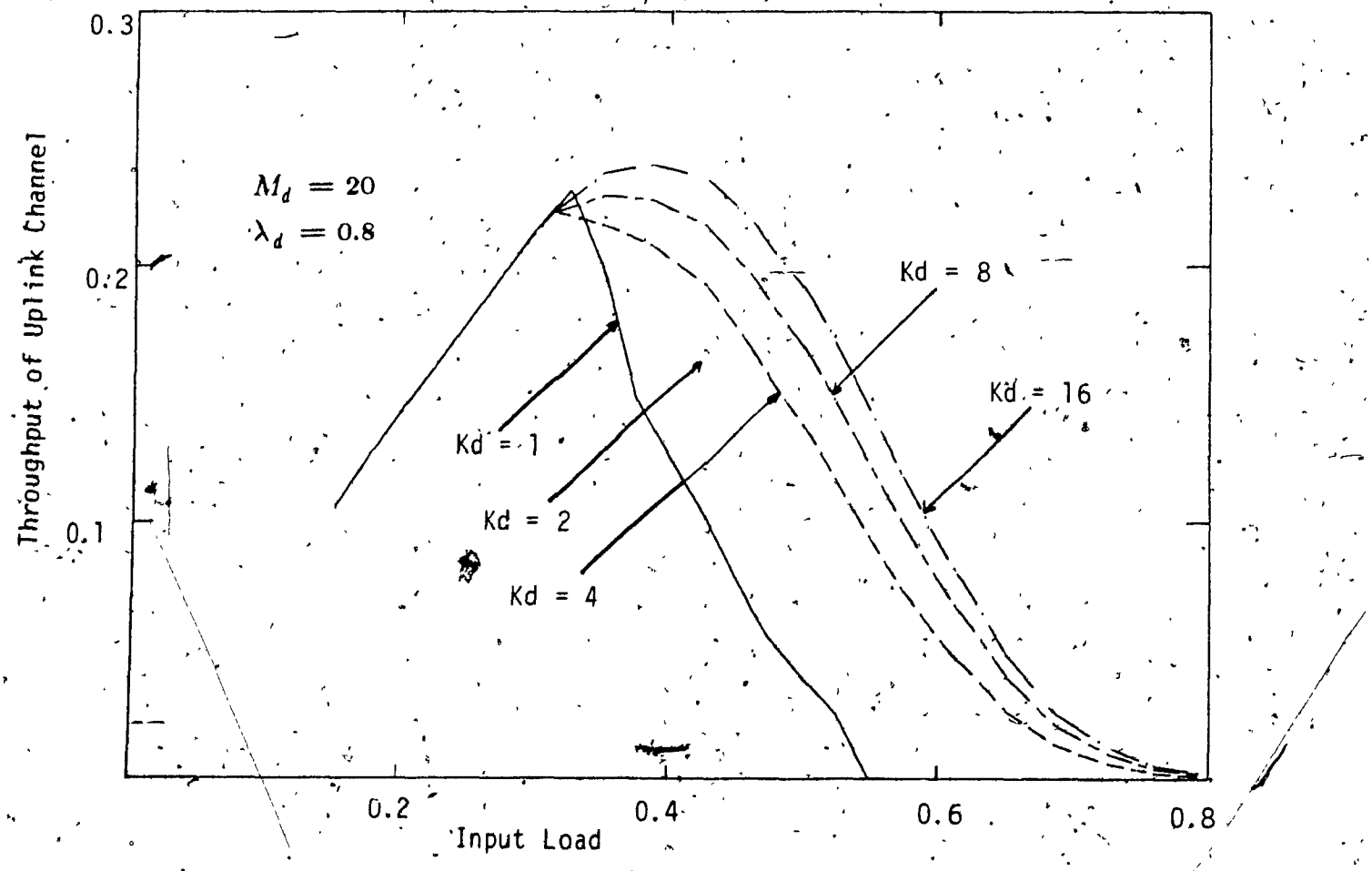

Figure (5.8) Throughput Performance of The Cellular Uplink Channel For a BFSK 2-Hop/Symbol Spread-Spectrum System (System A).

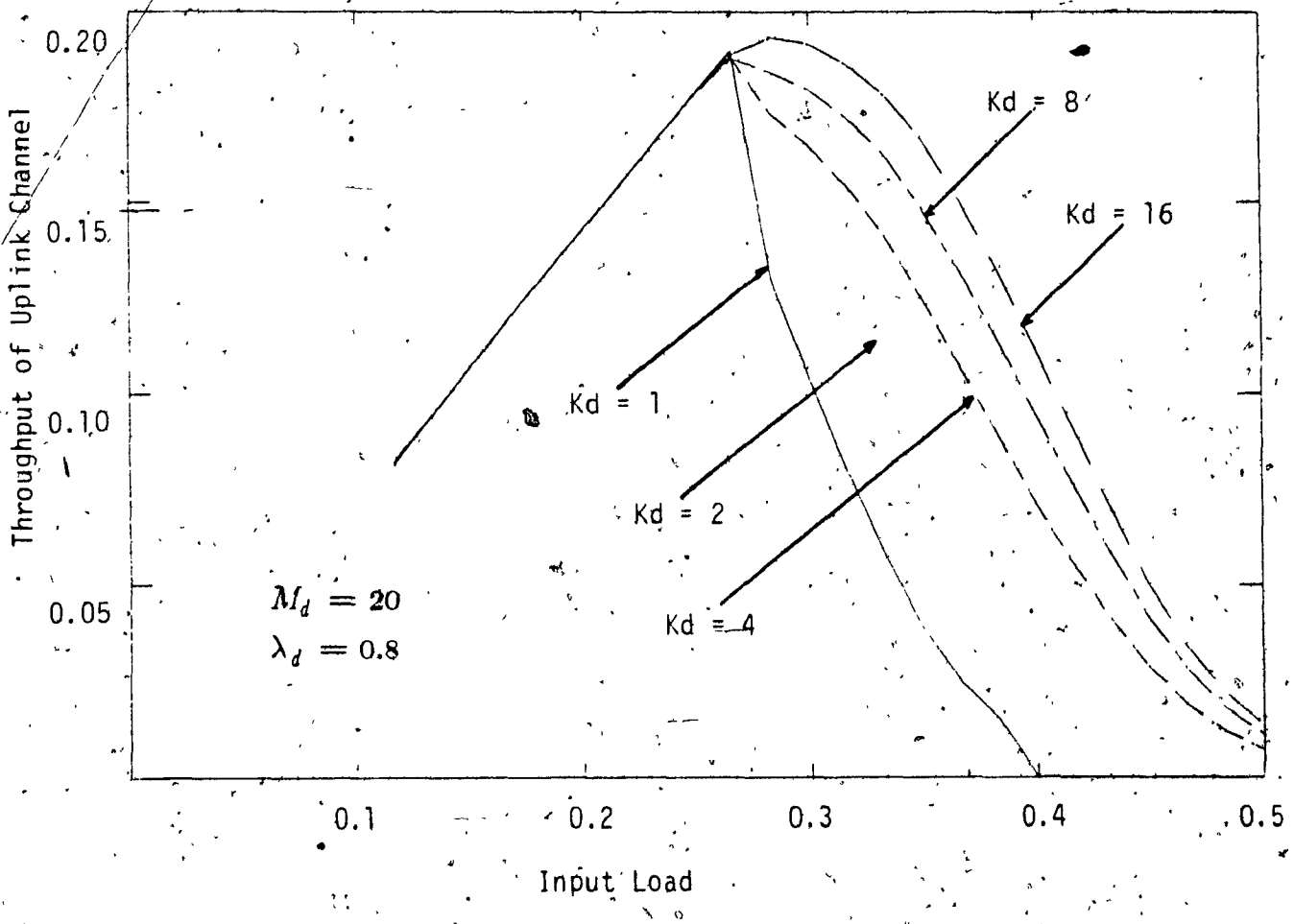

Figure (5.9) Throughput Performance of The Cellular Uplink Channel For a BFSK 4-Hop/Symbol Spread-Spectrum System (System B).

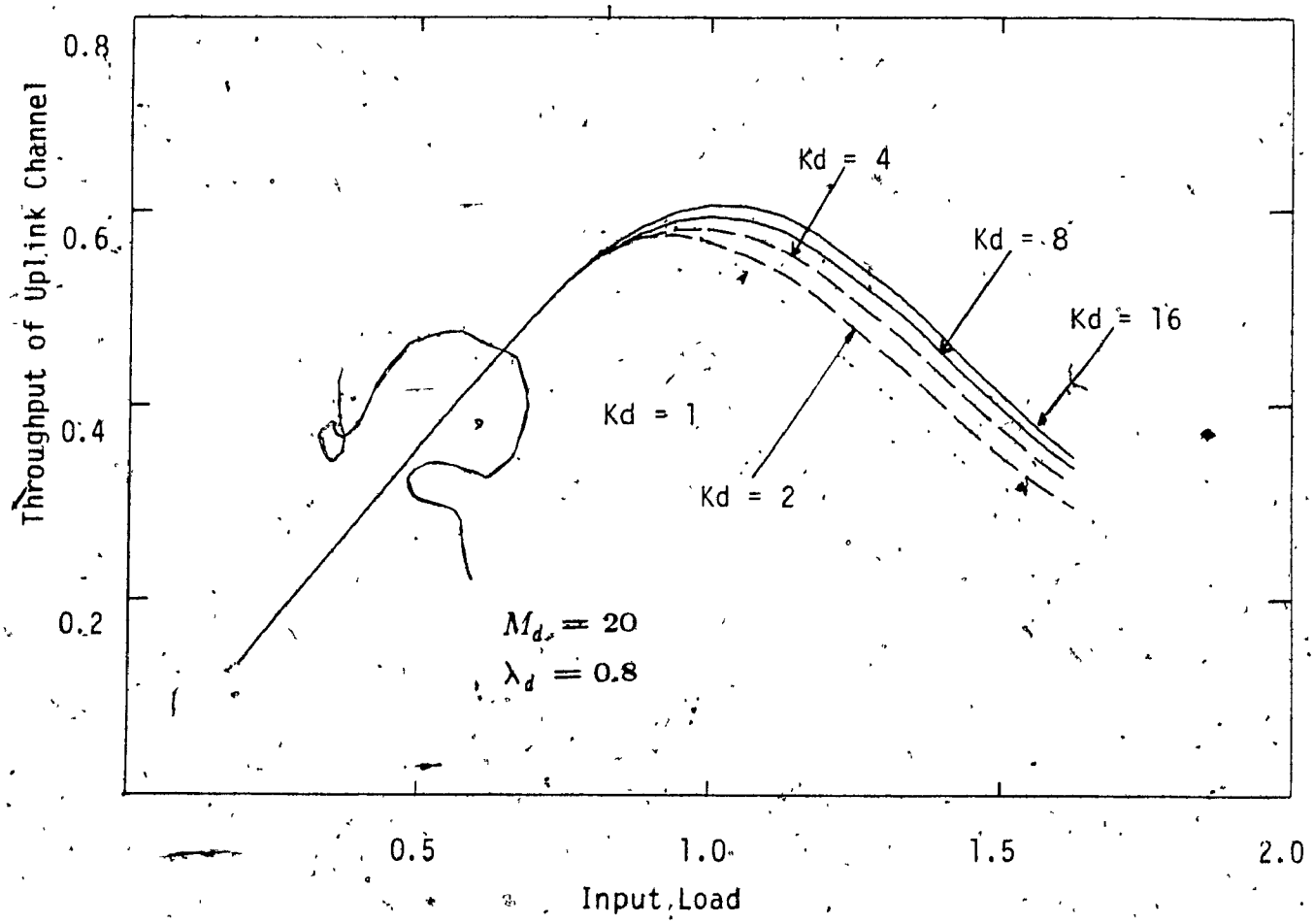

Figure (5.10) Throughput Performance of The Cellular Uplink Channel For a 4FSK 2-Hop/Symbol Spread-Spectrum System (System C).

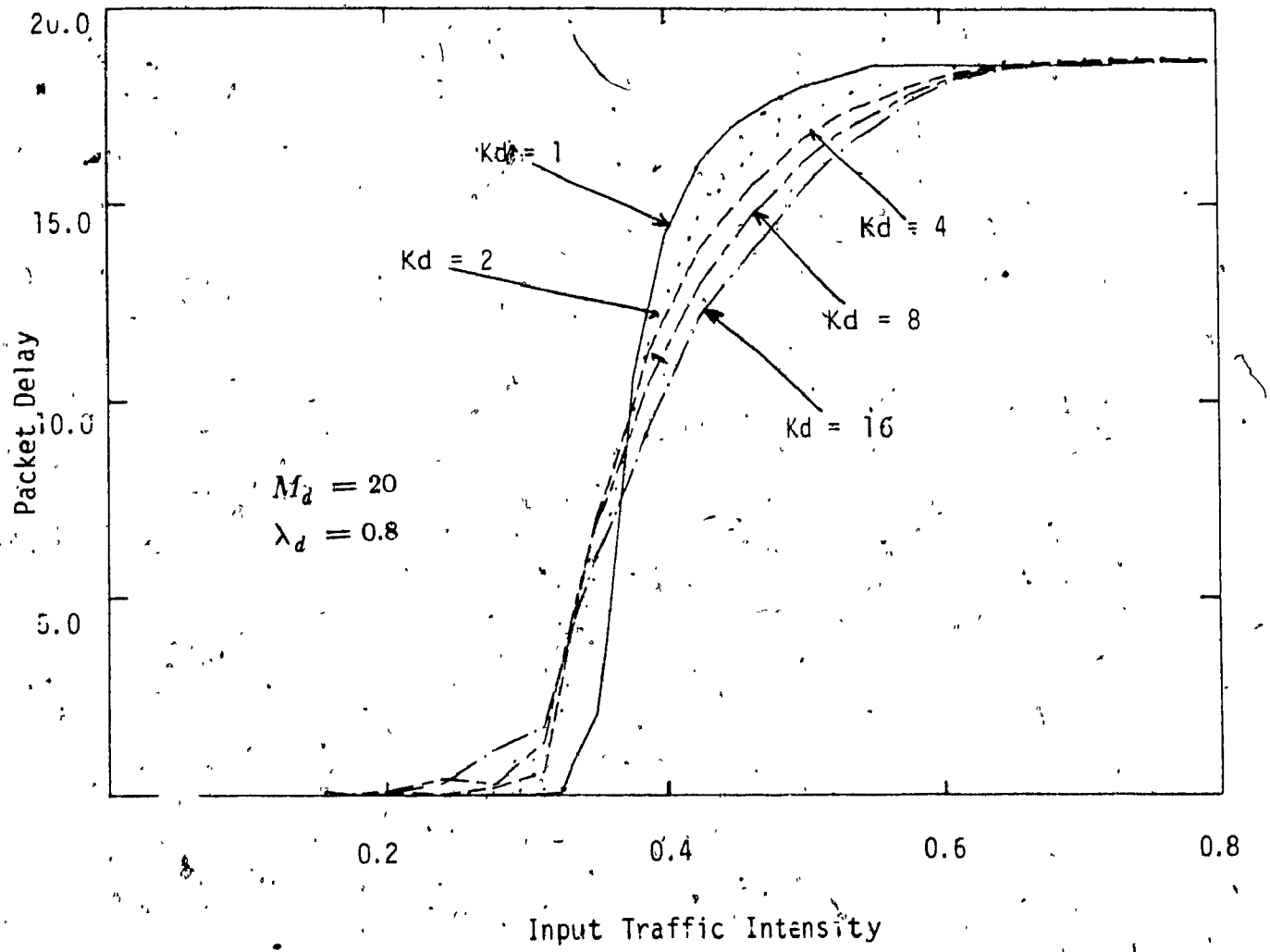

Figure (5.11) Delay Characteristics of The Cellular Uplink Channel For System A.

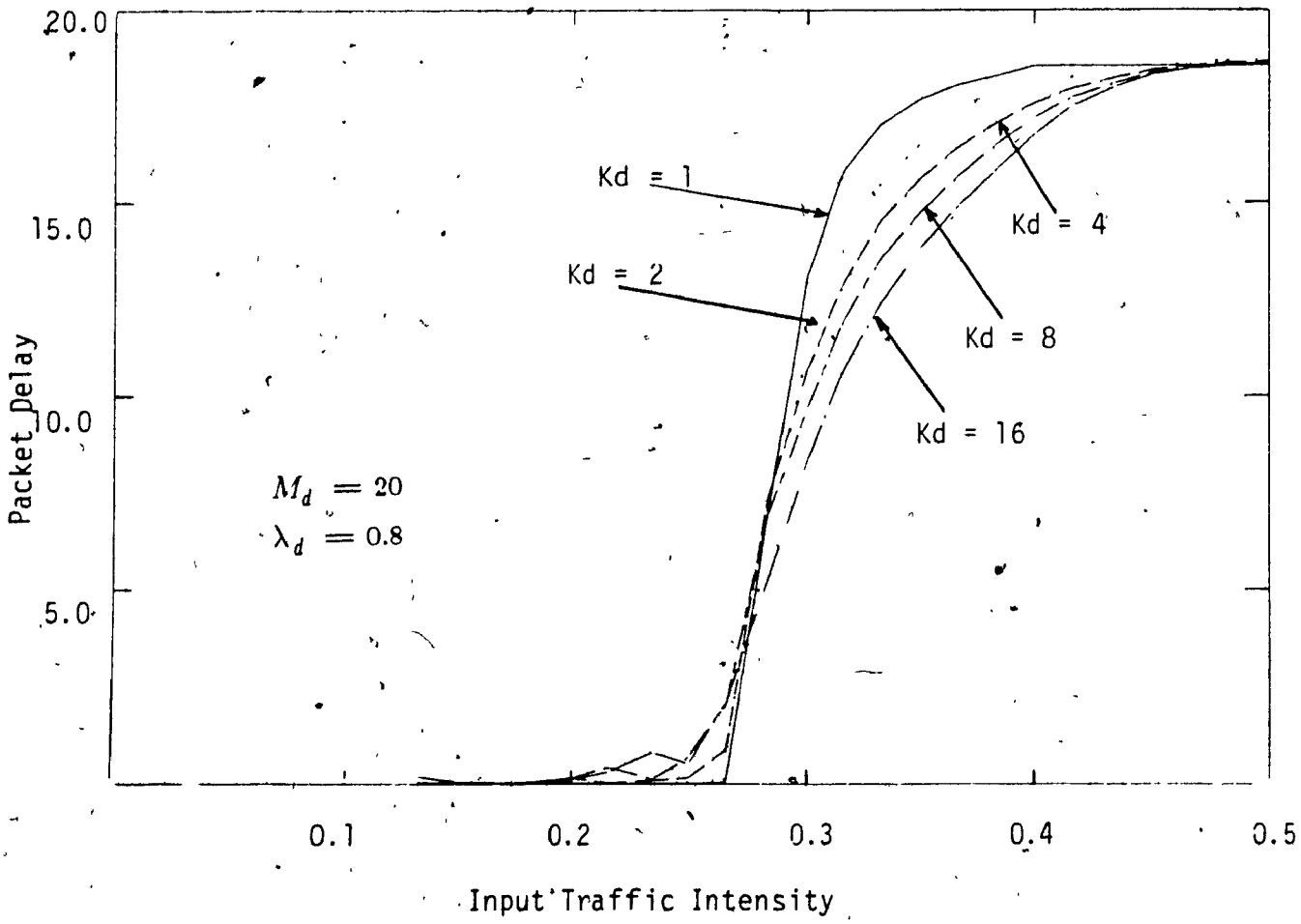

Figure (5.12) Delay Characteristics of The Cellular Uplink Channel For System B.

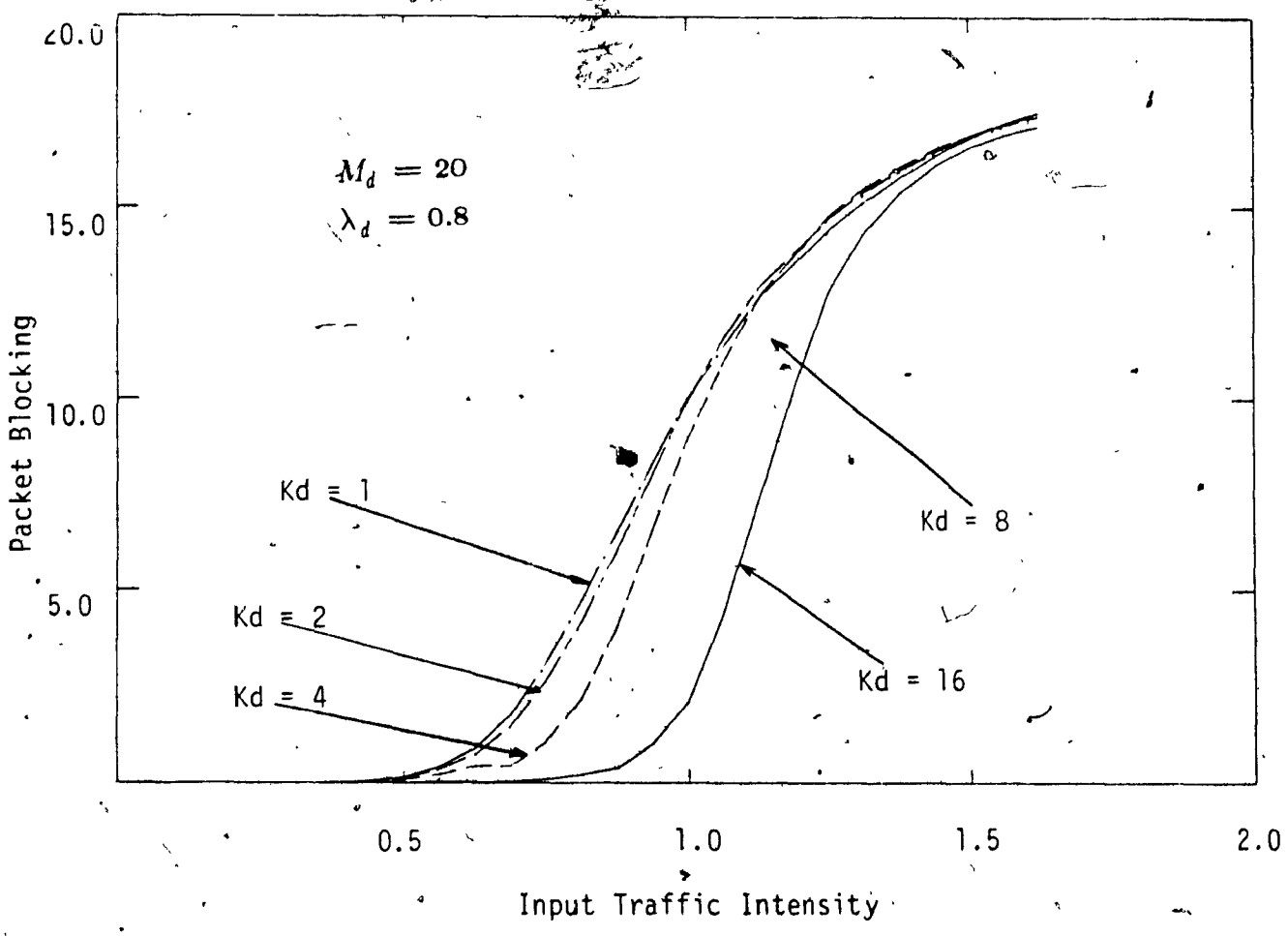

Figure (5.13) Delay Characteristics of The Cellular Uplink Channel For System C.

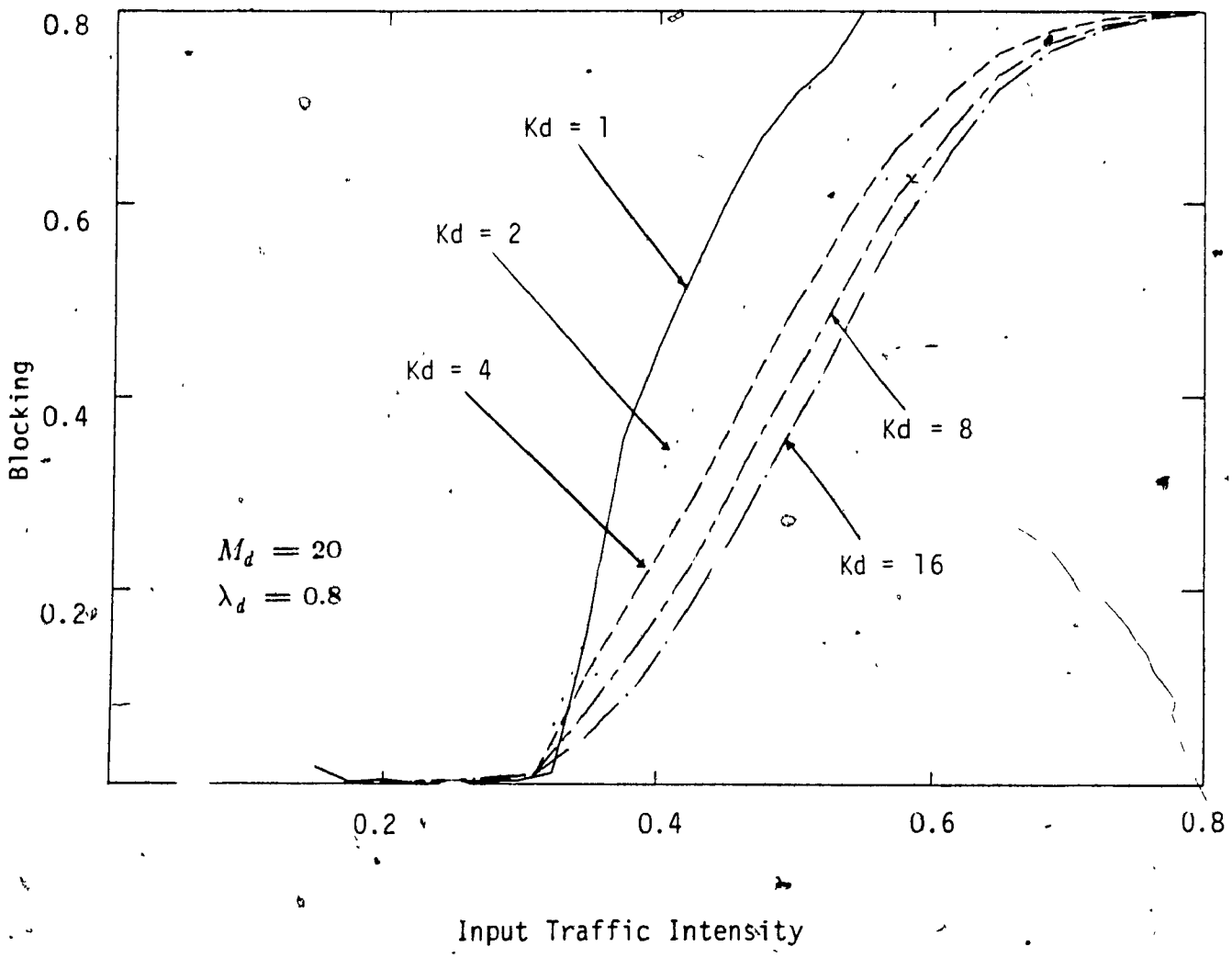

Figure (5.14) Blocking in The Cellular Uplink Channel of System A.

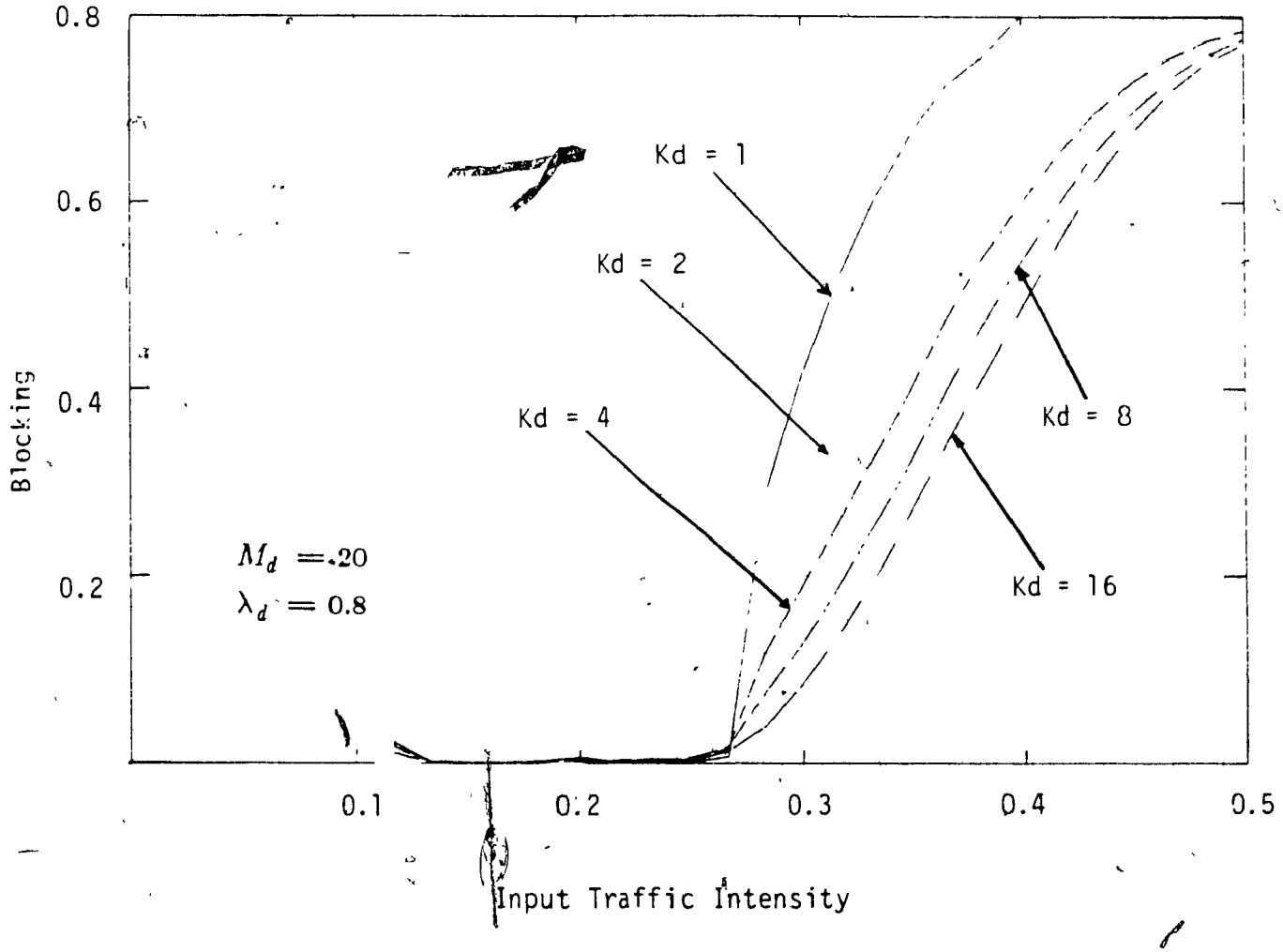

Figure (5.15) Blocking in The Cellular Uplink Channel of System B.

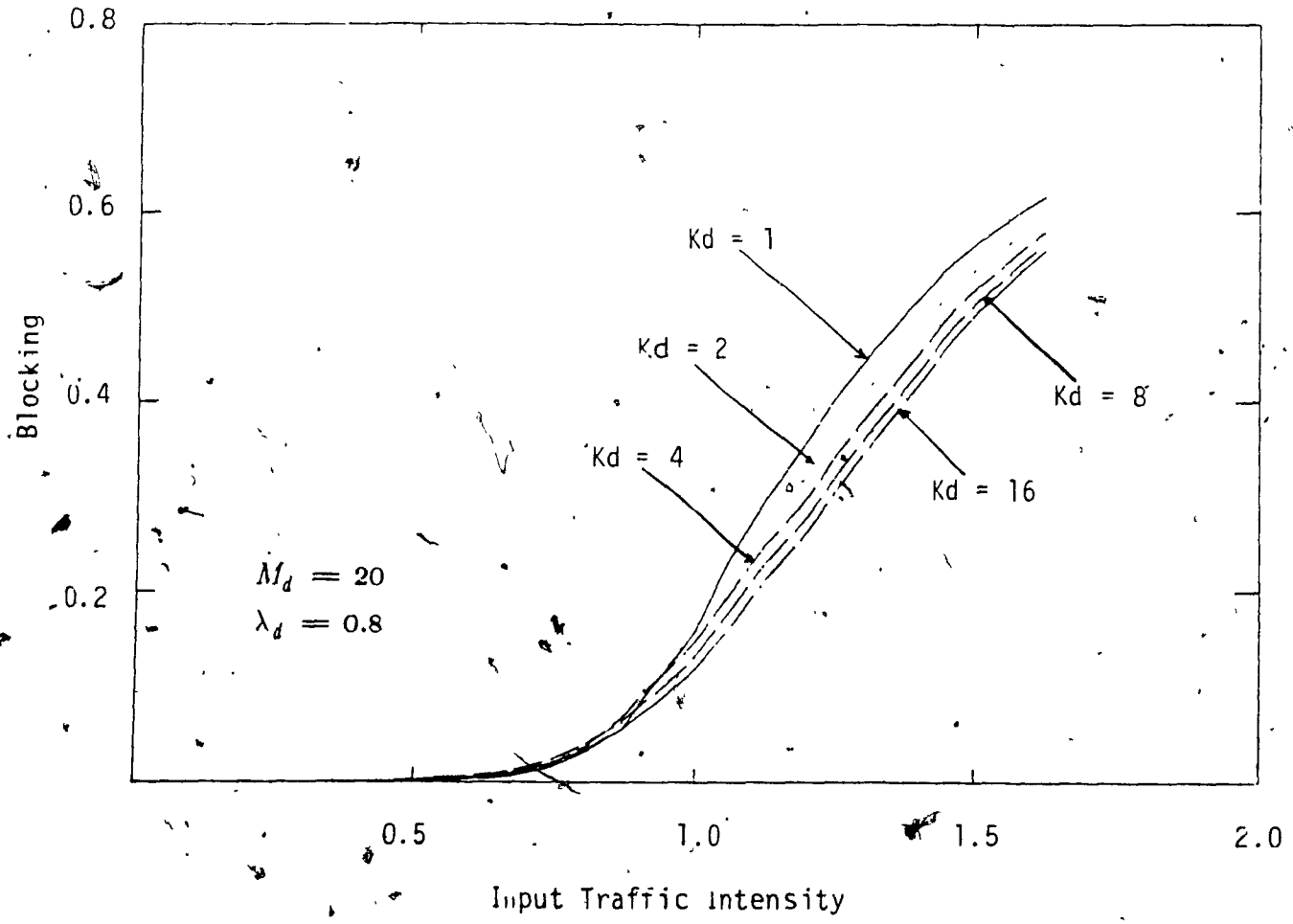

Figure (5.16) Blocking in the Cellular Uplink Channel of System C.

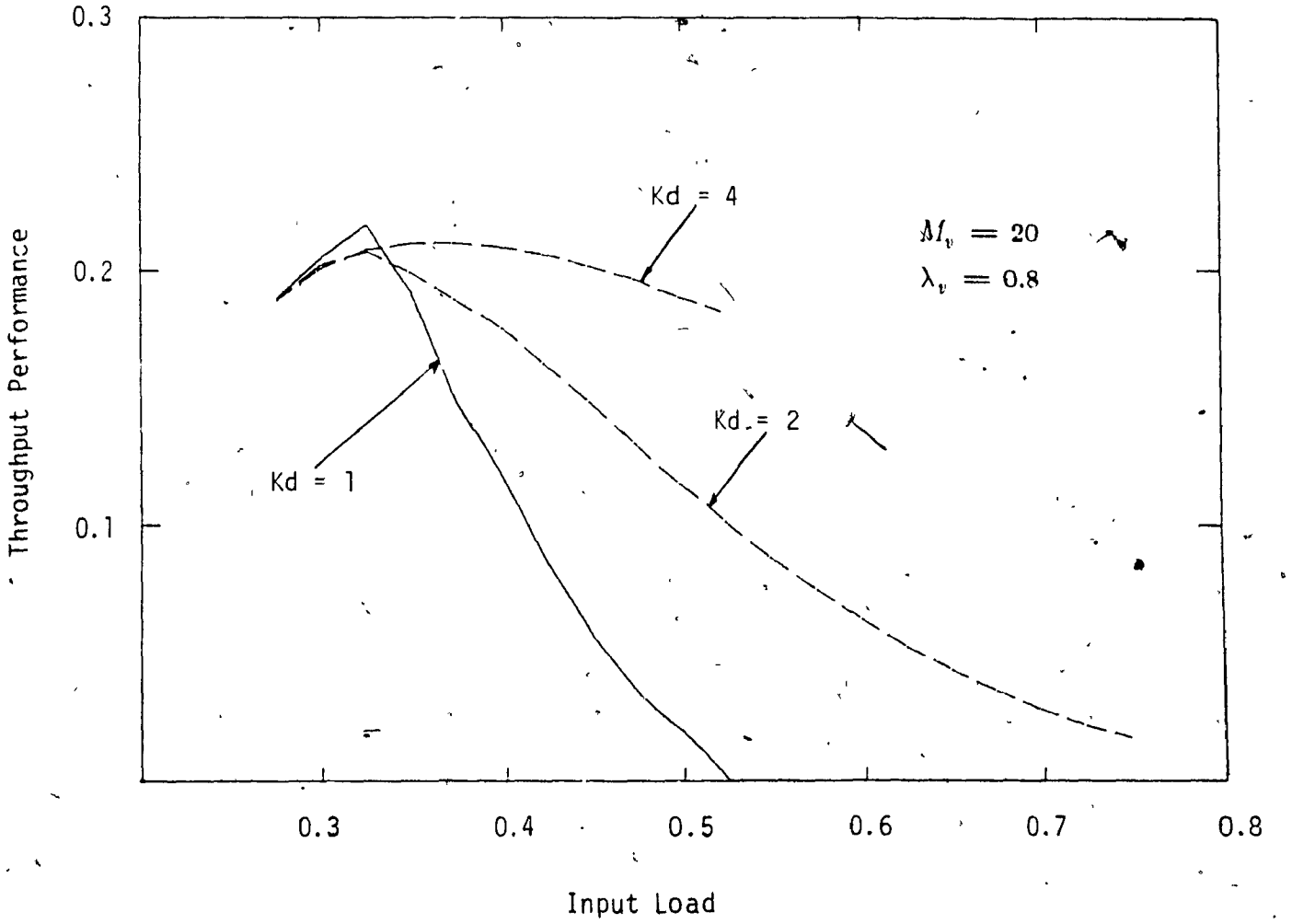

Figure (5.17) Throughput Performance of a BFSK 2-Hops/Symbol Spread-Spectrum System (System A) When The $M_d \lambda_d$ Component of The Load Varies.

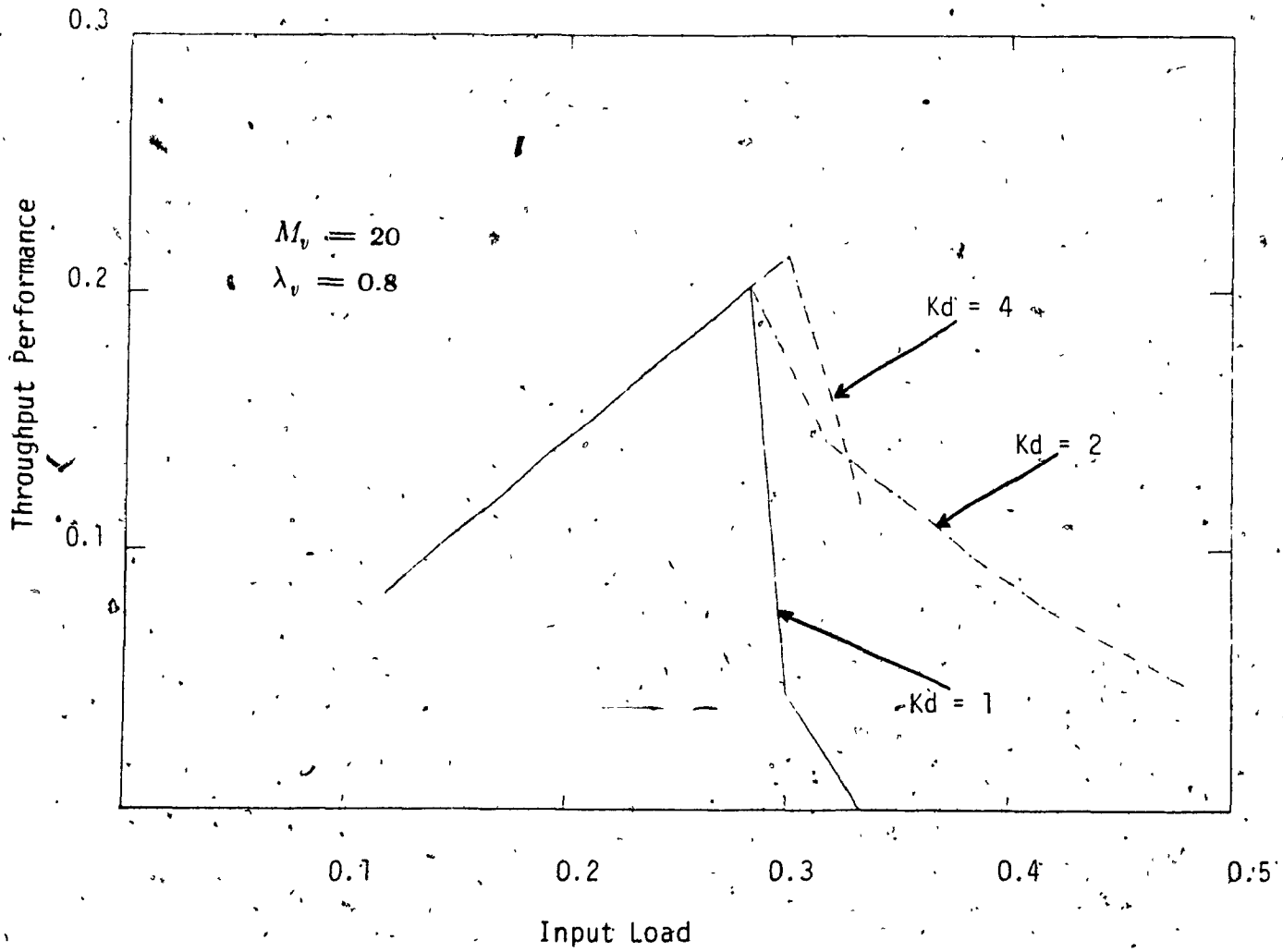

Figure (5.18) Throughput of The Cellular Uplink Channel For a BFSK 4-Hop/Symbol Spread-Spectrum System (System B) When The $M_d \lambda_d$ Component of the Load Varies.

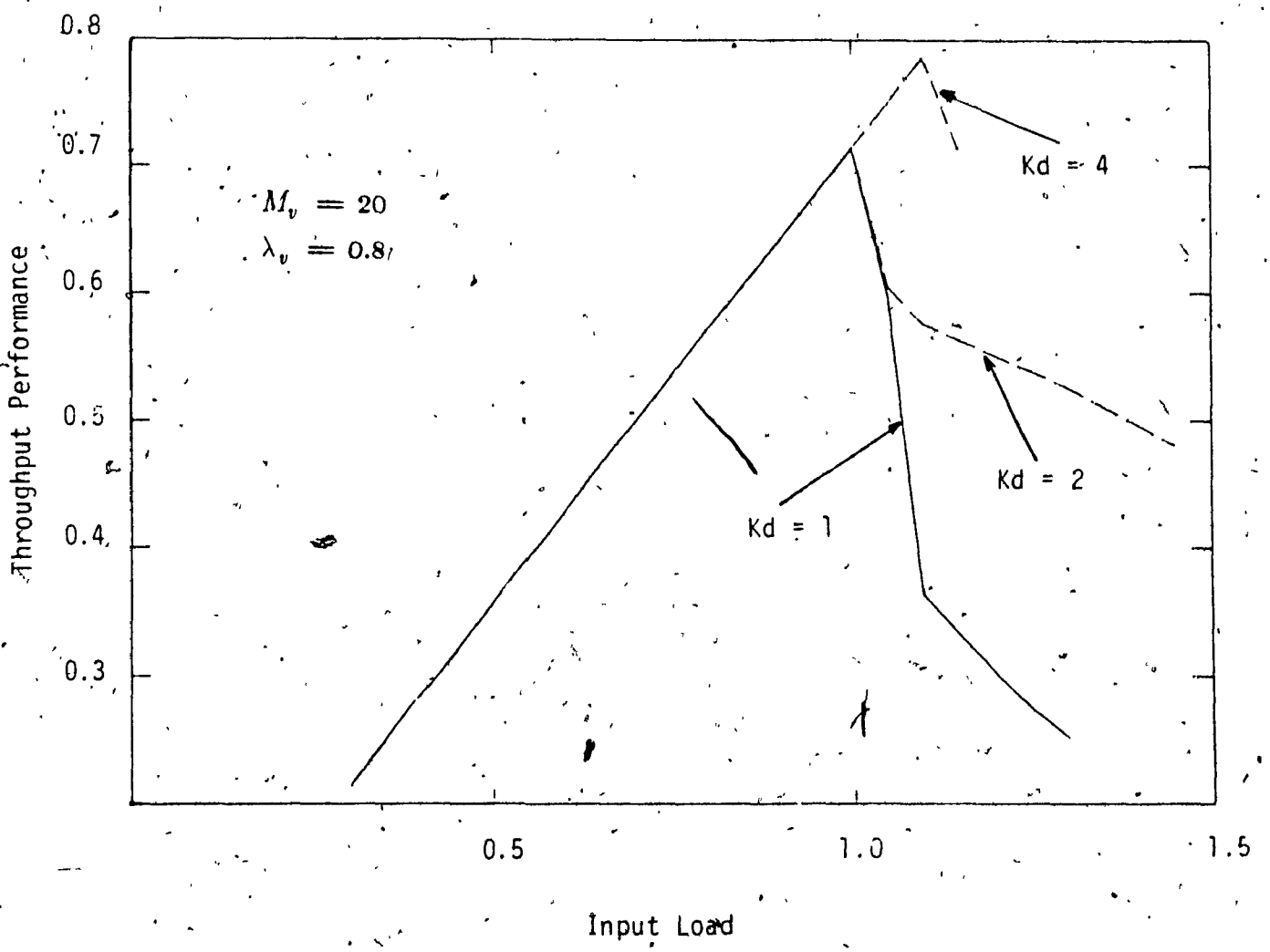

Figure (5.19) Throughput Performance of The Cellular Uplink Channel For a 4FSK 2-Hop/Symbol Spread-Spectrum System (System C) Changing The $M_d \lambda_d$ Component of The Load.

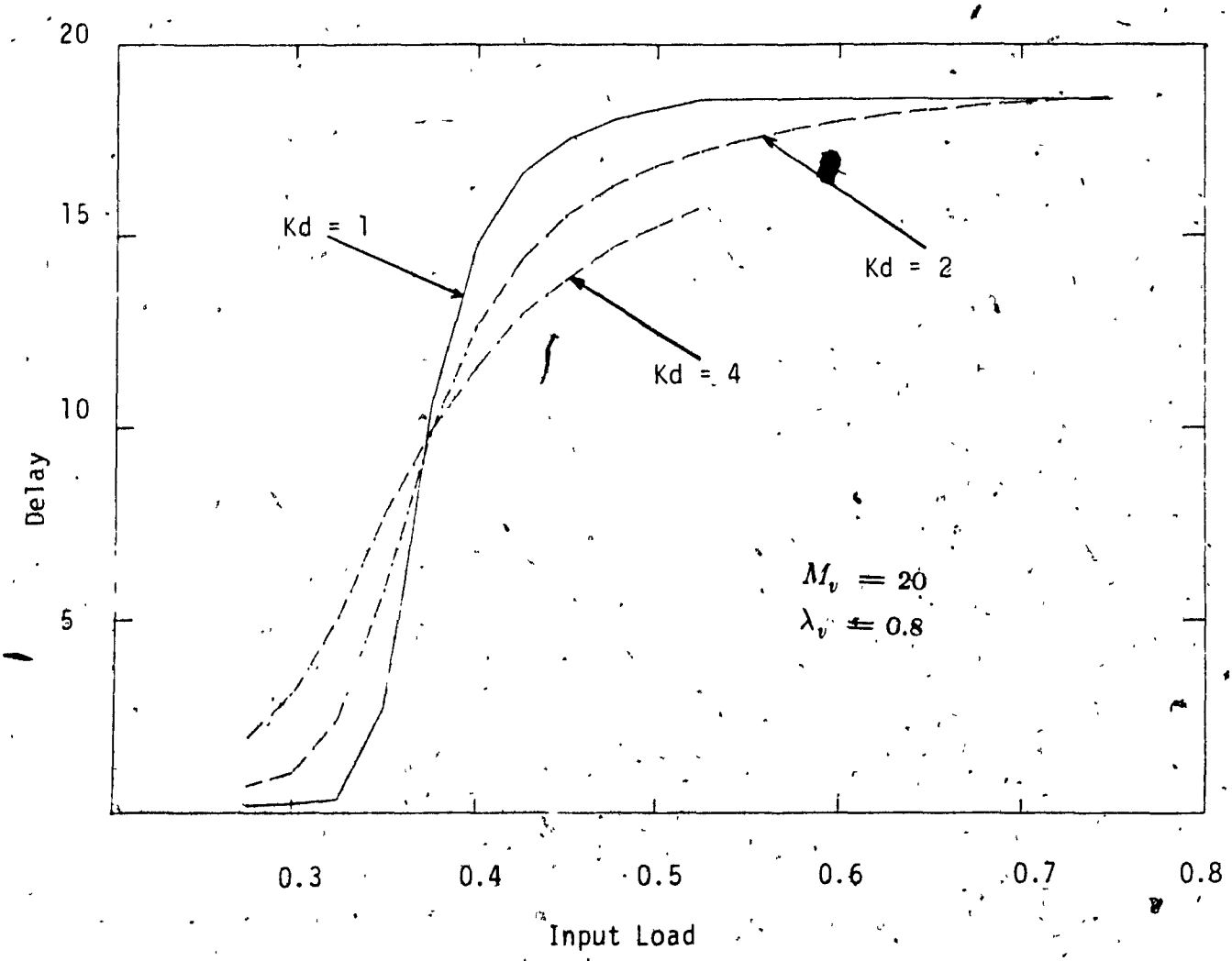

Figure (5.20) Delay Characteristics of The Cellular Uplink Channel For System A While Varying $M_d \lambda_d$.

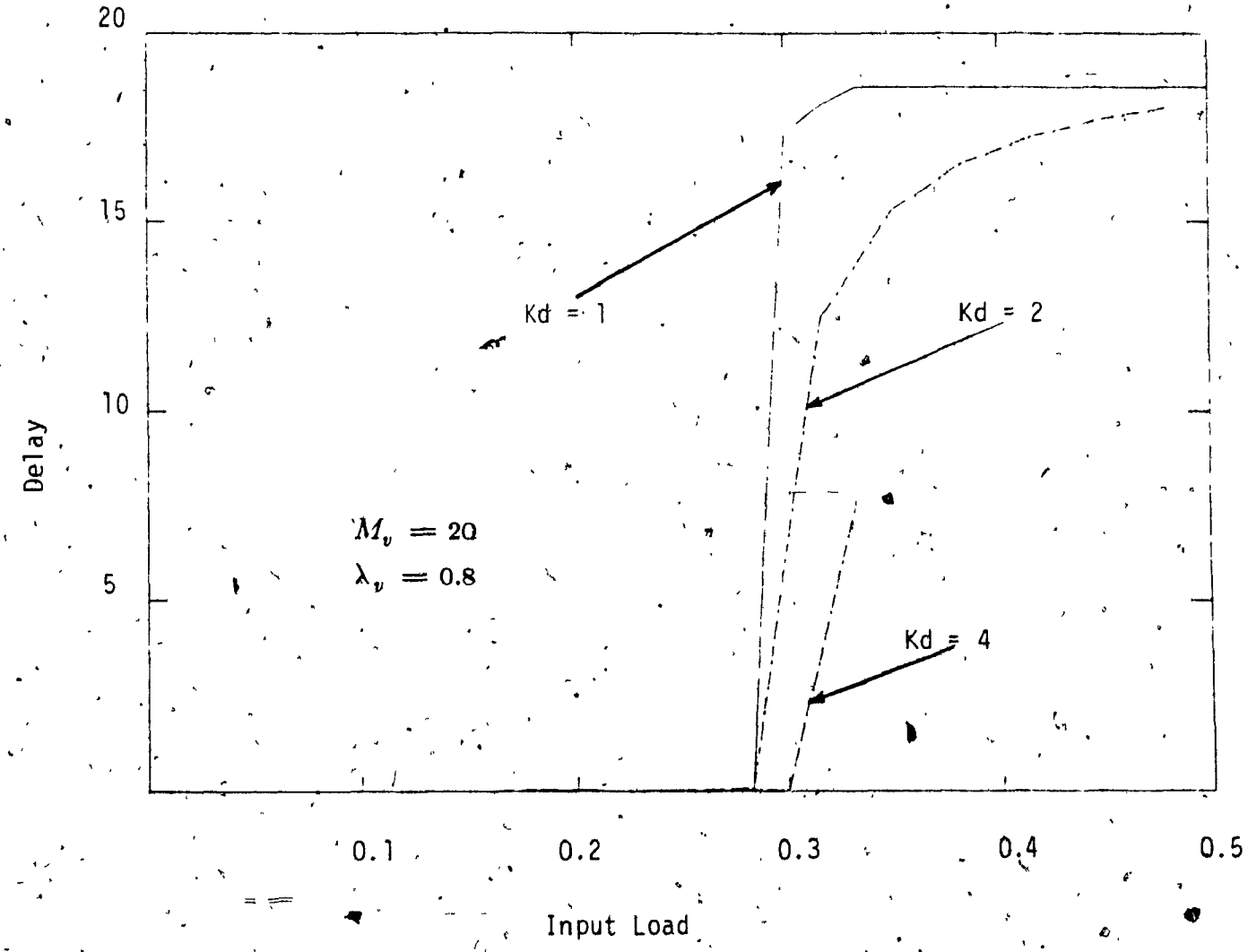

Figure (5.21) Delay Characteristics of The Cellular Uplink Channel For System B While varying $M_d\lambda_d$.

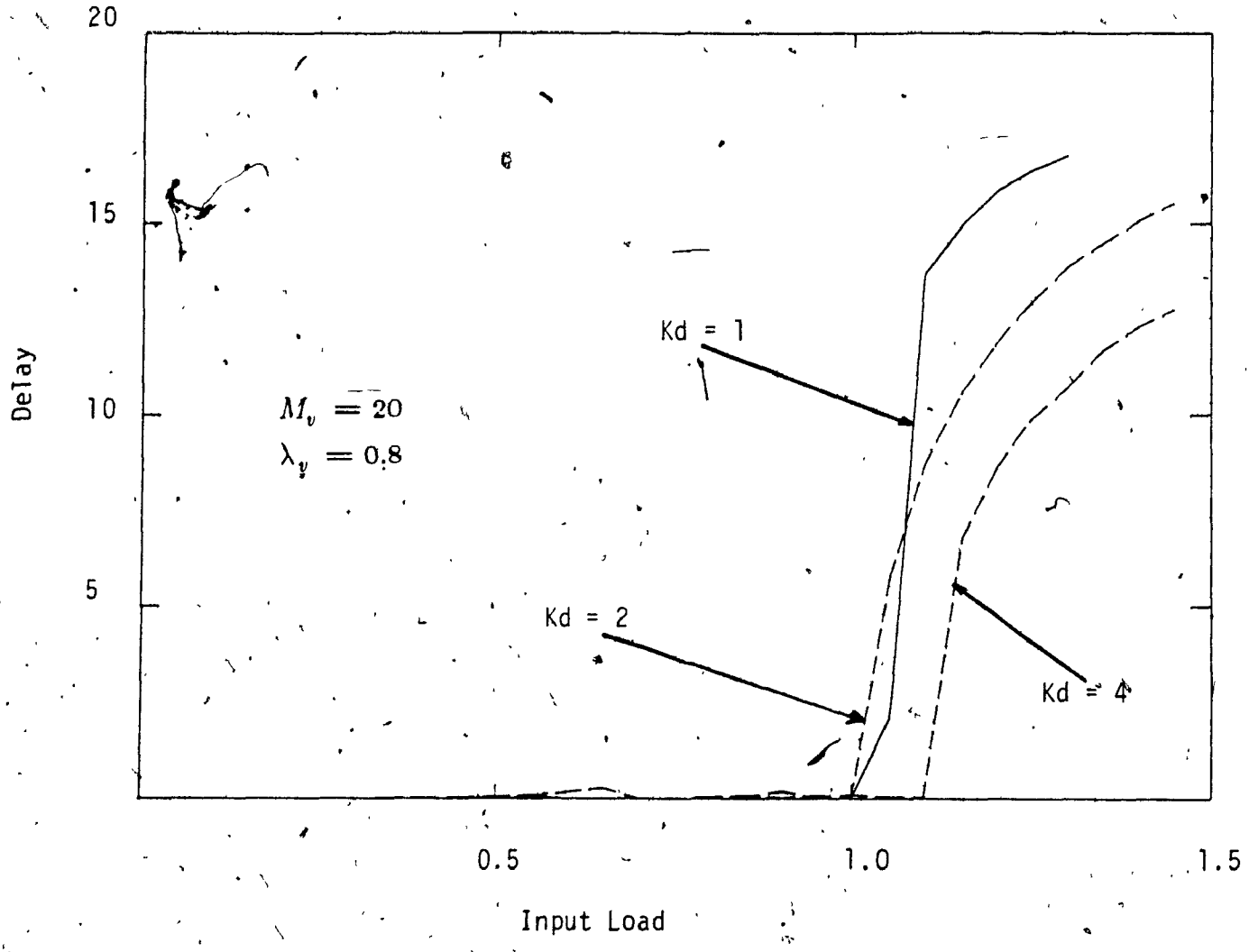

Figure (5.22) Delay Characteristics of The Cellular Uplink Channel For System C While Varying $M_d \lambda_d$.

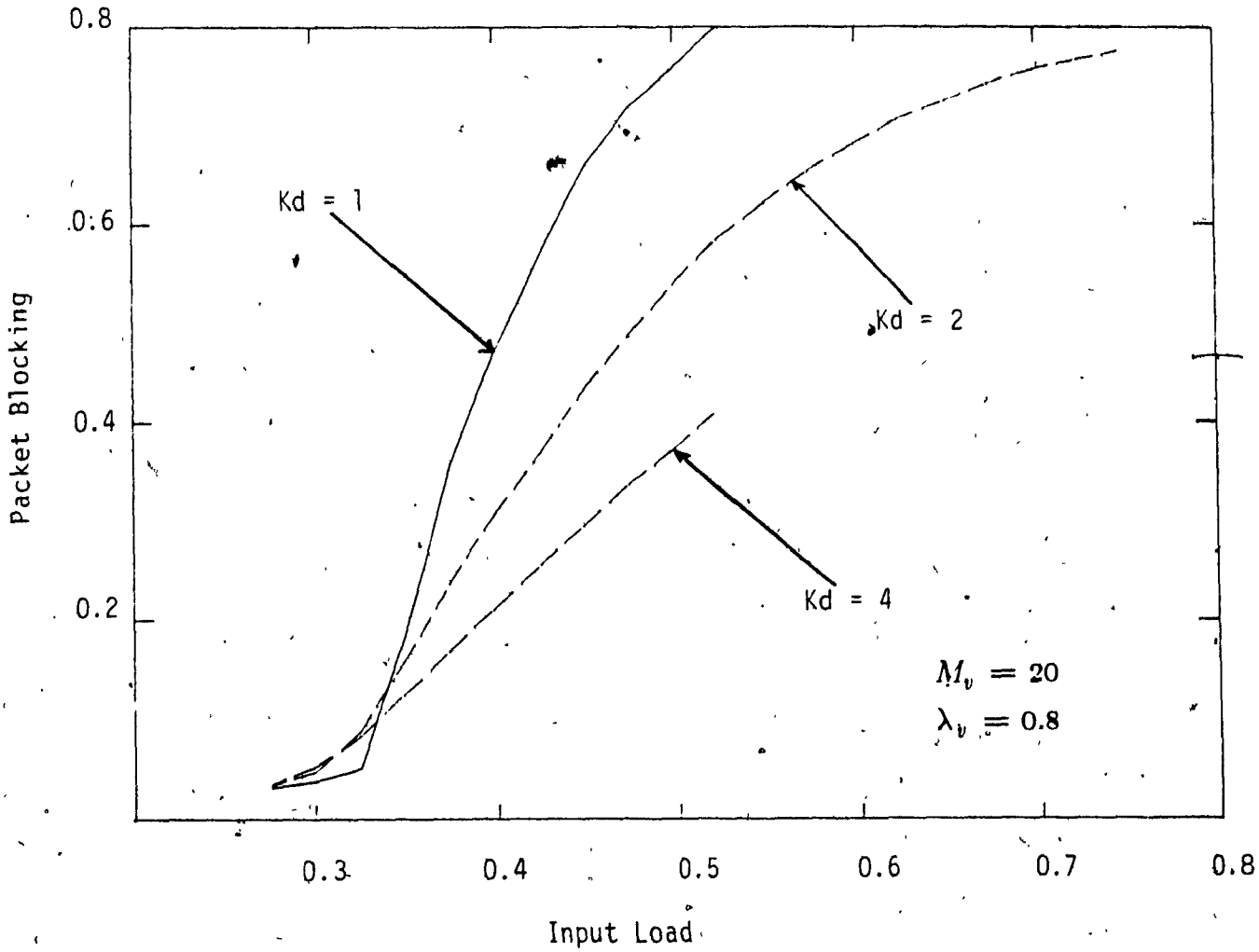

Figure (5.23) Blocking In The Cellular Uplink Channel of System A. While Varying The $M_d \overline{\lambda_d}$ Load Component.

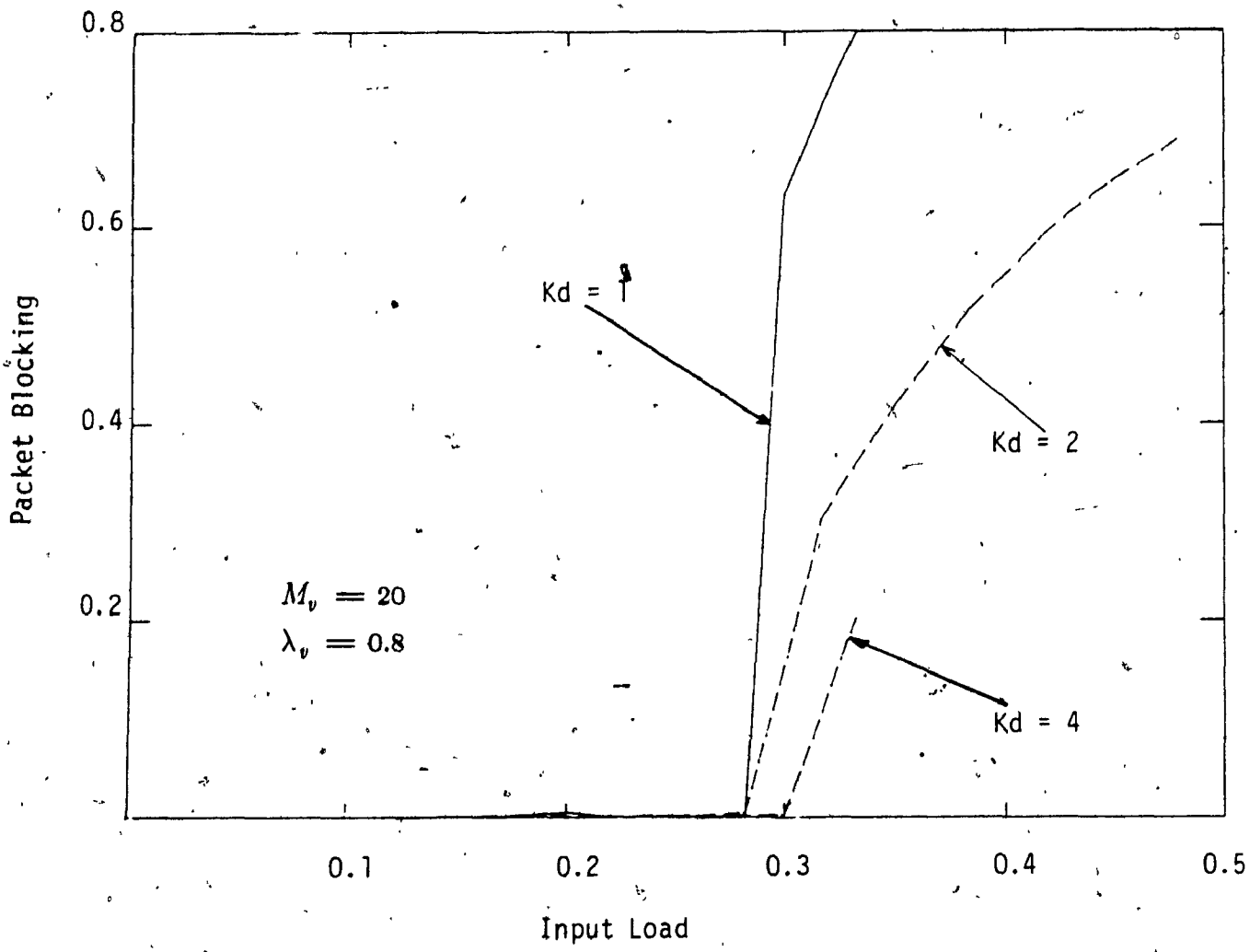

Figure (5.24) Blocking in The Cellular Uplink Channel of System B. While Varying The $M_d \lambda_d$ Load Component.

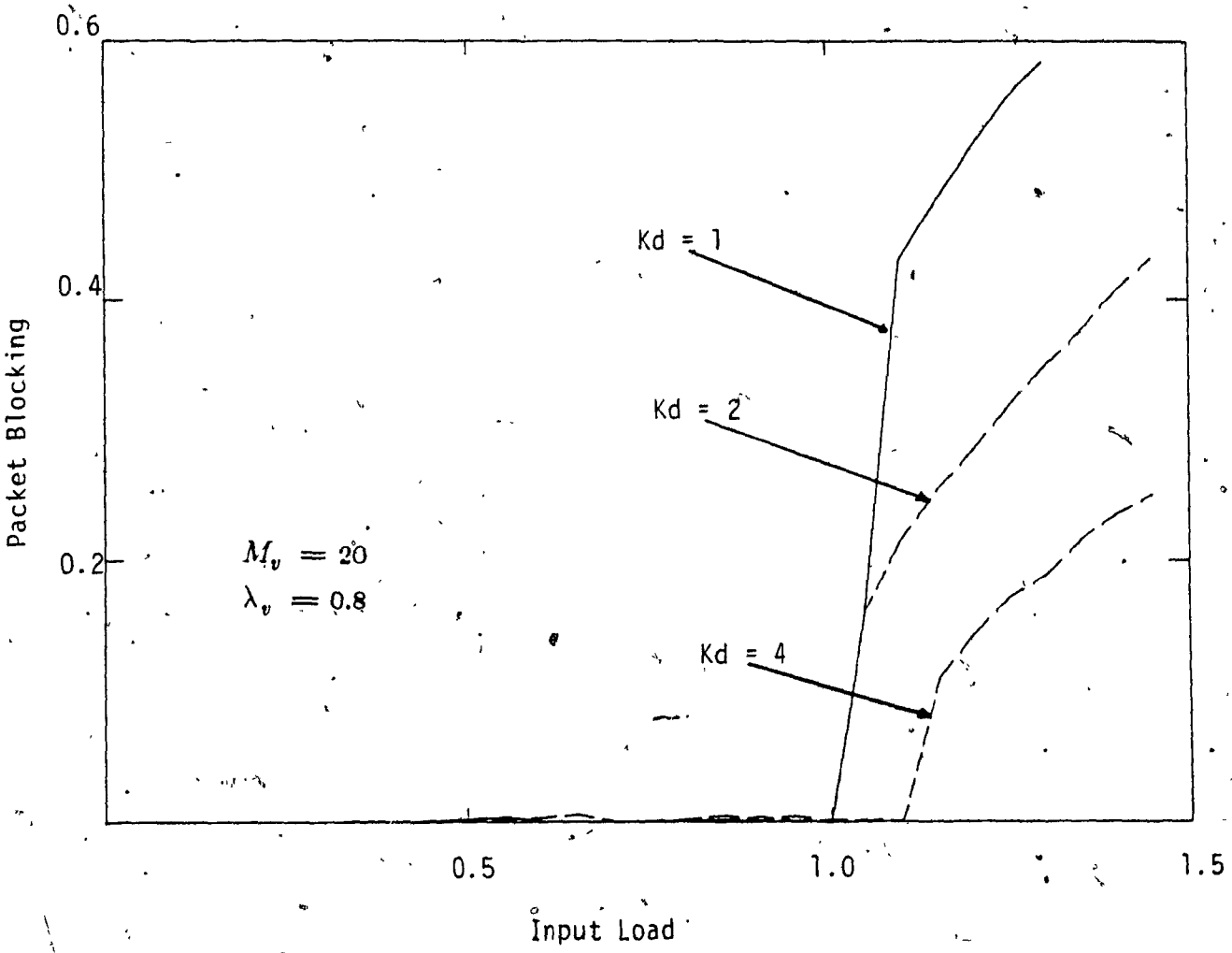

Figure (5.25) Blocking in the Cellular Uplink Channel of System C. While Varying The $M_d \lambda_d$ Load Component.

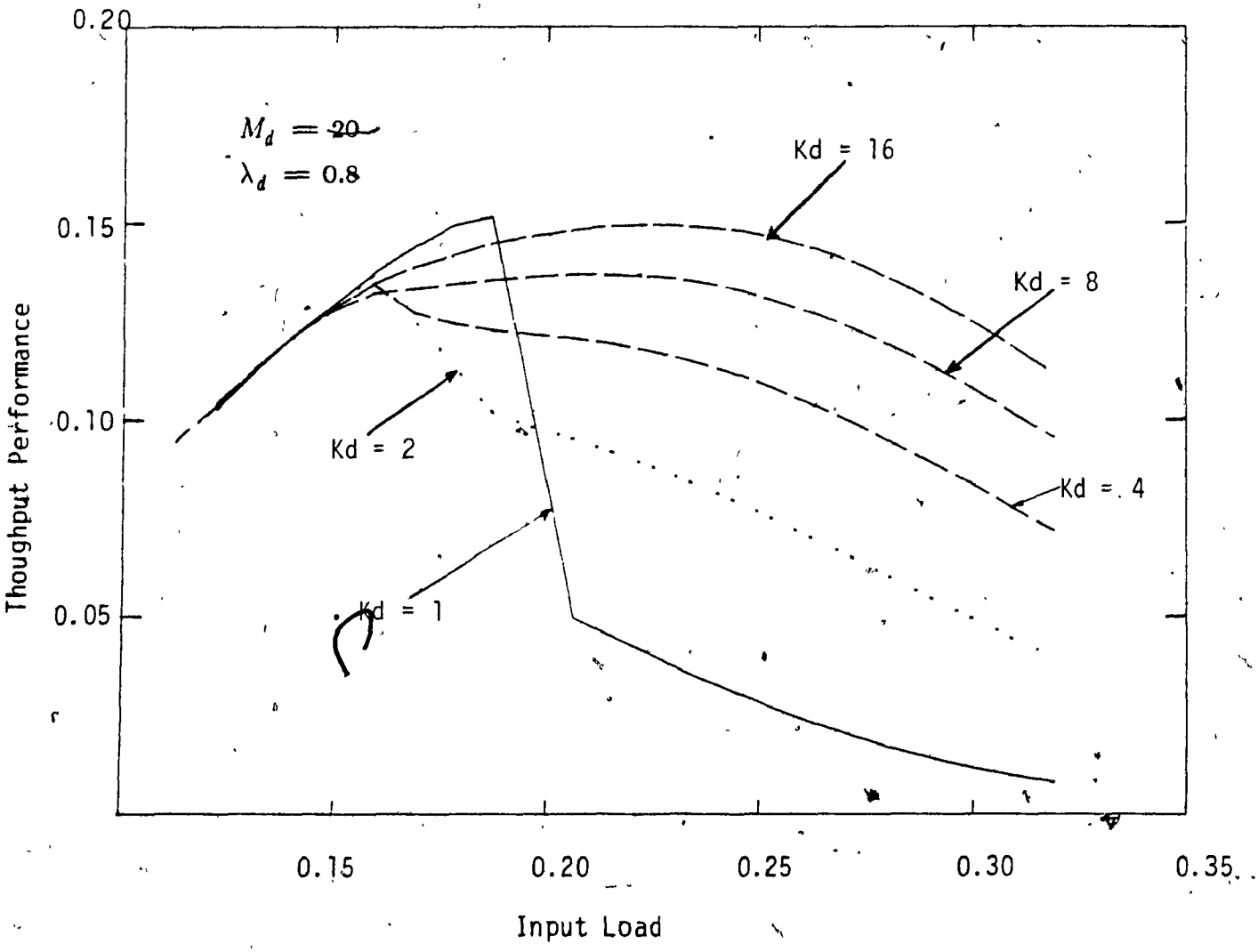

Figure (5.26) Throughput Performance of System A Using a (63,55) Hamming Code.

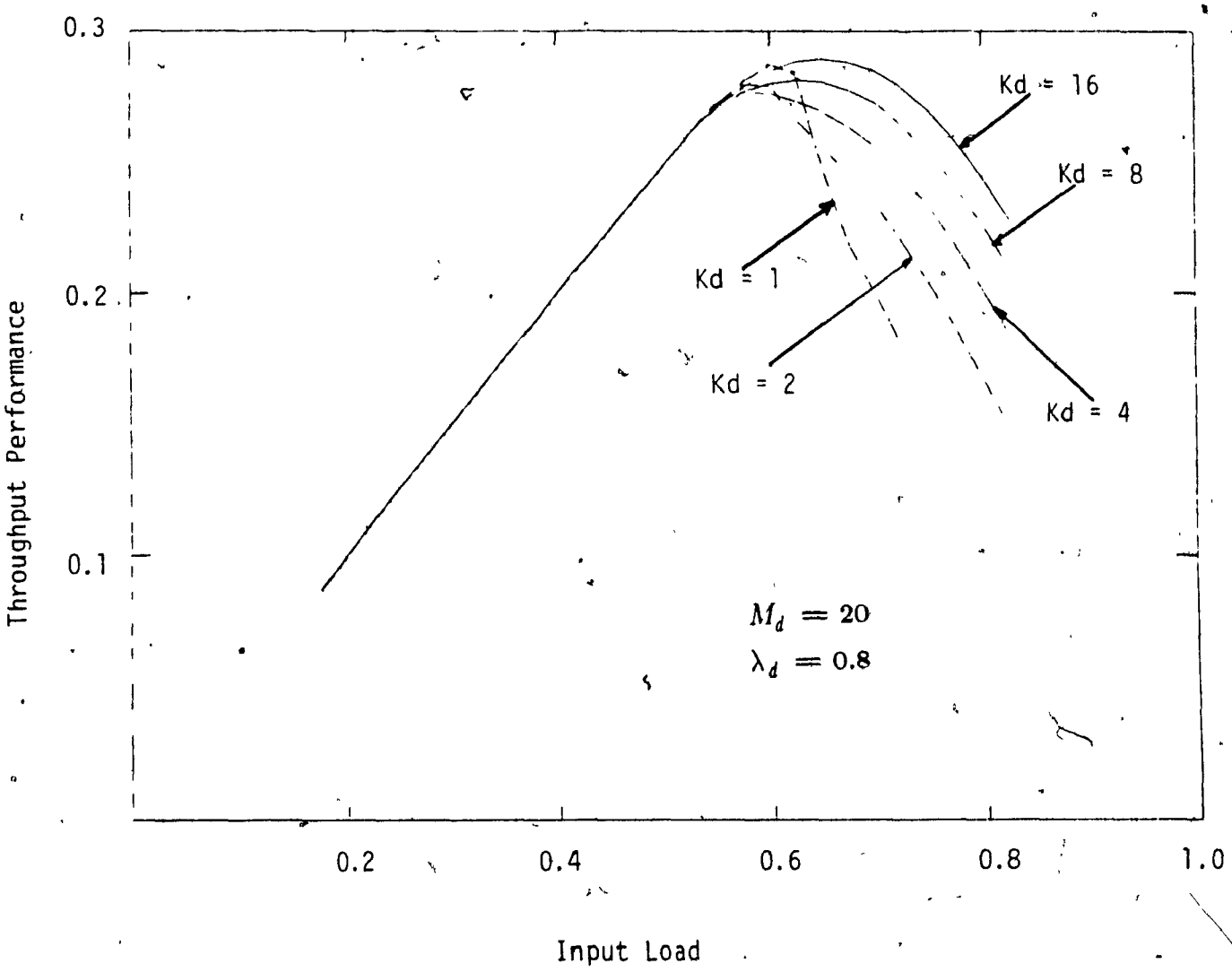

Figure (5.27) Throughput Performance of System A Using The Extended Golay Code.

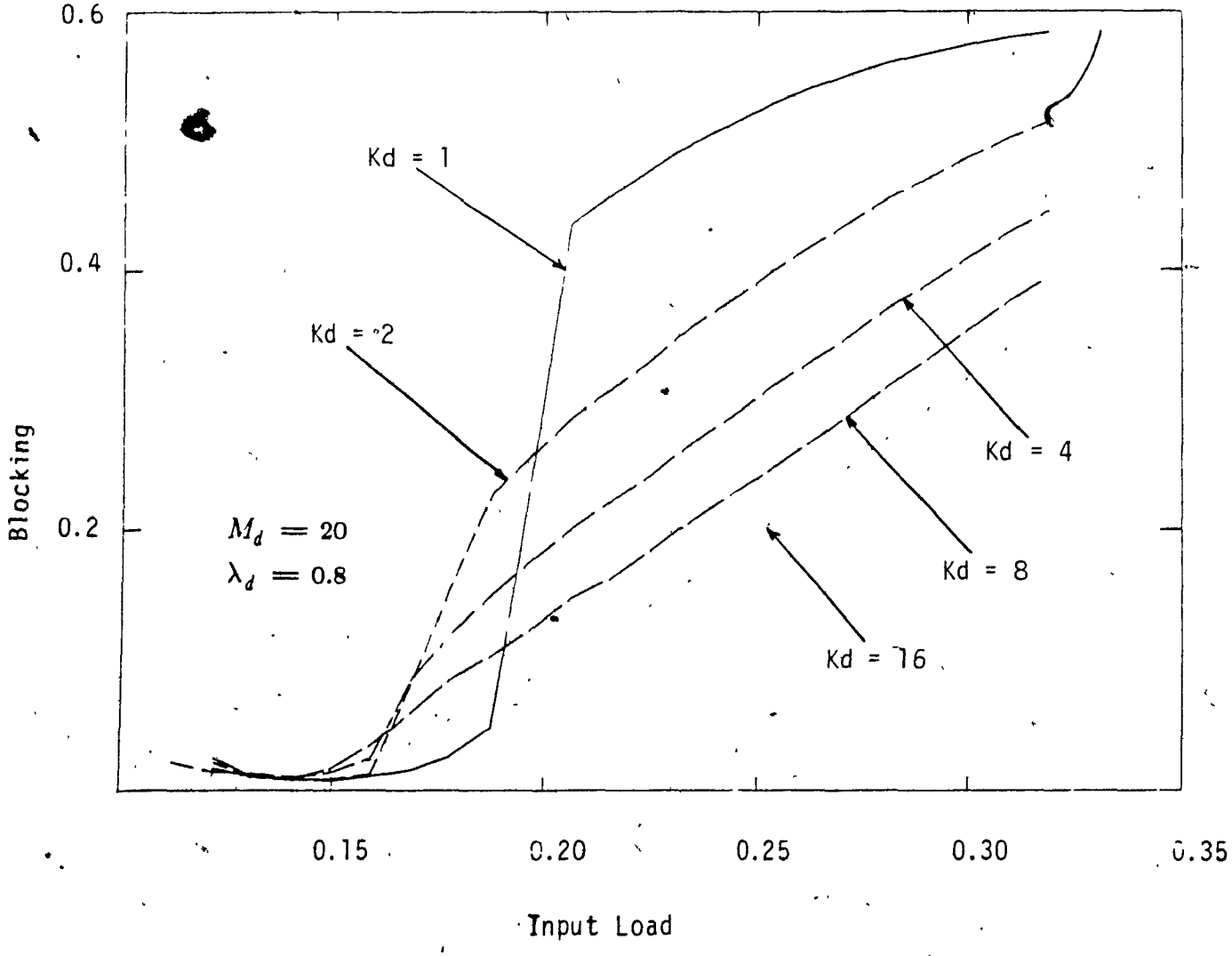

Figure (5.28) Probability of Packet Blocking For a (63,55) Hamming Code.

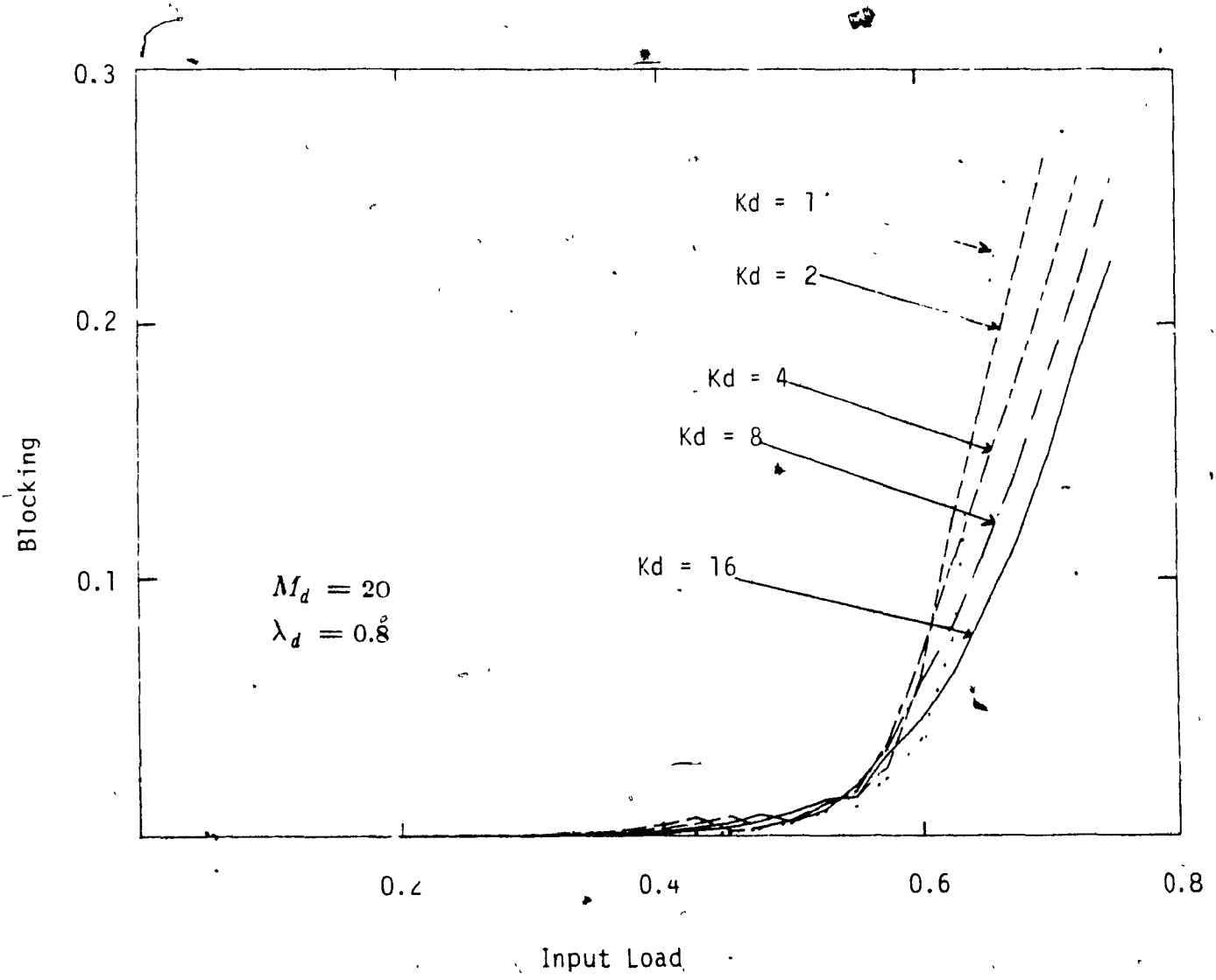

Figure (5.29) Probability of Packet Blocking Using The Extended Golay Code.

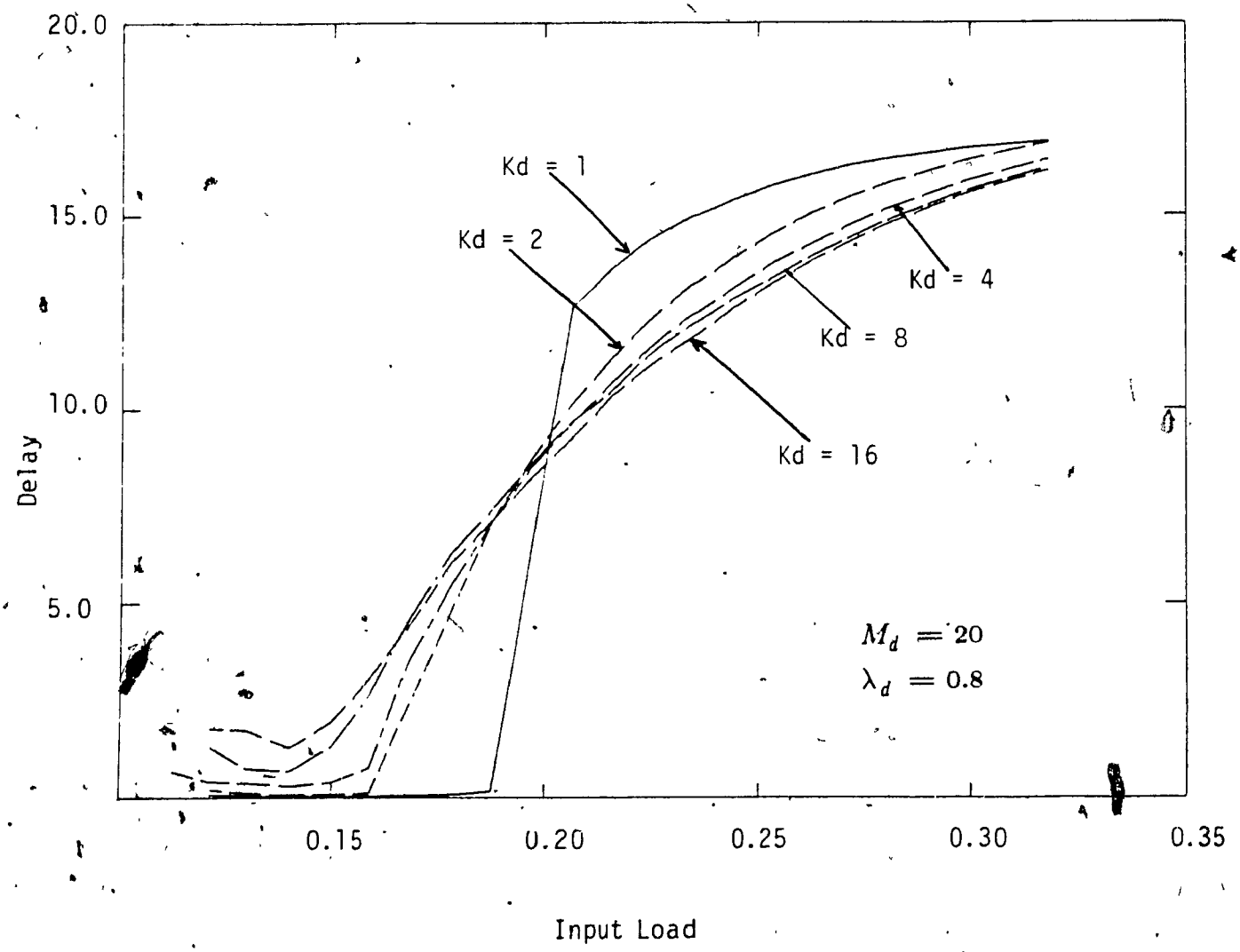

Figure (5.30) Delay Characteristics of System A Using a (63,55) Hamming Code.

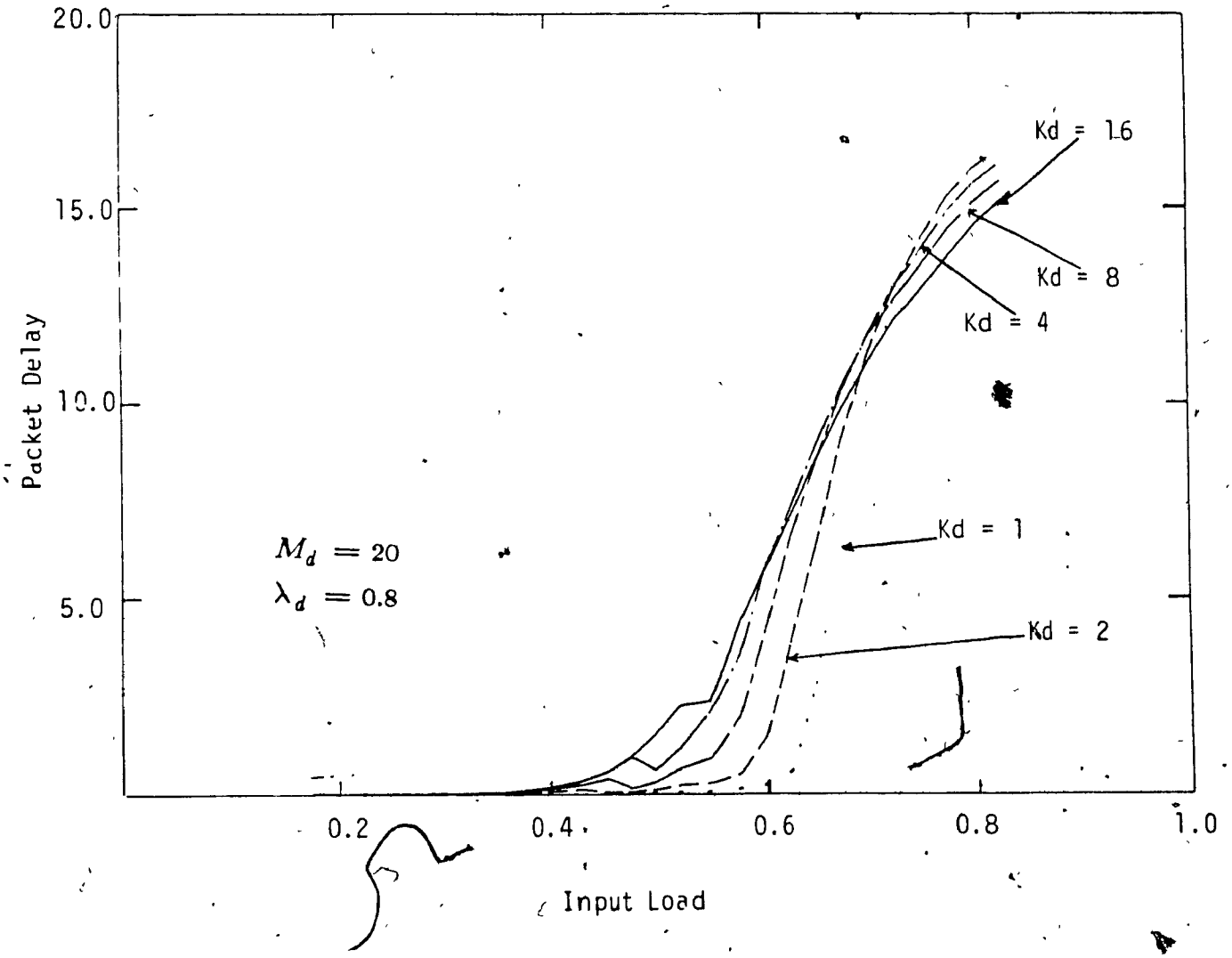

Figure (5.31) Delay Characteristics of System A Using The Extended Golay Code.

5.7 Comparison

In this section we compare the network throughput performance obtained in the previous section with the results of Cooper [14]. Cooper proposed a mobile cellular network using non-coherent frequency hopping techniques with Rayleigh faded signals. Each mobile user was assigned a unique set of time-frequency coded waveforms.

The fundamental unit of system efficiency is the number of successful calls/MHz (satisfied by the probability of error) for each cell denoted as U/B per cell, is also called Erlangs/Mhz. To determine the capacity of the mobile system, the interference contribution of other users must be analyzed. If we consider a cell that is circular in shape with equal area of the hexagon cell. Each user is modeled as a unit area d_a and transmits with an intensity of $W(r)$ $Watts/m^2$.

To aid in the determination of the total contribution computation, the cell structure is illustrated in Figure (5.34). The total contribution from each element d_a at base station Y_i is

$$dP = W(r)/r^{\alpha} D_a \qquad (5.27)$$

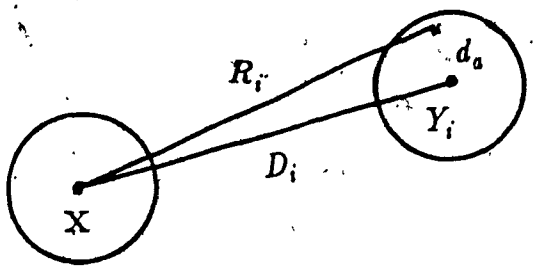

Figure (5.34) Cell Structure.

where α is the propagation law for mobile terrain. The received power from an elements in cell Y_i is denoted C, so we can state that $C = W(r)/r^{\alpha}$. Then the total accumulated power at the base station Y_i is

$$P = \int_A \frac{W(r)}{r^{\alpha}} dA = C\pi R_s^2 \tag{5.28}$$

thus

$$W(r) = P\frac{r^{\alpha}}{\pi R_s^2} \tag{5.28}$$

The base station X in another cell receives each element of power from the Y_i cell as

$$dP_{Y_i} = \frac{W(r)}{R_i^{\alpha}} dA \tag{5.29}$$

By employing the cos rule for the distance between users in cell Y_i and base station X, we get

$$P_{Y_i} = P_r^{\alpha} \frac{dA}{\pi R_s^2 (D_i^2 + r^2 - 2D_i r\cos\theta)^{\alpha/2}} \tag{5.30}$$

By summing over the contributions of the total power from all interfering cells N and dividing by the power P, we have the ratio

$$K_v = 1/\pi R_s^2 \sum_{i=1}^{N} \int_0^{l_s} \int_0^{2\pi} r^{\alpha} + \frac{1}{(D_i^2 + r^2 - 2D_i r\cos\theta)^{\alpha/2}} dr\, d\theta \tag{5.31}$$

If each cell contains U number of active users, then the interference contribution from users in adjacent interfering cells is $K_v U$ and the interference from

within the cell of concern is (U-1). Thus the ratio of signal power for one mobile user to the total interference power is

$$\frac{S}{I} = \frac{1}{(U-1)+(K_v U)} = \frac{1}{U(K_v+1)} \tag{5.32}$$

The signal to noise at the n bank receiver is

$$\frac{S}{I} = B\frac{t_1}{n}\frac{1}{(1+K_v)U} \tag{5.33}$$

where $1/t_1$ is the bandwidth of each filter and B is the total available bandwidth of the FH system. By rearranging equation (5.33) we get

$$\frac{U}{B} = \frac{1}{(n/t_1)(S/T)(1+K_v)} \tag{5.34}$$

Since $t_1 = \log_2 N/nR$ and the signal to noise is $S/I = (E_b/N_0)(\log_2 n/n^2)$. Thus by substituting

$$\frac{U}{B} = \frac{1}{R(E_b/N_0)(1+K_v)} \tag{5.35}$$

Including the speech time to total time ratio K_s in an average conversation we get

$$\frac{U}{B} = \frac{1}{R(E_b/N_0)(1+K_v)}\frac{1}{k_s} \tag{5.36}$$

Cooper selected the value of the bit rate as R = 30 Kbit/sec and a signal to noise ratio of 8 dB. Typically the value $K_v = 1$ is normally used after digital computation and we get U/B = 5.28 Erlang/Mhz.

Cooper fixes the data demodulated probability of error (or corresponding performance, since a specific probability of error corresponds to a certain signal

to noise ratio S/R. He then finds the maximum number of users that can operate full time within the above performance constraints (ie. U). Finally, dividing by U/B the traffic in Erlangs/Mhz is obtained.

For fair comparison with our Spread-Spectrum cellular scheme, we divide the total traffic per cell from all data and voice users by the Spread-Spectrum Bandwidth (per cell), and multiply by the probability of packet success, ie

$$\frac{(\lambda_v M_v + \lambda_d M_d)}{BW} * P_s \qquad (5.37)$$

It is easily seen that our analysis is more restricted then his. What we are effectively saying is that the packet has to be decoded successfully to be considered a success. In his case, the S/N ratio should not fall below a certain value for the transmission to be reliable. Our analysis includes both data and voice loads as opposed to considering only the voice case as Cooper described. Even if his S/N ratio is high enough, few bits of a certain packet may be erroneously detected, thus rendering the packet usless and cutting down the throughput.

Our analysis is also more realistic by the inclusion of the traffic variations. While in his case, users are operating full time, However, in our case, we are not exaggerating the value of the input traffic since each value of M_d or M_v is multiplied by its activity ratio λ_d or λ_v.

We compare the capacity of the three spread-spectrum systems obtained in Chapter Five with the capacity obtained by Cooper as depicted in Table (5.2). The capacity values were calculated using the throughput performance curves for Spread-Spectrum Systems A, B, and C with the (63,45) BCH code and a maximum possible transmitter back-off of 16 (*ie.* $K_d = 16$).

Table (5.2). Capacity Performance Comparisons.

Proposed System	Capacity Performance
Spread-Spectrum Network Proposed by Cooper	5.28
System A	10.65
System B	8.26
System C	26.56

The best performance achieved in this fair basis comparison was System C which employs the 8 Bank 4 hop spread-spectrum design, with almost 5 times the capacity obtained for the spread-spectrum network proposed by Cooper.

CHAPTER SIX

CONCLUSIONS

In the previous chapters, a plan for a high-capacity spread-spectrum mobile communications network has been outlined in both theoretical study and possible system implementations.

The FH/MFSK modulation techniques which provides the best system performance in terms of the probability of error is the 8-FSK 4 Hop/Symbol system design. Which is expected because of the large frequency diversity employed in this system. Better performance margins can be obtained for even higher frequency diversity techniques, but for economic and bandwidth considerations, practical systems must be designed with the tradeoff between better performance and a more complicated design.

Using the probability of error results obtained in Chapter Three for several FH/MFSK parameters an overview of the performance of a cellular mobile network was investigated. The basic cellular system requires non- overlapping uplink and downklink channels between the mobile users and the cell base stations along with a frequency reuse scheme to keep the overall spread spectrum network bandwidth as low as possible. The throughput performance, blocking, and average packet delay characteristics were studied for three different FH systems using three forward-error-correcting codes. The packet size employed in the analysis was 504 bits, allowing the block size of each FEC code to fit evenly into the packet. Various levels of packet backoff in the ARQ retransmission waiting time were also examined.

It was found that in general, the best throughput performance is obtained for larger values of the retransmission waiting time. However, this implies an

increase in the average packet delay time. The performance of the BFSK 2 hop/Symbol system was studied using (63,45) BCH code, (63,55) Hamming code, and an extended Golay code. We found that as the number of correctable bits per block increased, the throughput performance improves regardless of the code redundancy introduced.

We also discovered some interesting results of the delay characteristics for the cellular uplink channel. The packet delay obtained for low values of BO are less than that of higher values of BO upto a specific load point. Above this load point, the opposite is true, so if the network is operated below the crossover point, a smaller transmitter buffer size can be employed with relatively good average packet delay in the SS uplink channel.

Further study can be attempted in the calculations of the probability of bit error for various spread-spectrum systems. The assumptions that we made in our analysis of a maximum of 3 interfering users hopping onto the intended user's signal can be increased. This will allow accurate probability of error calculations to be performed for spread-spectrum systems with smaller processing gains then we considered in this analysis. Cellular mobile networks in heavily-loaded traffic areas may choose to use more cells per area as compared to low average load areas, thus the bandwidth of each cell must be reduced to keep the overall network bandwidth the same. With probability of error results obtained for cells with smaller processing gains calculated, the network characteristics can be analyzed.

Of course, increasing the number of possible interfering signals per hop requires an extremely large number of calculations, but can be done with powerful computers within a reasonable amount of time if the redundancies in the time- frequency matrix are deleted, as discussed in appendix A.

APPENDIX A

To alleviate the huge computational requirements of equation (3.9) which can easily exceed 10^{14} convolutions and summations for a single point on the P_e graph, we use the fact that some of the patterns in the time-frequency matrix (Figure (3.3)) are redundant. The P_e calculations need to be determined once for each unique pattern and then multiplied by a factor representing the number of times the pattern occurs.

First we examine how redundant patterns of interferers can exist in each receiver bank after L hops. This corresponds to a row in the time-frequency matrix. As stated before, the summation of the L random variable outcomes of each hop in a specific row can be described by

$$Z_l = \sum_{j=1}^{L} \chi_{jl} \tag{A.1}$$

where χ_{jl} is the PDF of all received signals in hop j and row l after limiting. It is clear that the order of summation does not change the final result, thus any specific pattern of $(\chi_{1l}, \chi_{2l}, \chi_{3l}, \cdots, \chi_{Ll})$ only needs to be used in the calculation of equation (3.9) once.

The sequence of unique patterns in row j and the multiplicity factors M_j, is denoted as S_j and can be determined by

$$\sum_{i_{1l}=0}^{U_t-1} \sum_{i_{1l}+i_{2l}}^{U_t-1} \cdots \sum_{i_{1l}+i_{2l}+\cdots+i_{Ll}}^{U_t-1} (i_{1l}, i_{2l}, \cdots, i_{Ll}) M_j \tag{A.2}$$

where $0 < i_{2l}, i_{3l}, \cdots, i_{Ll} < U_{st}$ and the length of the sequence is denoted as L_S,

Processing the S_j sequences for each row, we now examine any redundancies that may exist in each hop or column in the time-frequency matrix. We assume that the intended signal after dehopping is always located in the top row of the matrix producing a Ricean distribution. To observe how the redundant patterns occur after L hops we use an example. Let us say for now that there are no interfering signals that hit the first row of the matrix, namely $(i_{11}, i_{21}, \cdots, i_{L1}) = 0$.

The remaining M-1 rows contain only the interferers' contribution with Rayleigh distributions. From equation (3.3) we see that at the decision circuit, the probability that the signal level of the first row after L hops exceeds all other M-1 signal levels is

$$P_c = \int_{-\infty}^{\infty} P_r(Z_2 < Z_1, Z_3 < Z_1, \cdots, Z_M < Z_1 / Z_1) P_r(Z_1) dZ_1 \qquad \text{(A.3)}$$

where $Z_1, Z_2, \ldots, Z_M$ are the decision variables after L hops of the M receiver banks.

Interchanging the variables Z_2 to Z_M leads to the same results for P_c. Thus we can obtain an antiredundancy scheme in the columns of the matrix by taking the xth unique pattern composed of elements of the sequences $S_2, S_3, \ldots, S_M$ This can be written in the form

$$\sum_{x_2}^{L_{S_2}} \sum_{x_2+x_3}^{L_{S_3}} \cdots \sum_{x_2+x_3+\cdots+x_M}^{L_{S_M}} S_2(x_2) S_3(x_3) \cdots S_M(x_M) \qquad \text{(A.4)}$$

Since the distribution for the top row of the matrix differs from the m-1 lower rows, no antiredundancy scheme can be employed to include the top row. So for each pattern of S_1 equation (A.4) must be used.

The elimination of the redundant patterns present in the rows and columns of the time-frequency matrix permit us to rewrite equation (3.9) as

$$P_c = \sum_{k_{11}}^{U_{st}} \cdots \sum_{k_{jl}}^{U_{st}} \cdots \sum_{k_{LM}}^{U_{st}} \sum_{i_{11}}^{U_t-1} \sum_{x_1+x_2}^{U_t-1} \cdots \sum_{x_1+x_2+\cdots+x_M}^{U_t-1}$$

$$Pr\,(c\,/k_{11}, \ldots, k_{LM}, i_{11}, \ldots, i_{LM})P\,(k_{11}, \ldots, k_{1M})*\ldots*P\,(k_{L1}, \ldots, k_{LM})*\ldots$$

$$\ldots*P\,(i_{11}, \ldots, i_{1M})*\ldots*P\,(i_{L1}, \ldots, i_{LM}) \qquad \text{(A.5)}$$

The total number of matrix patterns for low power users is U_t^{L*M}, and the number of unique matrix patterns for all low power users omitting the redundancies is.

$$(L_{S_j}+M-2)\left[\frac{L_{S_j}+m-1}{2}\right] \qquad \text{(A.6)}$$

where L_{S_j} is the antiredundancy sequence length for L hops and U_t active users, so that $L_{S_j} = (U_t+L-1)(U_t-L/2)$.

REFERENCES

[1] J. W. Schwartz, J. M. Aein, J. Kaiser, "Modulation Techniques for Multiple Access to a Hard-Limiting Satellite Repeater", *Proceedings of the IEEE.*, Vol 54, No. 5, pp. 763-776, May 1966.

[2] Jhong S. Lee, Leonard E. Miller, Robert H. French, "The Analyses of Uncoded Performances for Certain ECCM Receiver Strategies for Multihops/Symbol FH/MFSK Waveforms", *IEEE Selected Areas In Communications*, Vol Sac-3, No. 5, pp 611-618, September 1985.

[3] Lee D. Davisson, Laurence B. Milstein, "On the Performance of Digital Communication Systems With Bandpass Limiters-Part I: One Link System", *IEEE Trans. on Communications*, pp 972-975, October 1972.

[4] Ray W. Nettleton, George R. Cooper, "Performance of a Frequency-Hopped Differentially Modulated Spread-Spectrum Receiver in a Rayleigh Fading Channel", *IEEE Trans. on Vehicular Tech.*, Vol. VT-30, No 1, February 1981.

[5] Jhong S. Lee, Leonard E. Miller, Young K. Kim, "Probability of Error Analyses of a BFSK Frequency-Hopping System with Diversity Under Partial-Band Jamming Interference--Part II: Performance of Square- Law Nonlinear Combining Soft Decision Receivers", *IEEE Trans. on Communications*, Vol. Com-32, No. 12, pp 1243-1250, December 1984.

[6] On-Ching Yue, "Performance of Frequency-Hopping Multiple-Access Multilevel FSK System with Hard-Limiting and Linear Combining", *IEEE Trans. on Communications*, Vol. Com-29, No 11, pp 1687-1694, November 1981.

[7] G. Elnarsson, "Address Assignment For a Time-Frequency-Coded, Spread-Spectrum System", *Bell System Tech. Journal*, Vol. 59, No. 7, pp 1241-1255, September 1980.

[8] Kung Yao, "Error Probability of Asynchronous Spread-Spectrum Multiple Access Communication Systems", *IEEE Trans. on Communications*, Vol. Com-25, No. 8, pp 803-808, August 1977.

[9] Said Elnoubi, R. Singh and S.C. Gupta, "Performance of Frequency Channel Assignment Schemes in Combined Mobile Telephone and Dispatch Systems", *IEEE ICC Conference Proceedings*, Vol. 2, pp. 24.4.1-24.4.5, 1980.

[10] Tsun-Yee Yan, Charles C. Wang, "Mathematical Models for Cochannel Interference in FH/MFSK Multiple-Access Systems", *IEEE Trans. on Communications*, Vol. Com-32, No. 6, pp 670-678, June 1984.

[11] D. J. Goodman, P. S. Henry, V. K. Prabhu, "Frequency-Hopped Multilevel FSK for Mobile Radio", *Bell System Tech. Journal*, Vol. 59, No. 7, pp

1257-1275, September 1980.

[12] William C. Y. Lee, "Elements of Cellular Mobile Radio Systems", *IEEE Trans. on Vehicular Tech*, Vol VT-35, pp. 48-56, May 1986.

[13] Leonard Schiff, "Traffic Capacity of Three Types of Common User Mobile Communication Systems", *IEEE Trans. of Communication Tech.*, Vol Com-18, No. 1, pp. 12-22, February 1970.

[14] Samual A. Musa and Wasyl Wasylkiwskyj, "Co-Channel Interference of Spread-Spectrum Systems in a Multiple User Environment", *IEEE Trans. on Communications*, Vol. Com-26, No. 10, pp.1405-1412, October 1978.

[15] George R. Cooper and Raymond W. Nettleton, "Spread-Spectrum Technique for High-Capacity Mobile Communications", *IEEE Trans on Vehicular Tech*, Vol. VT-27, No. 4, pp. 264-275, November 1978.

[16] Didier Verhulst, Michel Mouly, and Jacques Szpirglas, "Slow Frequency Hopping Multiple Access for Digital Cellular Radiotelephone", *IEEE Trans. on Vehicular Tech.*, Vol. VT-33, No. 3, pp. 179-190, August 1984.

[17] Shu Lin and Philip S. Yu, "A Hybrid ARQ Scheme with Parity Retransmission for Error Control of Satellite Channels", *IEEE Trans on Communications*, Vol. Com-30, No. 7, pp. 1701-1719, July 1982.

[18] H. O. Burton and D. D. Sullivan, "Errors and Error Control", *IEEE Proceedings*, Vol. 60, No. 11, pp. 1293-1301, November 1972.

[19] Vijay K. Bhargava, "Foward Error Correction Schemes For Digital Communications", *IEEE Communication Magazine*, pp. 11-19, January 1983.

[20] Jin-tuu Wang and Ming T. Liu, "Analysis and Simulation of The Mixed Voice/Data Transmission Systems (MVD) For Computer Communications", *IEEE National Telemetry Conference*, 1976.

[21] W. Wesley Peterson and E. J. Weldon, Jr., "Error correcting Codes", Second Ed., MIT Press.,1972

[22] Marvin K. Simon et al., "Spread-Spectrum Communications", Vol. I/II/III, Computer Science Press, Maryland, 1985.

[23] Rodger E. Ziemer, Roger L. Peterson, "Digital Communications and Spread-Spectrum Systems", MacMillan Publishing Co., New York., 1985.

[24] John G. Proakis, "Digital Communications", McGraw-Hill New York, 1983.

[25] Vijay K. Bhargava et al., "Digital Communications By Satellite", John Wiley & Sons., New York, 1981.

[26] Jeremiah F. Hayes, "Modeling and Analysis of Computer Communication Networks", Plenum Press, New York, 1984.

[27] Thomas Richard, "Introduction to Numerical Methods and Fortran Programming", John Wiley & Sons, New York, 1967.

[28] James S. Vandergraft, "Introduction to Numerical Computation", Academic Press, New York, 1978.

[29] J. LI. Morris, "Computational Methods in Elementary Numerical Analysis", John Wiley & Sons, Toronto, 1983.

[30] Robert B. Cooper, "Introduction to Queuing Theory", North Holland Inc., New York, 1981.

[31] Robert C. Dixon, "Spread-Spectrum System", John Wiley & Sons, New York, 1984.

[32] William C. Jakes Jr., " Microwave Mobile Communications", John Wiley & Sons, New York, 1974.

[33] Charles L. Weber, Gaylord K. Huth, Bartus H. Batson, "Performance Considerations of Frequency-Hopping Multiple Access", *IEEE Milcom Conference Proc.*, pp 69.4.1-69.4.5, 1980.

[34] S. J. Towalj, Robert McCaugheren, "An Integrated Land Mobile Telecommunication Radio System", *IEEE Montech'86 Conference Proc.*, pp 94-98, September 1986.

[35] V. H. MacDonald,"The Cellular Concept", *The Bell System Technical Journal*, Vol. 58, No. 1, pp. 15-41, January 1979.

[36] John Oetting, "Cellular Mobile Radio- An Emerging Technology", *IEEE Communications Magazine*, pp 10-15, November 1983.

[37] Z. C. Fluhr, P. T. Porter, "Control Architecture", *The Bell System Technical Journal*, Vol. 58, No. 1, pp. 43-69, January 1979.

[38] Andrew J. Viterbi, "Spread-Spectrum Communications- Myths And Realities", *IEEE Communication Magazine*, pp 11-18, May 1979.

[39] Nirode C. Mohanty, "Spread-Spectrum and Time Division Multiple Access Satellite Communications", *IEEE Trans. on Communications*, Vol. COM-25, No. 8, PP. 810-815, August 1977.

[40] I. Sabbagh, D.G. Appleby, "Adaptive Slow Frequency-Hopping System For Land Mobile Radio", *IEE Proceedings*, Vol. 132, Pt. F, No. 5, pp. 375-383, August 1985.